



บัณฑิตวิทยาลัย จุฬาลงกรณ์มหาวิทยาลัย
Graduate School, Chulalongkorn University
เสาหลักของแผ่นดิน

การตั้งตำรับแผ่นฟิล์มที่เตรียมจากไซโลกลูแคนเมล็ดมะขาม
ซึ่งผสมสารสกัดบัวบก

นางสาวจิรัญญา อัสনী

วิทยานิพนธ์นี้เป็นส่วนหนึ่งของการศึกษาตามหลักสูตรปริญญาเภสัชศาสตรมหาบัณฑิต
สาขาวิชาเภสัชกรรม ภาควิชาเภสัชกรรม
คณะเภสัชศาสตร์ จุฬาลงกรณ์มหาวิทยาลัย
ปีการศึกษา 2550
ลิขสิทธิ์ของจุฬาลงกรณ์มหาวิทยาลัย



บัณฑิตวิทยาลัย จุฬาลงกรณ์มหาวิทยาลัย
Graduate School, Chulalongkorn University
เสาหลักของแผ่นดิน

FORMULATION OF FILMS PREPARED FROM TAMARIND
SEED XYLOGLUCANS CONTAINING
CENTELLA ASIATICA EXTRACT

Miss Jirunya Assanee

A Thesis Submitted Partial Fulfillment of the Requirements
for the Degree of Master of Science in Pharmacy Program in Pharmaceutics
Department of Pharmacy
Faculty of Pharmaceutical Sciences
Chulalongkorn University
Academic Year 2007
Copyright of Chulalongkorn University



จรรยาบรรณ อักษรย่อ: การตั้งตำรับแผ่นฟิล์มที่เตรียมจากไซโลกลูแคนเมล็ดมะขามซึ่งผสมสารสกัดบัวบก (FORMULATION OF FILMS PREPARED FROM TAMARIND SEED XYLOGLUCANS CONTAINING *CENTELLA ASIATICA* EXTRACT) อ. ที่ปรึกษา: รศ. ดร.สุชาติ ชูติมา วรพันธ์, อ. ที่ปรึกษาร่วม: ผศ.ดร.ชำนาญ ภัทรพานิช, 161 หน้า.

การศึกษาระดับบัณฑิตยศึกษานี้เป็นการทำวิจัยและทำการทำให้ตะกอนนอนก้นของไซโลกลูแคนจากเมล็ดมะขามเพื่อคัดเลือกวิธีที่เหมาะสมในการสกัดไซโลกลูแคน พบว่า วิธีที่ 1 ซึ่งคัดเลือกเป็นวิธีที่เหมาะสมที่สุดโดยใช้การผสมแห้งเมล็ดมะขามกับเฮกเซนก่อนแล้วจึงผสมกับน้ำ และทำให้ตะกอนนอนก้นโดยการหมุนเหวี่ยงในทันที นอกจากนี้ได้ศึกษาหาสภาวะการพ่นแห้งที่เหมาะสมที่สุดด้วยวิธีพื้นผิวตอบสนอง ได้ศึกษาผลของปัจจัยเกี่ยวกับกระบวนการได้แก่ อุณหภูมิลมเข้า และอัตราการไหลของอากาศต่อปริมาณผลผลิตและปริมาณความชื้นโดยใช้วิธีการออกแบบส่วนประกอบกลางที่ผิว พบว่าโมเดลกำลังสองเหมาะสมเข้ากับเปอร์เซ็นต์ปริมาณผลผลิต และโมเดลเชิงเส้นเหมาะสมเข้ากับเปอร์เซ็นต์ความชื้น ($P < 0.05$) โดยใช้การพล็อตโอเวอร์เลย์สามารถหาสภาวะที่เหมาะสมที่สุดได้ และทดลองทำซ้ำพบว่าค่าเฉลี่ยของเปอร์เซ็นต์ปริมาณผลผลิตและเปอร์เซ็นต์ความชื้นที่ได้อยู่ในช่วงที่คาดการณ์ไว้ที่ระดับความเชื่อมั่น 95 เปอร์เซ็นต์ โดยมีค่า 50.04 ± 4.13 เปอร์เซ็นต์ และ 6.07 ± 0.37 เปอร์เซ็นต์ตามลำดับ แสดงว่าโมเดลดังกล่าวเหมาะสมเข้ากันได้กับผลการทดลองการศึกษาคคุณสมบัติของผงพ่นแห้งไซโลกลูแคน พบว่าค่าความเป็นกรด-ด่างของสารละลาย 1% น้ำหนักต่อปริมาตรของผงแห้งไซโลกลูแคนในน้ำเท่ากับ 7.83 ค่าการละลายของไซโลกลูแคนในน้ำประมาณ 6.28 มิลลิกรัมต่อมิลลิลิตร สารละลาย ไซโลกลูแคนมีการไหลแบบซูโดพลาสติก แผ่นฟิล์มที่เตรียมจากผงไซโลกลูแคนซึ่งผสมสารสกัดบัวบกในความเข้มข้นเทียบเท่ากับเอเชียติโคไซด์ 1 เปอร์เซ็นต์โดยน้ำหนัก เมื่อประเมินจากคุณสมบัติเชิงกลพบว่าฟิล์มมีลักษณะแข็งและเหนียว และมีคุณสมบัติยึดติดมีค่าแรงยึดติดเท่ากับ 3.70 ± 1.11 นิวตันต่อตารางเซนติเมตร ผลจากดีฟเฟอเรนเชียลสแกนนิ่งแคลอริเมตรี และพาวเดอร์เอ็กซ์เรย์ดิฟแฟรคชันแสดงให้เห็นว่าสารสกัดบัวบกอาจจะกระจายในแผ่นฟิล์มในระดับโมเลกุล และ/หรืออยู่ในรูปอสัณฐานแบบของแข็งกระจายตัว การปลดปล่อยเอเชียติโคไซด์จากแผ่นฟิล์มมากกว่า 50% ที่เวลา 8 ชั่วโมง การวิเคราะห์กลไกการปลดปล่อยของสารเอเชียติโคไซด์ พบว่าการปลดปล่อยเป็นสัดส่วนกับรากที่สองของเวลา แสดงได้ว่าสารเอเชียติโคไซด์อาจจะปลดปล่อยออกจากแผ่นฟิล์มโดยการแพร่ การศึกษาการซึมผ่านผิวหนังใช้ผิวหนังหน้าท้องของลูกหมูเป็นเมมเบรนโมเดล พบว่ามีเอเชียติโคไซด์ในผิวหนังอยู่ประมาณ 1.30 ± 1.28 เปอร์เซ็นต์ การตรวจพบเอเชียติโคไซด์ในปริมาณน้อยอาจเกิดจากการไฮโดรลิซิสของเอเชียติโคไซด์เป็นกรดเอเชียติคซึ่งเป็นสารออกฤทธิ์หนึ่งของสารสกัดบัวบก

ภาควิชา	เภสัชกรรม	ลายมือชื่อนิสิต.....
สาขาวิชา	เภสัชกรรม	ลายมือชื่ออาจารย์ที่ปรึกษา.....
ปีการศึกษา	2550	ลายมือชื่ออาจารย์ที่ปรึกษาร่วม.....



47876559033 : MAJOR PHARMACEUTICS

KEY WORD: XYLOGLUCAN / SPRAY DRYING / *CENTELLA ASIATICA* EXTRACT / TAMARIND SEED / ADHESIVE PROPERTY / FILM

JIRUNYA ASSANEE: FORMULATION OF FILMS PREPARED FROM TAMARIND SEED XYLOGLUCANS CONTAINING *CENTELLA ASIATICA* EXTRACT. THESIS ADVISOR: ASSOC. PROF. SUCHADA CHUTIMAWORAPAN, Ph.D., THESIS COADVISOR: ASST. PROF. CHAMNAN PATARAPANICH, 161 pp.

The process of defatting and sedimentation of xyloglucan from tamarind seed were investigated in order to select the appropriate method for xyloglucan extraction. The selected Method I was performed by soaking tamarind seed powder with hexane prior to mixing with water and then sedimentation by centrifugation. In addition, the optimized spraying condition was estimated by response surface methodology. The effect of two process parameters, inlet temperature and aspirator rate on yield and moisture content was studied. A face centered design showed a quadratic model fitted for %yield and a linear model for %moisture content ($P < 0.05$). The optimum region by overlay plot was carried out using the best condition to evaluate the repeatability of the spray-drying technique. The observed means obtained for %yield and %moisture content were in range of the prediction intervals at 95% confidence level as, $50.40 \pm 4.13\%$ and $6.07 \pm 0.37\%$, respectively. The result clearly showed that the model fitted the experimental data well. The properties of xyloglucan spray dried powder were determined. The pH value of 1%w/v solution of xyloglucan in water was 7.83. The solubility in water of xyloglucan was 6.28 mg/ml. The solution of xyloglucan exhibited typical pseudoplastic flow. The film prepared from xyloglucan powder containing *Centella asiatica* extract in equivalent amount of asiaticoside at 1%w/w, from mechanical property evaluation, was hard and tough and had good adhesive property with adhesive force of $3.703 \pm 1.11 \text{ N/cm}^2$. Differential scanning calorimetry and powder x-ray diffraction studies revealed that *Centella* extract might molecularly disperse with film formulation and/or exist in an amorphous state as a solid dispersion. The release of asiaticoside more than 50% from film formulation was achieved at 8 hours. The analysis of release mechanism showed that the release of asiaticoside was proportional to the square root of time, indicating that asiaticoside might be released from the film formulation by diffusion. The skin permeation study using porcine skin as model membrane showed that asiaticoside permeated into skin approximately $1.30 \pm 1.28\%$. The detection of small amount of asiaticoside permeated might be due to hydrolysis of asiaticoside to Asiatic acid, one of active compounds of *Centella* extract.

Department : Pharmacy

Student's Signature:

Field of Study : Pharmaceutics

Advisor's Signature:

Academic Year : 2007

Co-Advisor's Signature:



ACKNOWLEDGEMENTS

First of all, I would like to express my gratitude to my advisor Associate Professor Suchada Chutimaworapan, Ph.D. for suggesting the main topic of this study and for providing excellent working facilities. I am most grateful for her scientific guidance as well as for her advice, constant enthusiasm and encouragement, all of which made the completion of this study possible.

I would like to express my appreciation and grateful thanks to my co-advisor, Assistant Professor Chamnan Patarpanich, Ph.D. for his valuable suggestion and kindness during the analysis method.

I thank most sincerely the reviewers of this thesis, Associate Professor Uthai Suvanakoot, Ph.D., the chairman of my thesis examination committee, as well as other committee members. I am grateful to Associate Professor Thitima Pengsuparp, Ph.D. and Assistant Professor Pol. Lt. Walaisiri Muangsiri, Ph.D. for their constructive criticism and for giving me valuable suggestions for its improvement.

I am very grateful to Dr. Mukdawan Prakobvaitayakit and Dr. Angkana Tantituanont for spending her valuable time and suggestion for the statistical program. I am very grateful to Associate Professor Waraporn Suwakul, Ph.D. for spending her valuable time and suggestion for the *in vitro* release and skin permeation studies. I am very grateful to Dusadee Charnvanich for spending her valuable time and suggestion for the spray dried technique.

I appreciate to UNIDO for allowance of using reflective index detector. I would like to express my thank to Megazyme International Ireland Ltd. for providing xyloglucan standard, ADINOP Co., Ltd., Thailand for providing Sepicide[®] HB, and Associate Professor Sunanta Pongsamart, Ph.D. for allowance of using tensimeter.

My sincere thanks are to all staff members of Department of Pharmacy and Department of Manufacturing Pharmacy, Faculty of Pharmaceutical Sciences, Chulalongkorn University for helping and other persons whose names have not been mentioned here for their assistance and encouragement.

Finally, greatest thank to my parents for their everlasting love, understanding, encouragement, and continued support during the course of my education.

CONTENTS

	Page
THAI ABSTRACT.....	iv
ENGLISH ABSTRACT.....	v
ACKNOWLEDGEMENTS.....	vi
CONTENTS.....	vii
LIST OF TABLES.....	ix
LIST OF FIGURES.....	xi
LIST OF ABBREVIATIONS.....	xiii
CHAPTER	
I INTRODUCTION.....	1
II LITERATURE REVIEW	3
Botanical, Chemical and Pharmacological Aspects of	
<i>Tamarindus indica</i> (Linn.).....	3
Chemistry, physicochemical properties and application of	
xyloglucan from tamarind seed.....	4
Spray drying technique.....	10
Structure of skin.....	13
Transdermal drug delivery system.....	15
Wound healing.....	18
Botanical, Chemical and Pharmacological Aspects of	
<i>Centella asiatica</i> (Linn.).....	19
III MATERIALS AND METHODS.....	24
Materials.....	24
Apparatus.....	25
Methods.....	27
IV RESULTS AND DISCUSSION.....	51
Characterization of xyloglucan spray dried powder from	
tamarind seeds	51
Optimization of spray drying condition.....	59
Evaluation of physiochemical properties of xyloglucan powder from	
Tamarind seed.....	74

	Page
Evaluation of films prepared from tamarind seed and films	
Formulation prepared from tamarind seed containing	
<i>Centella asiatica</i> extract.....	79
V CONCLUSIONS.....	96
REFERENCES.....	99
APPENDICES.....	106
VITA.....	161

LIST OF TABLES

Table	Page
1	A face central design of two parameters38
2	Mixing ratio of absolute ethanol and tamarind seed xyloglucan solution.....40
3	Small central composite design of film formulations.....42
4	Composition of tamarind seed xyloglucan film formulations45
5	Comparison of the percentage yield, percentage moisture content and physical appearances xyloglucan spray dried powder from four different methods.....51
6	Data of calibration curve of xyloglucan by HPLC method55
7	The percentages of analytical recovery of xyloglucan by HPLC method.....55
8	Data of within run precision by HPLC method.....56
9	Data of between run precision by HPLC method.....56
10	Comparison of the percent of xyloglucan, total protein and fat of xyloglucan spray dried powder from four different methods and tamarind seed powder (mean \pm SD).....56
11	A face centered design matrix of two parameters and the observed responses.....60
12	ANOVA for response surface quadratic model of % yield.....61
13	ANOVA for linear model of %moisture content.....61
14	Model Summary Statistics of %yield and % moisture content.....62
15	Coefficients of the regression equation linking the responses to the experimental factors and major interactions (coded units).....62
16	The optimum region by overlay plot of two parameters and the observed responses.....67
17	Observed responses and 95% CI (confidence interval) of optimization spray dried condition.....68
18	The particle size distributions of the xyloglucan spray dried particles (mean \pm SD; n=3).....74
19	The viscosity value and rheology property of 1, 1.5 and 2%w/v of xyloglucan powder from tamarind seed (mean \pm SD).....75

Table	Page
20	The percentage of remained and reduced xyloglucan after added ethanol (Mean \pm SD).....76
21	The thickness and film weight data of films (mean \pm SD).....80
22	The force of adhesive data of films. (mean \pm SD).....82
23	The value of tensile strength and %elongation of classification of film.....82
24	Mechanical properties data of film and film formulation containing <i>Centella asiatica</i> extract (mean \pm SD).....84
25	The release data of asiaticoside from film formulation (mean \pm SD).....88
26	The percentage of asiaticoside from film formulations in donor of Franz diffusion cell and porcine skin.....90
27	The percentages labeled amount of asiaticoside in film formulation containing <i>Centella asiatica</i> extract in stability test (mean \pm SD).....91
28	Table Adhesive properties data of asiaticoside in film formulation in stability test (mean \pm SD).....91
29	Mechanical properties data of asiaticoside in film formulation in stability test (mean \pm SD).....92

LIST OF FIGURES

Figure		Page
1	<i>Tamarindus indica</i>	3
2	Tamarinds seed and kernel of tamarind seeds	4
3	The unit structures of oligosaccharides from tamarind xyloglucan.....	5
4	Structure of human skin in crosssection.....	14
5	A reservoir-type transdermal delivery device	16
6	a) A typical matrix-type transdermal delivery device b) An adhesive matrix device.....	17
7	A microreservoir transdermal delivery device.....	17
8	<i>Centella asiatica</i> (Linn.) Urban	20
9	Structures of the triterpenoids from <i>Centella asiatica</i> (Linn.).....	21
10	Diagram of xyloglucan extraction.....	29
11	Spray dryer (Model SD-06, Labplant, Ltd., UK).....	30
12	Soxhlet extraction.....	35
13	Spray dryer B-290 (Buchi Mini, Switzerland).....	37
14	Viscometer (RotoVisco RV1, Germany).....	39
15	The xyloglucan spray dried powder from four different methods	52
16	HPLC chromatograms of ultra pure water; (a) xyloglucan standard solution (b) sample solution and (c) absolute ethanol.....	54
17	Calibration curve of a by HPLC method.....	55
18	Scanning electron photomicrographs of xyloglucan spray dried powder from four different methods; a) Method I, (b) Method II, (c) Method III and Method IV.....	58
19	Response surface plot of % yield and linear regression plot of %moisture content; (a) response surface plot of % yield, (b) linear regression plot of %moisture content.....	65
20	The normal probability plots of the %yield and %moisture content.....	66
21	The optimum region by overlay plot of two responses (%yield and %moisture content) evaluated as a function of inlet temperature and %aspirator.....	67

Figure	Page
22	Xyloglucan spray dried powder of optimal spray dried condition 68
23	Scanning electron photomicrographs of xyloglucan spray dried powder from experimental design70
24	Rheogram of 1% w/v xyloglucan spray dried powder.....76
25	The DSC thermograms of standard xyloglucan and xyloglucan powder from tamarind seed.....77
26	X-ray diffractograms of standard xyloglucan and xyloglucan powder from tamarind seed78
27	Scanning electron photomicrographs of xyloglucan powder.....79
28	The appearance of films79
29	The DSC thermograms of <i>Centella asiatica</i> extract, film prepared from xyloglucan powder and film prepared from xyloglucan powder containing <i>Centella asiatica</i> extract.....85
30	X-ray diffractograms of <i>Centella asiatica</i> extract, film prepared from xyloglucan powder and film prepared from xyloglucan powder containing <i>Centella asiatica</i> extract.....86
31	The release profiles of asiaticoside from film formulation.....87
32	Cumulative release per unit area, Q , for asiaticoside as a function of square root time from film formulation.....89
33	DSC thermograms of film formulation after stress condition (40° C, 75% RH).....94
34	X-ray diffractograms of film formulation after stress condition (40° C, 75% RH).....95

LISTS OF ABBREVIATIONS

A°	=	Angstrom
ANOVA	=	analysis of variance
°C	=	degree Celsius
CCD	=	Central Composite Design
CI	=	confidence interval
cm	=	centimeter
CV	=	coefficient of variation
df	=	degree of freedom
DSC	=	differential scanning calorimetry
et al.	=	<i>et alii</i> , 'and others'
g	=	gram
hr	=	hour
HPLC	=	high performance liquid chromatography
kv	=	kilovolt
mg	=	milligram
min	=	minute
mJ	=	millijoule
ml	=	milliliter
mm	=	millimeter
mm ²	=	square millimeter
mPas	=	millipascal
MPa	=	millipascal.second
MW	=	molecular weight
N	=	Newton
n	=	sample size
pH	=	the negative logarithm of the hydrogen ion concentration
R ²	=	coefficient of determination
RH	=	relative humidity
RI	=	reflective index
rpm	=	round per minute

s	=	second
SD	=	standard deviation
TECA	=	titrated extract of <i>Centella asiatica</i>
TTF	=	total triterpenic fraction
TTFCA	=	total triterpenoid fraction of <i>Centella asiatica</i>
µg	=	microgram
µm	=	micrometer
USP/NF	=	The United States Pharmacopoeia/National Formulary
UV	=	ultraviolet
w/v	=	weight by volume
w/w	=	weight by weight

CHAPTER I

INTRODUCTION

Xyloglucan polysaccharide is found in the primary cell walls of higher plants such as apple, onion, corn and tamarind, etc (Hoffman et al., 2005). Xyloglucan from these plants are different in structural features and molecular weights, therefore different physicochemical properties including viscosity, solubility, gelling, freeze–thaw stability and film formation were reported. Sims et al. (1998) had studied the rheological properties of xyloglucans from three plants; *Nicotiana plumbaginifolia* cells, apple pomace and tamarind seeds. The result showed that xyloglucan from tamarind seeds gave the highest viscosity and the greatest stability over the acid pH range.

Xyloglucan polysaccharide derived from tamarind seed is composed of a (1-4)- β -D-glucan backbone chain which has (1-6)- α -D-xylose branches that are partially substituted by (1-2)- β -D-galactoxylose. The tamarind seed xyloglucan is composed of three units of xyloglucan oligomers with heptasaccharide, octasaccharide and nonasaccharide, which differ in the number of galactose side-chains (Kawasaki et al., 1999).

Tamarind seed xyloglucan possesses many attractive properties such as high viscosity, broad pH tolerance and adhesiveness. This led to its application as stabilizer, thickener, gelling agent and binder in food and pharmaceutical industries (Sumathi and Ray, 2002). In addition to these properties, tamarind seed xyloglucan showed non-carcinogenicity (Sano et al., 1996), sol to gel transition (Yamanaka et al., 2000; Shirakawa, Yamatoya and Nishinari, 1998), mucoadhesivity (Burgalassi et al., 1996), biocompatibility, high drug holding capacity and high thermal stability (Pongsawatmanit et al., 2006). This led to its application as an excipient in drug delivery system namely tablet (Sumathi and Ray, 2002) and in situ gelling formulations (Takahashi et al., 2002; Miyazaki et al., 2001; Suisha et al., 1998).

Centella asiatica extract is a mixture of triterpenes such as madecassic acid, asiatic acid and asiaticoside and used as wound healing agents (Cheng and Koo, 2000). The European Agency for the Evaluation of Medicinal Products Veterinary

Medicines Evaluation Unit (1998) reported that madecassic acid, asiaticoside and asiatic acid acted on fibroblast cells and equilibrated collagen fiber synthesis. The overall effects contributed to the restoration of elastic connective tissue, a reduction in fibrosis and a short in the time necessary for wound healing. The development of *Centella* extract into film attached on skin for wound healing might prolong the existence of the active substances on skin and sustained the action.

In this study, it has been aimed to develop the extraction method and to evaluate properties of extracted xyloglucan from tamarind seeds. Besides, this study also focused on development and evaluation of film formulations of extracted tamarind seed xyloglucan consisting of *Centella asiatica* extract.

The purposes of this study were:

1. To develop the extraction method of xyloglucan from tamarind seeds.
2. To evaluate properties of tamarind seed xyloglucan
3. To develop film formulations of tamarind seed xyloglucan containing *Centella asiatica* extract.
4. To evaluate properties of prepared films such as physicochemical properties, mechanical properties, *in vitro* release study, skin permeation and stability.

CHAPTER II

LITERATURE REVIEW

A. Botanical and Chemical Aspects of *Tamarindus indica* Linn.

Tamarindus indica, known as Ma-kam, is in Family Leguminosae which prefers tropical climate regions such as South East Asia, Africa and South America. Tamarind is a large tropical tree with a short massive trunk, ferny pinnate leaves, small yellow flowers and fat reddish brown pods. The tree can be 90 ft (27.4 m) high but is usually less than 50 ft (15.2 m). It has a short, stocky trunk, drooping branches and a domed umbrella shaped crown about as wide as the tree's height. The leaves are approximately 10 in (25.4 cm) length with 10-18 pairs of 1 in (2.5 cm) oblong leaflets. The flowers are about 1 in (2.5 cm) diameter, pale yellow with purple or red veins. They have five unequal lobes and borne in small drooping clusters. The velvety cinnamon brown pods are 2-6 in (5.1-15.2 cm) long, sausage shaped and constricted between the seeds. The pulp around the 8-10 seeds may be sweet but some extremely sour (Figure 1).



Figure 1 *Tamarindus indica*

Tamarind seed is covered with a black-brown husk (Figure 2). Tamarind seeds consist 30% of husk and 70% of kernel or endosperm. The husk contains 40% water soluble, 80% of which is a mixture of tannin and coloring matter. Kernel or

endosperm is white and component with 65% of non-fiber carbohydrate, 17% of protein, 7% of fat, 5-6% of crude fiber, 2-8% of ash and 4-5% of other components. The carbohydrates of seeds consist mainly of a polysaccharide composed of D-galactose, D-xylose and D-glucose in the ratio 1:2:3 (Lewis and Neelakantan, 1964).



Figure 2 Tamarind seeds and kernel of tamarind seeds

B. Chemistry, physicochemical properties and application of xyloglucan from tamarind seeds

Xyloglucan is major structural polysaccharides found in the primary cell walls of higher plants such as barley, rice, corn, onion, apple and tamarind seed, etc (Picout et al., 2003; Hoffman et al., 2005). Xyloglucans from plants are differentiated by the distribution of side chain residues and molecular weights. It has even been displayed to be different in properties such as viscosity, solubility, gelling, freeze–thaw stability and film formation (Sims et al., 1998).

1. Chemical structure of xyloglucan

Xyloglucan derived from tamarind a seed is composed of a (1-4)- β -D-glucan backbone chain which has (1-6)- α -D-xylose branches. The (1-6)- α -D-xylose branches are partially substituted by (1-2)- β -D-galactoxylose. The tamarind seed xyloglucan consists of three units of xyloglucan oligomers with heptasaccharide, octasaccharide and nanosaccharide, which have different numbers of galactose side-chains (Figure 3) (Kawasaki et al., 1999).

of suspension cultured *Nicotiana plumbaginifolia* cells, apple pomace and tamarind seeds with different structural features and molecular weights. They stated that viscous solution of tamarind seed xyloglucan displayed non-Newtonian behaviour. It has the highest molecular weight (880 kDa) and the highest viscosity among three xyloglucans. The viscosity of *Nicotiana* xyloglucan at 5% w/v and apple pomace xyloglucan at 5% w/v were almost equivalent to tamarind seed xyloglucan at 0.5% and 2% w/v, respectively. In addition, the viscosity of xyloglucan solution decreased when the temperature increased. There was no effect of pH on viscosity of three xyloglucans and stability over the acid pH range.

The toxicity and carcinogenicity of tamarind seed polysaccharide were studied in the diet to B6C3F₁ mice of both sexes for 78 weeks. This study showed that tamarind seed polysaccharide is neither toxic nor carcinogenic in mice with long-term dietary exposure (Sano et al., 1996).

Shirakawa et al. (1998) studied the changes in physiological function and properties of tamarind seed xyloglucan when it was modified by fungal β -galactosidase. The result demonstrated that the changes in solution viscosity accompanied with the removal of terminal galactose from tamarind seed xyloglucan. Xyloglucan by removing galactose residues had sol-gel transition points. It formed a gel on heating and reverted to a solution on cooling below the low temperature transition point. Subsequently, over the high temperature transition point, the gel reverted to solution again. For example, xyloglucan which a galactose removal ratio of 35%, solution changed to gel on heating at 40 °C and reverted to solution again at 80 °C. Xyloglucan which a galactose removal ratio of 58%, solution reverted to gel on heating at 5 °C and transformed to solution again at 110 °C.

In addition, tamarind seed xyloglucan forms gel at low temperature in the presence of ethanol. As a result, tamarind seed xyloglucan in 15% ethanol aqueous solution had gel-sol transition at 47 °C (Yamanaka et al., 2000).

3. Applications of Xyloglucan

Tamarind seed xyloglucan is used in food and pharmaceutical industries since its solution is very stable against heat, pH and shear. In the food industry, tamarind seed xyloglucan is widely used as a thickener, stabilizer, fat replaces, or starch modifier to improve rheological and thermal properties of many products, for example, ice cream, salad dressing, mayonnaise, noodles, stew, etc (Shirakawa and Yamatoya, 2003). Due to low stability against heat or shear, the physical properties of native starch pastes often limit commercial applications in products. Addition of hydrocolloids such as xyloglucan tamarind seed may improve textural properties and stability of native starch pastes in food products.

Pongsawatmanit et al (2006) investigated the influence of xyloglucan obtained from tamarind seed on rheological properties and thermal stability of tapioca starch. Tapioca starch and xyloglucan were prepared at different mixing ratios (10/0, 9/1, 8/2, 7/3, and 6/4) with 5% total polysaccharide concentration. The viscosity and thermal stability of these solution were determined. Consequently, the viscosity of the tapioca starch paste was lower than those of the tapioca starch and xyloglucan mixture. The tapioca starch and xyloglucan mixture gave higher apparent viscosity with increasing xyloglucan concentration. The change in the apparent viscosity with temperature of the tapioca starch alone was greater than those of the tapioca starch and xyloglucan mixture. The addition of a small amount of xyloglucan to tapioca starch might be useful to control the texture of food and to prevent the retrogradation of starch. Moreover, there were some studies on the effect of xyloglucan on rheological and thermal of corn starch and tapioca (Yoshimura et al., 1999; Temsiripong et al., 2005; Pongsawatmanit, Temsiripong and Suwonsichon, 2007) and the effect of xyloglucan on the concentration of gellan and formation of a network of gellan (Ikeda et al., 2004).

For the pharmaceutical application, xyloglucan was studied to be used as an alternative pharmaceutical excipient for sustained release. For example, xyloglucan was used to prepare mucoadhesive buccal patch, matrix tablet of both water-soluble and water insoluble drugs and in situ gelling formulations for rectal, ocular,

transdermal, intraperitoneal and oral drug delivery, it showed sustained release (Miyazaki et al., 2001; Suisha et al., 1998).

Different mucoadhesive polymers such as tamarind seed xyloglucan, polycarbophil, polyacrylic acid and xanthan gum were studied to investigate an innovative mucoadhesive controlled-release device for topical buccal drug delivery. Benzydamine and lidocaine were used as a model drugs in this study. Mucoadhesive properties of four non-medicated matrices prepared by different polymers were determined. The tamarind seed xyloglucan containing matrix was the best mucoadhesive properties. The devices containing the salts of benzydamine and the complex of lidocaine showed zero-order release kinetics *in vitro*. The patches adhered for over 8 hours to the upper gums of the volunteers, and were perfectly tolerated (Burgalassi et al., 1996).

Tamarind seed xyloglucan and crosslinking tamarind seed xyloglucan with epichlorohydrin were used to prepare the microspheres of both water-soluble drugs; such as acetaminophen, caffeine, theophylline and salicylic acid, and water insoluble drugs such as indomethacin. Releasing behaviors of these drugs were determined. About 50% of total loading of drug releases in 5, 5.5, 7 and 10 hours for caffeine, acetaminophen, theophylline and salicylic acid, respectively. The total release of indomethacin in the first 5 hours is about 10% of total load of the tablet. As a result, tamarind seed xyloglucan can be used for controlled releasing both water-soluble and water insoluble types of drugs. Crosslinking tamarind seed xyloglucan could be sustained for longer period than with tamarind seed xyloglucan (Sumathi and Ray, 2002). In addition, there was the study of controlled caffeine released from tamarind seed xyloglucan tablets and sustained release of verapamil hydrochloride (Sumathi and Ray, 2003; Kulkarni et al., 1997).

A sustained release of gel formation *in situ* following the oral administration of diluted aqueous solutions of tamarind seed xyloglucan was investigated by the *in vitro* and *in vivo* studies. Xyloglucan was modified by partially degraded by β -galactosidase in order to eliminate 44% of galactose residues. The enzyme-degraded xyloglucan could form gels at concentrations 1.0% and 1.5% w/w at 37 °C. *In vitro*,

the releasing indomethacin and diltiazem from the enzyme-degraded xyloglucan gels followed square root-time kinetics over a period of 5 hours at 37°C and pH 6.8. In vivo, plasma concentrations of indomethacin, after oral administration to rats of chilled 1% w/w aqueous solutions of the enzyme-degraded xyloglucan containing dissolved drug were determined. The release of indomethacin was sustained over a time period of at least 7 hours. Bioavailability of indomethacin from xyloglucan gel formed in situ was increased approximately threefold compared with the suspension. As a result, the enzyme-degraded xyloglucan gel had potential as vehicles for oral delivery (Kawasaki et al., 1999).

4. Xyloglucan extraction

Many methods of xyloglucan extraction were report. For example, Suttananta (1986) extracted xyloglucan from seed kernel by hot water at 92-98 °C for 60 minutes. The slurry was filtered through muslin or sieves no. 80 and was then centrifuged at 3,200 rpm for 30 minutes. The solution was precipitated by 1-1.5 volumes of ethanol. The precipitant was dried by oven at 50-60 °C for 8-12 hours and milled. A yield of approximately 30% was obtained.

In 1990, Molinarolo, Thompson and Stratton reported the extraction of xyloglucan from tamarind seed after the defatting. Then treated tamarind kernal powder (TKP) was dispersed in a small amount of distilled water prior to extraction for one-half hour in boiling distilled water. The suspension was filtered through coarse grade filter paper in a Buchner funnel and then through a layer of diatomaceous earth in a medium grade fritted glass filter funnel. The solution was precipitated by 96% ethanol and drained on cheesecloth and squeezed out to remove as much alcoholic liquid as possible. The precipitate was stirred with 50% ethanol and the liquid was squeezed out. The sample was then concentrated in vacuum to remove ethanol and then freeze dried. Approximately 33% yield was obtained.

Sumathi and Ray (2002) extracted xyloglucan from tamarind seed powder. Tamarin kernel powder was dispersed in 200 ml of cold water. The slurry was added into 800 ml of boiling water. The solution was boiled for 20 minutes under stirring

condition in a water bath. It was kept overnight so that most of the proteins and fibers settled out and was then centrifuged at 5000 rpm for 20 minutes. The supernatant was separated and was precipitated by twice volume of absolute ethanol. The precipitant was washed with absolute ethanol, diethyl ether and petroleum ether and then dried at 50-60 °C under vacuum. The dried material was ground and sieved.

Tamarind seed kernels were dissolved in water by stirring at room temperature. Subsequently, the slurry was centrifuged for 15 minutes at 8,000 rpm to remove insoluble ingredients. Isopropanol was added drop by drop to the supernatant up to a isopropanol concentration of 70 %. The precipitant was separated by centrifugation at 8,000 rpm for 10 minutes, washed by 70 % isopropanol aqueous solution, and dried in a vacuum at 500 °C for 24 hrs (Hiroshi et al., 2002).

In addition, xyloglucans were extracted by mixing tamarind seed powder with water at 25 °C. The slurry was centrifuged at 10,000 rpm for 20 minutes and the supernatant passed sequentially through Millipore filter membranes with pore sizes of 3 and 0.8 mm. Then, the solution was precipitated with two volumes of 96% ethanol and washed with acetone (Freitasa et al., 2005).

C. Spray drying technique

Spray drying is the most common industrial process for removal of solvent involving particle formation and drying such as beverages, flavors, milk, plant extracts, pharmaceuticals, plastics and polymers etc. The spray dryer system consists of a feed pump, an atomizer, an air heater, an air dispenser, a drying chamber and a system for exhausting air cleaning and powder recovery. There are three main phenomena in spray dry process as follows: (Shabde and Hoo, 2008).

1. Atomization of the liquid feed
2. Drying of the droplets once they are formed
3. Motion of the droplet to model the spray drying process

For this process, a sample such as solution, emulsion, slurry and suspension, etc, is atomized in a spray drying chamber. Heat is supplied to the liquid mixture by

passing a hot air to the liquid under controlled temperature and airflow conditions. The contact between the droplets and the hot air results in the solvent in the liquid mixture evaporates and the droplets converted into solid particles. The solid particles are continuously discharged from the drying chamber and recovered from the exhaust air using a cyclone or a bag filter.

The parameters influencing yield and powder properties such as particle size and size distribution, particle shape, moisture content and bulk density are concentration of the sample, inlet and outlet air temperatures, main air flow rate and liquid feed flow rate.

The spray drying parameters were determined in relation to particle size and the yield of the resultant powder. Chawla et al. (1994) investigated on pump speed, aspirator level, inlet temperature and the concentration of the aqueous salbutamol sulphate solution dried. The yield percentages of the spray dried material relied on the several factors such as the aspirator level, the feed concentration and the interaction between the pump and the feed concentration. An increase in any of these factors, or interacting factors, led to an increase in product yield. It was found that spray drying produced spherically shaped particles of salbutamol sulphate with a mass median diameter of 4.5 μm (laser diffraction), mean Feret's diameter (image analysis) of 1.58 μm and a mass median aerodynamic diameter of 9.7 μm (cascade impaction), i.e., particles sufficiently small in diameter for use in inhalation formulation.

Billona et al. (2000) investigated the effects of five parameters on production yields and moisture contents of spray-dried products. These factors concerned concentration of solution feed (drug concentration, colloidal silica concentration and polymer:drug ratio), inlet temperature and feed rate. Yields could be considerably increased by reducing feed rate. An increase in inlet temperature improved yields when the feed rate was high. An increase of feed rate led to higher moisture contents, especially at low inlet temperature; however, a higher inlet temperature promoted a decrease of residual moisture. The total feed concentration (drug concentration and colloidal silica concentration) also greatly affected yields and

moisture content. When the concentration of the solution feed increased, the drying process is greater. Polymer:drug ratio had significant effect of the formulations.

The effect of process variables on the degradation and physical properties of spray dried insulin intended for inhalation was investigated by [Stahl et al. \(2002\)](#).

Factorial experimental design was applied to evaluate the effects of feed flow rate, nozzle gas flow rate, inlet air temperature and aspirator capacity on the degradation and physical properties of spray dried insulin intended for inhalation. It was found that the degradation of insulin was not dependent on the nozzle gas flow rate. However, a decrease in the nozzle flow resulted in an increase in the yield. They also stated that the atomization energy could be decreased by decreasing nozzle flow and thus producing enlarged droplets. It was also found that larger particles dried by these droplets enable these particles to be easily captured through the centrifugal force in the cyclone. Not only increasing aspirator capacity but also increasing inlet air temperature led to a decrease in moisture content as a result of higher efficient drying caused by an increase in the supplies of heat energy. This relationship between moisture content and outlet air temperature was in agreement with the spray-dried β -galactosidase study of [Broadhead et al. \(1994\)](#). Due to the reduction of the outlet air temperature caused by increasing feed flow, drying capacity was lower but moisture content in the powder product was higher. The investigators also reported that an increase in inlet air temperature led to an expansion of the particle size.

Advantages of spray drying ([Master, 1979](#)):

1. A single-step operation from liquid feed to dry product.
2. An ability to operate in applications that range from aseptic pharmaceutical processing to ceramic powder production.
3. A potential design to virtually any capacity required.
4. A constant powder quality constant during the entire run of the dryer.
5. A continuous and adaptable operation for full automatic control.
6. A great variety of spray dryer designs meeting various product specifications.
7. A possible application for both heat-resistant and heat sensitive products.

8. An durable process even though the abrasive corrosive, flammable, explosive or toxic feedstock if the pump working
9. An potential application for the different of solution feedstock such as slurry, paste, gel, suspension or melt form.
10. A characteristic particle from the product a high bulk density and, in turn, rapid dissolution (large surface area)
11. A non-contraction metal surfaces until dried, reducing corrosion problems.
12. A dry product specifications meeting through dryer design and operational flexibility.

D. Structure of skin

The skin is the largest organ of the human body, accounting for approximately 10% of total the body mass of an average person, and it covers an average area of 1.7 m². Its function is to prevent loss of water and other components of the body to the environment and protect the body from a variety of environmental insults. The skin also has important immune and sensory functions, helps to regulate body temperature, and synthesizes vitamin. The skin composes of 70% water, 25% protein and 2% lipids. The remainder includes trace minerals, nucleic acids, glycosoaminoglycans, proteoglycans and numerous other chemicals. The skin consists of three main layers: epidermis, dermis and subcutaneous tissue as depicted in Figure 4.

The viable epidermis is the topmost layer of the skin. It is a complex multiply-layered membrane, approximately 100-150 µm thick. About 95% of the viable epidermis layer is composed of keratinocytes. Other cell types in its are melanocytes, Langerhans cells and Merkel cells (mechanoreceptors). The viable epidermis contains four layers.

1. Stratum germinativum or basal layer
2. Stratum spinosum or spinous layer or prickly layer
3. Stratum granulosum or granular layer
4. Stratum lucidum

The stratum corneum or the horny layer is the top layer of the skin, where its thickness depends on the region of the body and can be from about 10 microns to several hundred microns. Furthermore, it is consisted of layers of dead, flattened

keratinocytes by surrounding a lipid matrix. The lipid matrix is jointly active as a brick-and-mortar system which has a difficulty of penetrates. It is interesting to note that the stratum corneum is a majority of barrier to transdermic delivery.

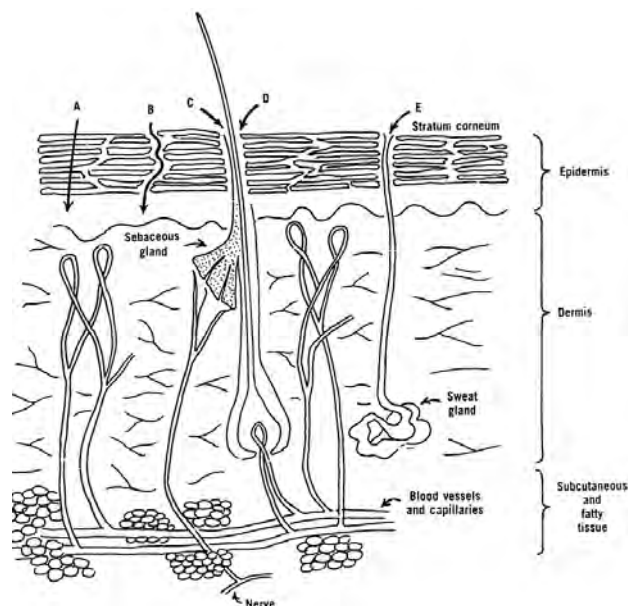


Figure 4 Structure of human skin in crosssection

The central layer of the skin, the thickest of the skin layers, 3-5 mm thick, being location between the epidermis and subcutaneous tissue is called as the dermis or courium. It has a composition of a matrix of connective tissue woven from several fibrous proteins; such as collagen, elastin and reticulin, that tightly surround by an amorphous ground substance of mucopolysaccharide. Moreover, there also are several compositions of the dermis such as sebaceous glands, sweat glands, hair follicles and a small number of nerve and muscle cells. The supply of blood maintains the dermal concentration of a permeated drug as a very low level, the essential driving force for transdermal permeation is contributed by a consequence of different concentration across the epidermis.

Eventually, the deepest layer of the skin being located under the dermis and containing mostly of fat cells is called as subcutaneous tissue. There are several advantages of subcutaneous tissue such as maintenance of regulated temperature,

contribution of nutritional support and mechanic protection , carrying the principal blood vessels and nerving the skin and may contain sensory pressure organs (Williams, 2003; Wille, 2006).

E. Transdermal drug delivery system

Alternatively, the delivery of systemically acting drugs can apply the skin to deliver transdermal drugs. There are several advantages for using skin as an alternative route over oral drug administration (Wang et al., 2002).

1. A circumvention of a variety of influences on gastro-intestinal absorption such as pH, food intake and gastro-intestinal motility.
2. A circumvention of the hepatic metabolism, which be suitable for drugs with a low bioavailability.
3. A delivery of transdermic drug resulting in proving a constant, controlling drug input, decreasing the variation in drug plasma levels, reducing the side effects particularly of drugs with a narrow therapeutic window.
4. An increase in patient compliance.
5. A quick termination of therapy by simple removal of the system from the skin.

There are two traditional designs of transdermic drug delivery devices (Tyle, 1988).

1. Reservoir-type devices

The drug in a reservoir-type system is kept in a reservoir from its diffusion via a rate-limiting membrane to the site of absorption. This form of system can get a benefit, which is the near-constant release rate of drug from device, when the stratum corneum is not the principal rate-limiting barrier for the diffusion of drugs and rate control from the desirable device. There are four main compositions of the drug in a reservoir-type system; backing membrane, reservoir of drug, rate limiting membrane and adhesive layer. The rate-limiting membrane is microporous or nonporous membrane. There are several methods of a control of a releasing rate such as varying the polymer ratios, drug reservoir formulation, permeability coefficient of the rate

controlling membrane and thickness of the adhesive. Many designs in this system are appearances such as

- a). Hercon device
- b). Multireservoir rate-limiting devices
- c). Devices with rate-limiting adhesive layer
- d). Drug reservoir gradient transdermal device
- e). Microencapsulated drug reservoir-type devices
- f). Transdermal devices with Hollow reservoir etc.

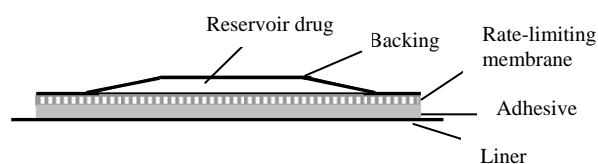


Figure 5 A reservoir-type transdermal delivery device

2. Matrix-type transdermal devices

In a matrix-type of devices, the drug is a uniform dispersion all through a hydrophilic or lipophilic polymer matrix. Subsequently, the hydrophilic or the lipophilic polymer matrix is cured into a polymeric disk of predetermined thickness and surface area. The matrix is subsequently glued to aluminum foil sealed to drug impermeable backing via an absorbent pad. Occasionally, the polymer matrix is not only a reservoir of drug but also adhesive. There are several factors influenced on the release rate of polymer-matrix system such as the initial drug loading dose, solubility and diffusion coefficient of drug in polymer matrix.

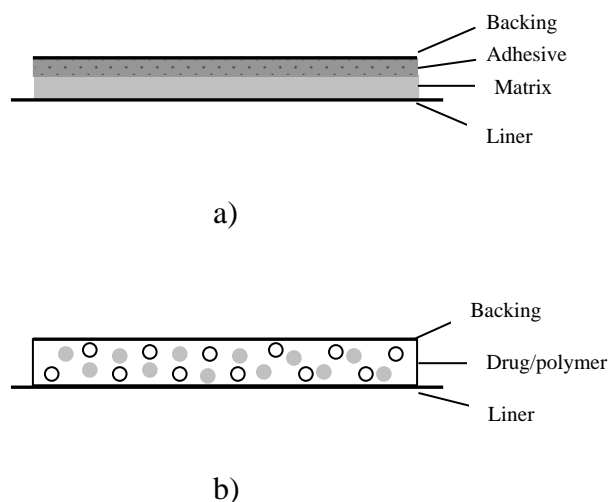


Figure 6 a) A typical matrix-type transdermal delivery device

b) An adhesive matrix device

Furthermore, ‘microreservoir or microsealed transdermal delivery device’ is the hybrid of the reservoir and matrix types of system. The preparation of an aqueous suspension of drug for this system is in a water-soluble polymer. The dispersion of the suspension into lipid-soluble polymer with high-speed-shear force is the formation of microscopic spherical reservoir with the drug entrapped. Instantly, the system is the crosslink of the addition of polymeric crosslinking agents and the formation of matrix, which is attachment to an aluminum foil plate at the back. There is a peripheral adhesive ring in the system (Mathiowitz et al., 1999; Hadgraft and Guy, 2002).

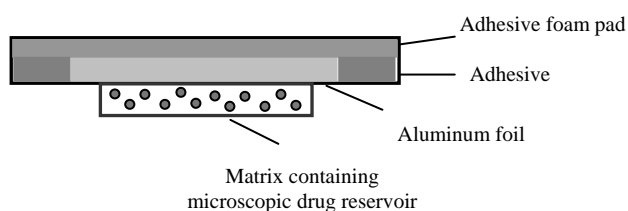


Figure 7 A microreservoir transdermal delivery device.

F. Wound healing

Wound healing is necessarily applied to remove invaded pathogen from the damaged tissue of the body and completely or partially remodel injured tissue. The phases of normal wound healing consist of hemostasis, inflammation, proliferation, and remodeling.

Initially, tissue injury clearly responds to the wound of devitalized tissue and foreign material and then the stage for subsequent tissue healing and regeneration are formed. The initial vascular responds to both a brief and transient period are vasoconstriction and hemostasis. A 5-10 minute period of intense vasoconstriction is subsequent to active vasodilation in company with increased capillary permeability. An aggregation of platelets within a fibrin clot generate a variety of growth factors and cytokines, by setting the stage for an orderly series of events resulting in tissue repair.

The second phase of wound healing is the inflammatory phase which represents as erythema, swelling, and warmth. It is frequently liked to the pain. An increase in vascular permeability, which leads to migration of neutrophils and monocytes into the surrounding tissue, is affected from inflammation. The first line prevention of infection is contributed by the neutrophils engulfing debris and microorganisms. In case of non-contamination after the first few days post-injury, neutrophil migration ends. Furthermore, in case of persistiveness of acute inflammatory phase as result of wound hypoxia, the release of hypoxia, infection, nutritional deficiencies, medication use, or other factors is to the patient's immune response, possibly interfering with the late inflammatory phase. The convention of monocytes in the tissue to macrophages, which is used for a digestion and a kill of bacterial pathogens, scavenged tissue debris and an elimination of remain neutrophils, is in the late inflammatory phase. In order to transit wound inflammation of macrophages to wound repair, a variety of chemotactic and growth factors including the stimulation of cell migration, proliferation, and formation of the tissue matrix, are repaired.

The subsequent proliferative phase is dependent on the formation of granulation tissue and epithelialization. The size of the wound also has effect on its period. The stimulation of the migration and activation of wound fibroblasts for the production of a variety of substances essential to wound repair, involving glycosaminoglycans (mainly hyaluronic acid, chondroitin- 4-sulfate, dermatan sulfate, and heparan sulfate) and collagen, is released by chemotactic and growth factors. The formation of an amorphous, gel-like connective tissue matrix is necessity for cell migration. It is essential that new capillary growth associated with the advancing fibroblasts into the wound for the contribution of metabolic needs. Both vascular integrity and strength of new capillary beds has been a responsibility to improper cross-linkage of collagen fibers. Near the beginning of the proliferation phase fibroblast activity is limitable to cellular replication and migration. Approximately the third day after wounding the growing mass of fibroblast cells start for synthesizing and secreting determined quantities of collagen. A continue rise in collagen levels last approximately three weeks. The tensile strength of the wound is evaluated by the quantities of secreted collagen over this approximately three weeks.

Wound remodeling, involved by a reorganization of new collagen fibers, a formation of more organized lattice structure which continue progress for an increase in wound tensile strength, is the final phase of wound healing. The remodeling process lasts no more than 2 years. It is interesting to note that 40-70 percent of the strength of undamaged tissue can be achieved in four weeks (MacKay and Miller, 2003).

G. Botanical, Chemical and Pharmacological Aspects of *Centella asiatica* (Linn.)

1. Botanical aspects of *Centella asiatica* (Linn.)

Centella asiatica (Linn.) of the family Apiaceae (Umbelliferae) is commonly found in parts of India, Asia and the Middle East. It is known as Buabok, Pegaga, Luei Gong Gen, Tung Chain, Vallarai and Daun Kaki Kuda.

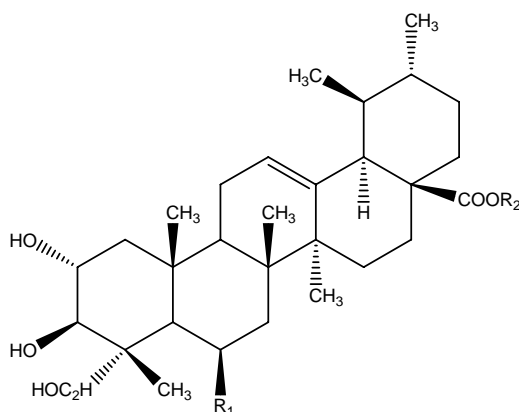
Centella asiatica (Linn.) is a perennial, herbaceous creeper growing up to 30 cm in height with fan-shaped leaves. The stems are slender, creeping stolons, green to reddish green in color. It has long-stalked, green, reniform leaves with rounded apices which have smooth texture with palmately netted veins. The leaves are borne on pericladial petioles, around 20 cm. The rootstock consists of rhizomes, growing vertically down. They are creamish in color and covered with root hairs. The flowers are pinkish to red in color, born in small, rounded bunches (umbels) near the surface of the soil. Each flower is partly enclosed in two green bracts. The hermaphrodite flowers are minute in size (less than 3 mm), with 5-6 corolla lobes per flower. Each flower bears five stamens and two styles (Figure 8).



Figure 8 *Centella asiatica* (Linn.) Urban

2. Chemical components of *Centella asiatica* (Linn.)

Centella asiatica (Linn.) contains a wide range of other substances such as triterpenoid glycosides (saponins) , phytosterols and a volatile oil consisting of vallerin, camphor, cineole and an unidentified terpene acetate. The substances of therapeutic interest are the saponin-containing triterpene acids and their sugar esters, the most important being asiatic acid, madecassic acid, asiaticoside and madecassoside (Figure 9) (Shim et al., 1996; Lawrence, 1967).



Compound	R ₁	R ₂
Asiaticoside	H	glu-glu-rham
Madecassoside	OH	glu-glu-rham
Asiatic acid	H	H
Madecassic acid	OH	H

Figure 9 Structures of the triterpenoids from *Centella asiatica* (Linn.)

3. Pharmacological activities of *Centella asiatica* (Linn.)

Centella asiatica has been used for hundreds of years as the traditional medicine of many asiatic countries to treat dermatological conditions. It is used to support faster healing of small wounds, chaps and scratches, superficial burns and, as an oral preparation, for atonic wounds and hypertrophic healing. *Centella* also has been used traditionally as an anti-inflammatory, particularly for eczema, and also for minor itching and insect bites. The active ingredients of *Centella asiatica* which claimed to possess wound healing properties are madecassic acid, asiaticoside and asiatic acid (The European Agency for the Evaluation of Medicinal Products Veterinary Medicines Evaluation unit, 1998). They promoted fibroblast proliferation and type-I collagen synthesis. The overall effects contributed to the restoration of elastic connective tissue tissue, a reduction in fibrosis and a short in the time necessary for wound healing (Lu et al., 2004).

Ether undefined alcohol or aqueous extracts or one of the following extracts; TECA, TTFCA, or TTF are mostly applied for clinical studies of *Centella asiatica*. The extracts TECA (titrated extract of *Centella asiatica*) and TTFCA (total triterpenoid fraction of *Centella asiatica*) combine a comprisal of asiatic acid (30%), madecassic acid (30%), and asiaticoside (40%). The centella extract TTF (total triterpenic fraction) is a comprisal of asiatic acid and madecassic acid (60%) in a doubt definition of ratio, in association with asiaticoside (40%) (Brinkhaus et al., 2000). Centella has potentially developed connective tissue integrity by elevating antioxidant levels in wound healing and enhancing capillary permeability (Shukla et al., 1999; Belcaro, Grimaldi and Guidi, 1990).

Shukla et al. (1999) studied the effect of asiaticoside on the wound healing in guinea pigs punch and streptozotocin diabetic rats. The 0.2% asiaticoside solution in guinea pig punch wounds produced 56% increase in hydroxyproline, 57% increase in tensile strength, increased collagen content and better epithelisation. The 0.4% asiaticoside solution in streptozotocin diabetic rats increased hydroxyproline content, tensile strength, collagen content and epithelisation thereby facilitating the healing. These results indicated that asiaticoside exhibits significant wound healing activity in normal as well as delayed healing models and was the main active constituent of *Centella asiatica*.

The investigation of *Centella* extract affecting on the protection of ethanol induced gastric lesions in rats. The 50% ethanol in the gastric ex-vivo chamber model was used the reduction of gastric transmucosal potential difference and an acceleration of its recovery resulted from *Centella* extract. Before a significant inhibition of gastric lesions formation (58% to 82% reduction) by ethanol administration and a reduce in mucosal myeloperoxidase (MPO) activity in a dose dependent manner, Oral administration of *Centella* extract (50 mg/kg, 0.25 g/kg and 0.50 g/kg) was applied. Consequently, it was suggested by Cheng and Koo (2000) that the prevention of ethanol by *Centella* extract induced gastric mucosal lesions by strengthening the mucosal barrier and a decrease in the damaging effects of free radicals.

The potentiality of the wound-healing ethanolic extract of *Centella asiatica* in both normal and dexamethasone suppressing wound healing was investigated by Shetty et al. (2006). Wistar albino rats were incision, excision, and dead space wounds models. A significant increase in the wound breaking strength in incision wound model compared with controls ($P < 0.001$) resulted from the extract of *Centella asiatica*. It was found that the extract-treated wounds epithelize faster, and a significant increase in the rate of wound contraction was apparent when compared with control wounds ($P < 0.001$). The content of wet and dry granulation tissue weights, granulation tissue breaking strength, and hydroxyproline in a dead space wound model resulted in an increase in statistically significant levels.

The extract of *Centella asiatica* affected on attenuating the known effects of dexamethasone healing in all wound models ($P < 0.001$, $P < 0.05$). As a result, wound healing is significantly promoted by the extract of *Centella asiatica*. This extract has ability for defeating the wound-healing suppressing action of dexamethasone in a rat model.

CHAPTER III

MATERIALS AND METHODS

Materials

1. Absolute Ethanol, AR grade (Merck, Germany)
2. Acetonitrile, HPLC grade (Lab Scan Co., Ltd., Thailand)
3. Acetic acid glacial 100% (Lab Scan Co., Ltd., Thailand, lot no.A8401E)
4. Cupper sulfate (Ajax, Finechem, lot no. A171)
5. Bovine serum albumin (BSA) (Sigma-aldrich, Inc., Germany)
6. Dipotassium hydrogen phosphate (Merck, lot no. A687601601)
7. Disodium carbonate (Ajax, Finechem, lot no. A463)
8. Ethylenediaminetetra acetic acid calcium disodium salt (Sigma-aldrich, Inc., USA, lot no. ED2SC)
9. Folin-Ciocalteu reagent (Merck, Germany, lot no. OC683903)
10. Glycerin (Srichand United Dispensary Co., Ltd., Thailand)
11. Hexane (Mallinckrodt Baker, Inc., USA)
12. Petroleum ether (Lab Scan Co., Ltd, Thailand)
13. Phospholic acid (J.T. Baker, USA, lot no. 0260-03A262673045)
14. Potassium dihydrogen phosphate (Merck, Germany, lot no. A315973 127))
15. Methanol, HPLC grade (Lab Scan Co., Ltd., Thailand)
16. Mineral oil (Aketong chemical co., Ltd, Thailand)
17. Propylene glycol (Srichand United Dispensary Co., Ltd., Thailand)
18. Sepicide[®] HB (ADINOP, Thailand, lot no. T70211)
19. Sodium chloride (Merck, Germany, lot no.K32104204 324)
20. Sodium dihydrogen phosphate, anhydrous (Asia Pacific Chemicals Limited, batch no. F2F136)
21. Sodium hydrogen phosphate (APS Finechem, batch no.FOJ067)
22. Sodium hydroxide (Mallinckrodt Chemical, Mexico, lot no.7708MVHV)
23. Sodium potassium tartrate (Farmitalia Carlo Erba)
24. 70% Sorbitol solution (Srichand United Dispensary Co., Ltd., Thailand)
25. Standard asiaticoside 90% (Guangxi Chemical Corporation, China)

26. Standard triamcinolone acetonide 99.86% (RCV, lot no. 7629/M2)
27. Standard xyloglucan (Megazyme International Ireland Ltd, Ireland, lot no. 00401)
28. Tamarind seed
29. Titrated extract of *Centella asiatica* (TECA) (Guangxi Chemical Import and Export Corporation, China, batch no. 050523)
30. Tween 80 (Srichand United Dispensary Co., Ltd., Thailand)

Apparatuses

1. Analytical balance (Model AX105, Mettler Toledo, Switzerland)
2. Centrifuge (Hitachi himac CR20B3, Japan)
3. Differential scanning calorimeter (DSC822^c, Mettler Toledo, Switzerland)
4. Disposable syringe filter nylon 13 mm, 0.45 μm (Chrom Tech, USA)
5. Dry cabinet (Model GH-197, Ampore House, Taiwan)
6. High performance liquid chromatography system
 - Automatic sample injector (SIL-10A, Shimadzu, Japan)
 - Communications bus module (CBM-10A, Shimadzu, Japan)
 - Column (Alltima HP C18, 5 μm , 150mm x 4.6mm, lot no.3461)
 - Column (Sugar Pak I, 6.5mm x 300mm, lot no.002437211A)
 - Liquid chromatograph pump (LC-10AD, Shimadzu, Japan)
 - Precolumn (μ Bondapak C18, 10 μm , 125 A^o, Water Corporation, Ireland)
 - Precolumn (Sugar-PakTM II, Water Corporation, Ireland)
 - RI detector (RID-10A, Shimadzu, Japan)
 - UV-VIS detector (SPD-10A, Shimadzu, Japan)
7. Homogenizer (Model EURO-D, Memmert, Germany)
8. Modified Franz Diffusion cells (Crown Glass Company, USA)
9. Magnetic stirrer (Model RCT basic, KIKA[®] Works Guangzhou, China)
10. Moisture analyzer balance (Model HB43, Mettler Toledo, Switzerland)
11. pH meter (Orion model 420A, Orion Research Inc., USA)
12. Rotary evaporator (Buchi heating bath B-490, Switzerland)
13. Scanning electron microscope (Model JSM-T220A, Jeol, Japan)
14. Sonicator (Model TP680DH, Elma, Germany)

15. Spray dryer (Model SD-06, Labplant, Ltd., UK)
16. Spray dryer B-290 (Buchi mini, Switzerland)
17. Soxhlet extraction (Chatcharee holding Co., Ltd, Thailand)
18. Stability cabinet (Eurotherm Axyos, Germany)
19. Stopwatch (Heuer, Switzerland)
20. Ultrasonicator (Crest Ultrasonics, Malaysia)
21. Universal tensiometer (Tinius olsen, Model H5KS 1509)
22. UV-Visible Spectrophotometer (UV-1601, Shimadzu, Japan)
23. Viscometer (RotoVisco RV1, Germany)
24. Vortex mixer (Vortex Ginies-2, Scientific Industries, USA)
25. Water bath (Model WB22, Becthai Co., Ltd., Thailand)
26. X-ray diffractometer (Model JDX-3530, Jeol, Japan)

Methods

A. Investigation of xyloglucan extraction and preparation of xyloglucan powder from tamarind seeds

1. Preparation of tamarind seed powder

Tamarind seeds were soaked in water for 2-3 days. The seed embryo was manually removed and then they were dried under sunlight. The dried mass were milled and sieved.

2. Xyloglucan extraction process

Generally, the extraction of xyloglucan was composed of two processes as follows:

2.1 Defatting process with hexane

The extraction of fat by hexane might be done with either mixing hexane directly with dried tamarind seed powder or mixing hexane with slurry of tamarind seed powder in water.

2.2 The sedimentation by centrifugation

The slurry of defatted tamarind seed powder in water might be centrifuged to sediment undissolved fraction of the powder either immediately or left standing overnight.

Thus, four methods of xyloglucan extraction were designed and investigated as depicted in Figure 10.

Method I

Tamarind seed powder was firstly soaked with hexane overnight by packing in a percolator. The percolate was slowly collected on the next day. Then, the powder was removed from the percolator and dried in a hot air oven under 60°C. Thirty grams of dried powder were mixed with 60 volumes of distilled water to make slurry using a homogenizer for 90 min at 90°C (Somsiri, 1997). The slurry was then centrifuged at 12,000 rpm for 30 min at 25°C. The supernatant liquid was removed for the spray drying.

Method II

Tamarind seed powder was firstly soaked with hexane overnight by packing in a percolator. The percolate was slowly collected on the next day. Then, the powder was removed from the percolator and dried in a hot air oven under 60°C. Thirty grams of dried powder were mixed with 60 volumes of distilled water to make slurry using a homogenizer for 90 min at 90°C. The slurry was left standing overnight and then centrifuged at 12,000 rpm for 30 min at 25°C. The supernatant liquid was removed for the spray drying.

Method III

Thirty grams of tamarind seed powder were mixed with 60 volumes of distilled water to make slurry using a homogenizer for 90 min at 90°C. The extraction of fat was performed by the addition of hexane in triplicate. The slurry was then centrifuged at 12,000 rpm for 30 min at 25°C. The supernatant liquid was removed for the spray drying.

Method IV

Thirty grams of tamarind seed powder were mixed with 60 volumes of distilled water to make slurry using a homogenizer for 90 min at 90°C. The extraction of fat was performed by the addition of hexane in triplicate. The slurry was left standing overnight and then centrifuged at 12,000 rpm for 30 min at 25°C. The supernatant liquid was removed for the spray drying.

3. Spray drying condition

The supernatant solution was dried in spray dryer (SD-06, Labplant, Ltd., UK) (Figure 11) at a condition of inlet temperature of $160\pm 2^\circ\text{C}$, feed rate 167.17 ml per hour (pump = 2), spray air flow 300 cubic meter per hour (fan = 50) and slow deblocker.

The collected xyloglucan spray dried powders prepared under different methods of xyloglucan extraction (Method I-IV) were characterized and compared.

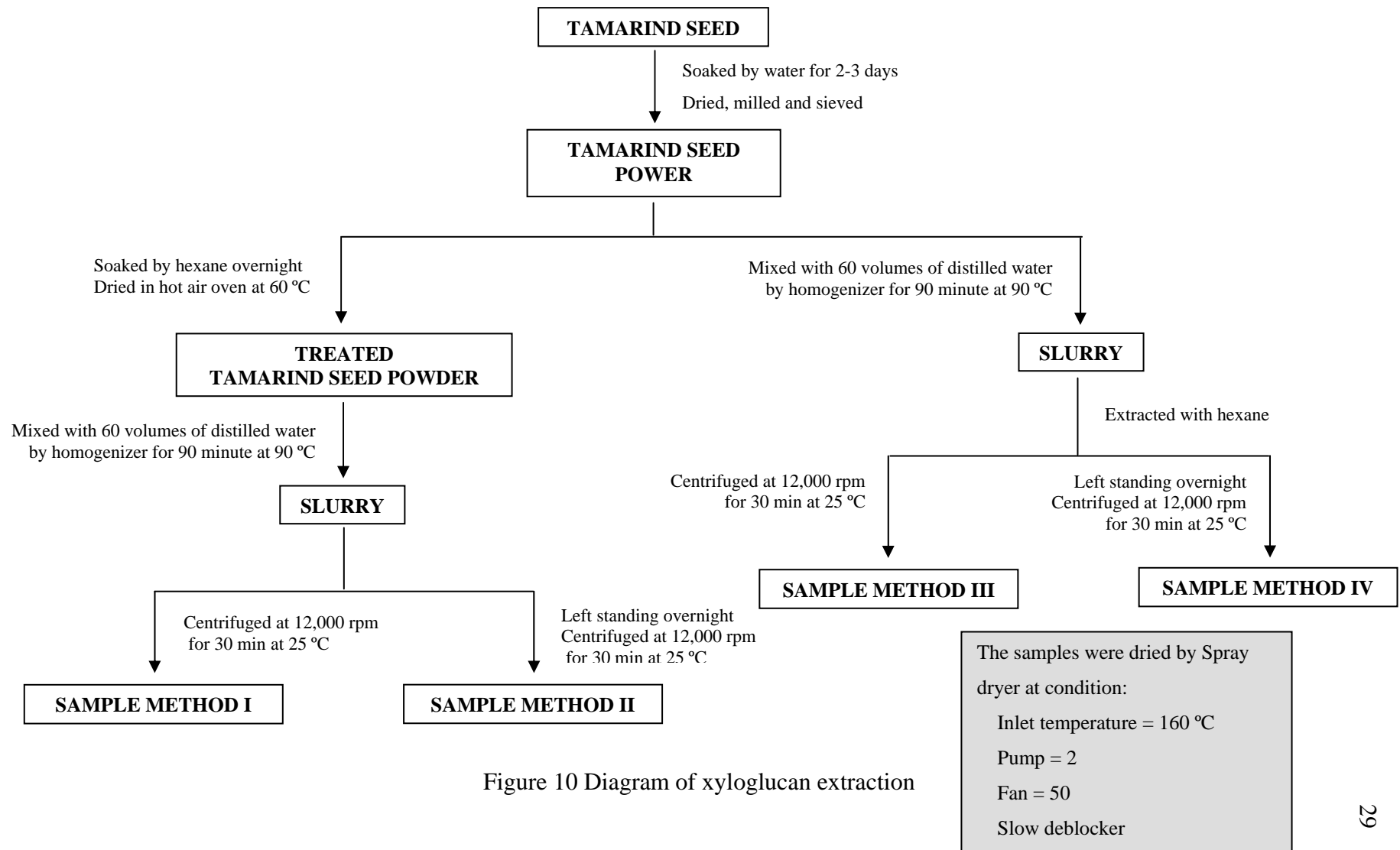


Figure 10 Diagram of xyloglucan extraction



Figure 11 Spray dryer (Model SD-06, Labplant, Ltd., UK)

B. Characterization of xyloglucan spray dried powder from Tamarind seeds.

To determine the appropriate method for the xyloglucan extraction, the xyloglucan spray dried powders prepared by four different methods of defatting and sedimentation were studied.

1. Percentage yield

The calculation of percentage yield (w/w) was the weight of the dried powder recovered from collecting chamber divided by the sum of the initial weight of tamarind seed powder and multiplied with 100.

2. Xyloglucan content

The determination of xyloglucan content of xyloglucan spray dried powder was performed by high performance liquid chromatography (HPLC), which was developed in this investigation.

2.1 Chromatographic Condition

The chromatographic conditions for the analysis of active constituents from xyloglucan were as follows (modified from Megazyme International Ireland Ltd):

Column	:	Sugar Pak I [®] 6.5 mm x 300 mm
Precolumn	:	μBondapack C18, 10 μm, 125Å°
Mobile phase	:	Ultra pure water
Injection volume	:	100 μl
Flow rate	:	0.6 ml/min
Detector	:	RI detector
Temperature	:	80 °C
Runtime	:	15 min

The mobile phase was freshly prepared, filtered through 0.45 μm membrane filter and then degassed by sonication for 30 min before using.

2.2 Standard Solution

- Preparation of standard stock solutions

The 125 mg of xyloglucan were accurately weighed and transferred into a 25 ml volumetric flask, ultrapure water was used to dilute and adjust to volume. The stock solution had the final concentration of xyloglucan of 5000 μg/ml.

- Preparation of standard solutions

The solutions of 400, 500, 600, 700, 800, 900 μl of xyloglucan standard stock solution were pipetted and added into 5 ml volumetric flasks. The dilution to volume with ultra pure water gave the final concentrations of 400, 500, 600, 700, 800, 900 μg/ml of xyloglucan, respectively.

The standard solutions were freshly prepared and used for the HPLC determination. As a result, the standard curve between concentration and peak area was plotted.

2.3 Validation of the HPLC method

The analytical parameters used in the assay validation of the HPLC assay method were specificity, linearity, accuracy and precision.

2.3.1 Specificity

The specificity of the method was determined by comparing the test results from analyses of xyloglucan in ethanol with standard solutions. Under the chromatographic conditions used, the peak of xyloglucan must be completely separated from and not be interfered by the peaks of ethanol.

2.3.2 Linearity

The linearity was determined from the coefficient of determination (R^2). Six concentrations of standard solutions and three replicates of each concentration were prepared and analyzed. The relation between the peak area and concentrations were plotted and the least square linear regressions were calculated.

2.3.3 Accuracy

The accuracy of an analytical method is the closeness of test results obtained by that method to the true value. Five sets of three concentrations (low, medium, high) of xyloglucan at 450, 650, 850 $\mu\text{g/ml}$ were prepared and analyzed, respectively. The accuracy of the method was determined from the percentage of recovery. The percentage of recovery of each concentration was calculated from the estimated concentration to know concentration multiplied by 100.

2.3.4 Precision

a) Within run precision

The within run precision was determined by analyzed five sets of three concentrations (low, medium, high) of xyloglucan at 450, 650, 850 $\mu\text{g/ml}$ in the same run. Peak area of xyloglucan was calculated and the percent of coefficient of variation (%CV) of each concentration was determined.

b) Between run precision

The precision during the operation run was determined by analyzing three concentrations (low, medium, high) of xyloglucan at 450, 650, 850 $\mu\text{g/ml}$ on five different runs. Peak area of xyloglucan was calculated and the percent of coefficient of variation of each concentration was determined.

Acceptance criteria:

For accuracy, the percentage of recovery should be within 98-102% of each nominal concentration, whereas the percent coefficient of variation for both within run precision and between run precision should be less than 2%.

The percentage xyloglucan content (w/w) was calculated as the amount of xyloglucan divided by the sum of the initial weight of tamarind seed powder and multiplied with 100

3. Total protein content

The determination of protein content in xyloglucan spray dried powder prepared from four extraction methods was performed by Lowry's method. Lowry's method for total protein is one of the most common colorimetric assays. This procedure is particularly sensitive because it employs two color forming reactions. It uses the Biuret reaction in which Cu^{2+} (in the presence of base) reacts with the peptide bond to give a deep blue color. In addition, Folin-Ciocalteu reagent, in which a complex mixture of inorganic salts reacts with tyrosine and tryptophan residues bovine serum albumin (BSA), was used as standard protein.

3.1 Standard Solution**Preparation of standard BSA stock solutions**

The 20 mg parts of BSA were accurately weighed and transferred into a 10 ml volumetric flask, diluted and adjusted to volume with ultrapure water. The stock solutions had the final concentrations of BSA of 2000 $\mu\text{g/ml}$.

The solutions of 25, 50, 75, 100, 125, 150 μl of BSA standard stock solution were added into glass tubes. The dilution to volume with ultrapure water gave final concentrations of 50, 100, 150, 200, 250, 300 $\mu\text{g/ml}$ of BSA, respectively.

The standard solutions were analyzed spectrophotometrically at 550 nm. The standard curve was plotted between concentration and absorbance.

3.2 Validation of the protein assay method

The analytical parameters were applied in the assay validation for linearity, accuracy and precision of spectrophotometric assay.

3.2.1 Linearity

Three sets of six concentrations of standard solutions ranging from 50 to 300 $\mu\text{g/ml}$. Linear regression analysis of the absorbance versus their concentrations was performed. The linearity was determined from the coefficient of determination (R^2).

3.2.2 Accuracy

The accuracy of an analytical method is the closeness of test results obtained by that method to the true value. The accuracy of the method was determined from the percentage of recovery. Five sets of three concentrations (low, medium, high) of BSA at 80, 160, 240 $\mu\text{g/ml}$ were prepared and analyzed, respectively. The percentage of recovery of each concentration was calculated from the estimated concentration to know concentration multiplied by 100.

3.2.3 Precision

a) Within run precision

The within run precision was determined by analyzing five sets of three concentrations of BSA at 80, 160, 240 $\mu\text{g/ml}$ in the same run. Absorbances of BSA were calculated and the percent of coefficient of variation (%CV) of each concentration was determined.

b) Between run precision

The precision during the operation run was determined by analyzing three concentrations of BSA at 80, 160, 240 $\mu\text{g/ml}$ on five different runs. Absorbance of BSA was calculated and the percent of coefficient of variation of each concentration was determined.

Acceptance criteria:

For accuracy, the percentage of recovery should be within 85-115% of each nominal concentration, whereas the percent coefficient of variation for both within run precision and between run precision should be less than 15%.

4. Fat content

The assay of fat content in xyloglucan spray dried powder was performed by AOAC.920.39. Amount of fat was calculated by the increased weight of flask multiplied with 100.

One gram of xyloglucan spray dried powder was packed in a filter paper and extracted with 300 ml of petroleum ether for 3 hour by soxhlet extraction (Figure 12). The petroleum ether extract was collected and evaporated under vacuum by rotary evaporator. The percentage fat content was calculated as the amount of fat, divided by the initial weight of tamarind seed powder and multiplied with 100.



Figure 12 Soxhlet extraction

5. Moisture content

A sample of xyloglucan spray dried powder was accurately weighed on the pan of moisture analyzer (Model HB43, Mettler Toledo, Switzerland). The temperature was set at 105°C and the maintainable constant weight for 20 s was detected. The sample was exposed to a halogen lamp until a constant weight was

obtained. The percentage moisture content was calculated automatically. The mean and standard deviation of three determinations were calculated.

6. Powder topography by scanning electron microscopy

The morphological feature of xyloglucan spray dried powder was displayed using scanning electron microscope (SEM), (JSM-T220A, Jeol, Japan). Powder samples were mounted onto aluminum stubs using double-sides adhesive tape and then sputter coated with a thin layer of gold before examination. The samples were imaged using a 15 kv electron beam. The magnifications of the photomicrographs of powder were $\times 500$ and $\times 2000$.

C. Optimization of spray drying condition

From the investigation of xyloglucan extraction method in topic B, the method I was selected. The spray drying solution was prepared from 600 grams of tamarind seed powder, the method was shown under method I. Sepicide[®] HB was added to the solution with the concentration of 0.5% w/v for preservation action. The solution was divided into 20 equal parts and kept frozen. The frozen was thawed at room temperature before spray drying process.

1. Preparation of spray drying solution

A Spray dryer B-290 (Buchi Mini, Switzerland) was used for the preparation of spray dried powder (Figure 13). The operating parameters were set with the feed rate of 10% and nozzle size of 0.7 mm. The spray drying solution was controlled at 37 °C through spray drying process. The inlet temperature and aspirator rate were set according to the experiment design. The resulting spray dried powders were collected and kept away from moisture until further investigations.



Figure 13 Spray dryer B-290 (Buchi Mini, Switzerland)

2. Optimization design: face centered design (FCD)

A face centered design is a central composite design with alpha equals to 1. For this purpose, a face centered design with two factors at two levels was used to study the response surface and to determine the combination of variables would produce the maximal yield and the minimal moisture content. The combination effect of inlet temperature and aspirator rate was studied by response surface methodology. The response surface plots indicated the effects of the factors on the percentage yield and percentage moisture content responses at each level of the factors. The face centered design in this study was 13 runs. The design matrix with responses was given in Table 1.

Table 1 A face central design of two parameters

Code	Parameters	
	Inlet temperature (°C)	Aspirator rate (%)
C1	(-) 120	(-) 80
C2	(+) 200	(-) 80
C3	(-) 120	(+) 100
C4	(+) 200	(+) 100
C5	(-) 120	(0) 90
C6	(+) 200	(0) 90
C7	(0) 160	(-) 80
C8	(0) 160	(+) 100
C9	(0) 160	(0) 90
C10	(0) 160	(0) 90
C11	(0) 160	(0) 90
C12	(0) 160	(0) 90
C13	(0) 160	(0) 90

Statistical analysis and a graphical optimization were performed using Design-Expert version 7.1 statistical software. The method basically consisted of overlaying the curves of the models according to the criteria imposed. The selection of conditions to overlay plot were range from 120-200 °C of inlet temperature and 80-100 % of aspirator rate. The main objective was to maximize %yield and minimize %moisture content.

3. Characterization of xyloglucan spray dried powder

The xyloglucan spray dried powders prepared from the 13 designed conditions in Table 1 was evaluated for percentage yield and moisture content (mention in topic B1 and B5). Additionally, size and size distribution were also studied.

D. Determination of physicochemical properties of xyloglucan powder from tamarind seeds.

1. pH

The pH of 1%w/v xyloglucan powder from tamarind seeds was measured by using pH meter. The measurements were done in triplicate.

2. Solubility in water

The excess amount of weighed xyloglucan powder was added into 10 ml of distilled water and left shaking at room temperature for 24 hrs. The mixture was centrifuged and filtered through a 0.45 μm membrane filter. The determination of amount of xyloglucan which dissolved in distilled water was performed by HPLC method. The examination was performed in triplicate.

3. Viscosity and rheology property

Viscosity and rheology property of xyloglucan solution was measured by using viscometer (RotoVisco RV1, Germany) (Figure 14). The cone C35/1° Ti was selected in the experiment. The viscosity and rheology measurements were made on solutions of tamarind seed xyloglucan powder dissolved in distilled water at 1, 1.5 and 2% w/v. The measurement was performed in triplicate.



Figure 14 Viscometer (RotoVisco RV1, Germany)

4. Incompatibility of xyloglucan and ethanol

The 1% w/v of tamarind seed xyloglucan solution was prepared and studied for the incompatibility of xyloglucan and ethanol. Tamarind seed xyloglucan solution was added with ethanol in different mixing ratios, mixed thoroughly and left at room temperature for 24 hrs (Table 2). These liquid were centrifuged and filtered through 0.45 μm membrane filter. The determination of amount of xyloglucan was performed by HPLC method. The examination was performed in triplicate.

Table 2 Mixing ratios of absolute ethanol and tamarind seed xyloglucan solution

%ethanol (v/v)	1% tamarind seed xyloglucan solution (ml)	Amounts of added ethanol (μl)
0	5.00	-
1	4.95	50
2	4.90	100
3	4.85	150
4	4.80	200
5	4.75	250

5. Thermal analysis by differential scanning calorimetric method

The differential scanning calorimetric (DSC) thermogram was determined by using differential scanning calorimeter (DSC822e, Mettler Toledo, Switzerland). A highly sensitive ceramic sensor in the DSC instrument was used to measure the difference between the heat flows to the sample and reference crucibles. The samples (3-5 mg) were accurately weighed into standard aluminum pans (40 μl) and then sealed. The DSC runs were conducted over a temperature range 30-330 $^{\circ}\text{C}$ at rate of 10 $^{\circ}\text{C}/\text{min}$. All tests were performed under a nitrogen atmosphere of 2 ml/min.

6. Powder X-ray Diffractogram

Powder X-ray diffractograms were carried out by using powder X-ray diffractometer (Bruker AXS model D8 Discover, Germany) with Cu-K radiation as the source of X-rays. The measurement conditions were set as voltage of 40 kV, current of 40 mA, scanning speed of 0.3 $^{\circ}/\text{min}$ in the 0.02° angle range of 0.8-30 $^{\circ}$.

7. Morphology

Morphology of xyloglucan powder was examined by scanning electron microscope (SEM), (JSM-T220A, Jeol, Japan).

8. Determination of size and size distribution

Particle size analysis was performed on a sample of powder suspended in light mineral oil as a non-dissolving dispersion medium. The samples were analyzed by using a laser light scattering (Mastersizer S, Malvern, UK). The mean and standard deviation of three determinations were calculated.

E. Formulation of films prepared from tamarind seed xyloglucan

1. Development of films formulation prepared from tamarind seed xyloglucan

The effect of concentration of combined plasticizers and concentration of tamarind seed xyloglucan in film formulations was determined using a small composite design (Table 3). From the results of preliminary study, the concentration ranges of glycerin and 70% sorbitol solution were 0-4% and 2-6% w/w, respectively, whereas the concentrations range of tamarind seed xyloglucan was 1-2% w/w. The formulations were shown in Table 4. The tamarind seed xyloglucan was dispersed in mixed solvent. The solvent mixture comprised of propylene glycol, Tween 80, glycerin, 70% sorbitol, Sepicide[®] HB, ethanol and distilled water. The mixture was poured into a plate. The casting mixture was dried by a hot air oven at 50°C for 24 hrs.

2. Evaluation of films prepared from tamarind seed

2.1 Physical Appearances

Color, transparency, flexibility and integrity of all films were visually observed. The thickness of film was measured by using a micrometer having a sensitivity of 0.01 mm.

Table 3 Small central composite design of film formulations

Film No.	tamarind seed xyloglucan	70% sorbitol solution	glycerin
1	(+) 2%	(+) 6%	(-) 0%
2	(+) 2%	(-) 2%	(+) 4%
3	(-) 1%	(+) 6%	(+) 4%
4	(-) 1%	(-) 2%	(-) 0%
5	(-) 1%	(0) 4%	(0) 2%
6	(+) 2%	(0) 4%	(0) 2%
7	(0) 1.5%	(-) 2%	(0) 2%
8	(0) 1.5%	(+) 6%	(0) 2%
9	(0) 1.5%	(0) 4%	(-) 0%
10	(0) 1.5%	(0) 4%	(+) 4%
11	(0) 1.5%	(0) 4%	(0) 2%
12	(0) 1.5%	(0) 4%	(0) 2%
13	(0) 1.5%	(0) 4%	(0) 2%
14	(0) 1.5%	(0) 4%	(0) 2%
15	(0) 1.5%	(0) 4%	(0) 2%

2.2 Film weight

The weight of films (1×1 cm²) was investigated using an analytical balance (Mettler Toedo, Switzerland), that has a sensitivity of 0.00001 g. The measurement was performed in 5 samples in each formulation.

2.3 Adhesive force

Tensile mucoadhesive experiments was examined by tensiometer (Tinius Olsen, Model H5KS 1509) with a 10 N load cell and a software-controlled program, QMat 4.10 S-Series-5K). The withdrawal and retune speeds were set at 15 mm/min. A probe was an aluminium cylinder having a diameter of 2.5 cm. A film product, whose the radius of a circle was 2.5 cm, was taped to the base of aluminium probe fixed to the mobile arm of the tensiometer (Tinmanee, 2004). A piece of porcine skin was securely set in place on a platform. Before testing, the piece of porcine skin was dropped with 100 µl distilled water. The film was brought into contact with the

porcine skin with a constant force of 0.1 N for 10 s. The value of the resistance to withdraw of the probe indicating the adhesive force of the film to porcine skin was displayed by adhesive force (N/cm^2). Five specimens were examined for one film formulation. A new porcine skin was replaced for each run.

2.4 Mechanical properties

Mechanical properties of films from tamarind seed xyloglucan were determined by using tensiometer (Tinius Olsen, Model H5KS 1509) with a 10 N load cell. The mechanical properties studied included the tensile strength, percent elongation at break, work of failure, and Young's modulus were evaluated. The measurements were done in five replicates. The procedure employed was based on the guideline of the American Society for Testing and Material ASTM (1995).

The film specimens were cut into small strips of 3×40 mm. The thickness of each strip was the averaged value of five separate measurements by using micrometer. The test machine was set according to conditions as follows:

Rate of grip separation	=	12 mm/min
Gauge length	=	5 mm
Loading weight	=	2 Newton
Temperature	=	37 ± 2 °C
Relative humidity	=	$24 \pm 3\%$

Five specimens were examined for one film formulation. After the specimen was ruptured, the breaking force and the change in length at the moment of rupture, were analyzed by the software-controlled program, QMat 4.10 S-Series-5K). The calculation of the mechanical properties of the films was as:

$$\text{Tensile strength (MPa)} = \frac{\text{maximum load}}{\text{original minimum cross-sectional area of the specimen}}$$

$$\% \text{ elongation} = \frac{\text{extension at the moment of rupture of the sample}}{\text{initial gauge length of the specimen}} \times 100$$

$$\text{Young's modulus} = \frac{\text{tensile stress}}{\text{elastic strain in tension}}.$$

Work of failure (mJ) = area of a curve plotting between force and extension

F. Formulation of films prepared from tamarind seed xyloglucan containing *Centella asiatica* extract

1. Prepared film from tamarind seed containing *Centella asiatica* extract

According to the evaluation of all films in topic E2.3, the formulation 6 with the highest adhesive force (N/cm²) value, was selected. *Centella asiatica* extract was weighed in an amount equivalent to 1% asiaticoside (w/w). *Centella asiatica* extract was dissolved in the solvent mixture comprised of 1.5% propylene glycol, 1% Tween 80, 2% absolute ethanol and distilled water.

2. The analysis of asiaticoside in *Centella asiatica* extract

The determination of asiaticoside content was performed by high performance liquid chromatography, HPLC).

2.1 Chromatographic Condition

The chromatographic conditions for the analysis of asiaticoside from *Centella asiatica* were as follows (Kongthong, 2004):

Column	:	Alltima [®] HP C18, 5 μm, 150 mm x 4.6 mm
Precolumn	:	μBondapack C18, 10 μm, 125A°
Mobile phase	:	Acetonitrile: 10mM phosphate buffer pH 6.8, (35:65)
Injection volume	:	20 μl
Flow rate	:	0.8 ml/min
Detector	:	UV detector at 210 nm
Temperature	:	ambient
Run time	:	9 min
Internal standard	:	triamcinolone acetonide

The mobile phase was freshly prepared, filtered through 0.45 μm membrane filter and then degassed by sonication for 30 min before using.

Table 4 Composition of tamarind seed xyloglucan film formulations

Ingredient	Rx (w/w)														
	1	2	3	4	5	6	7	8	9	10	11	12	13	14	15
Xyloglucan powder	2	2	1	1	1	2	1.5	1.5	1.5	1.5	1.5	1.5	1.5	1.5	1.5
Propylene glycol	1	1	1	1	1	1	1	1	1	1	1	1	1	1	1
Tween 80	1.5	1.5	1.5	1.5	1.5	1.5	1.5	1.5	1.5	1.5	1.5	1.5	1.5	1.5	1.5
Ethanol	2	2	2	2	2	2	2	2	2	2	2	2	2	2	2
70% Sorbitol solution	6	2	6	2	4	4	2	6	4	4	4	4	4	4	4
Glycerin	0	4	4	0	2	2	2	2	0	4	2	2	2	2	2
Sepicide [®] HB	0.5	0.5	0.5	0.5	0.5	0.5	0.5	0.5	0.5	0.5	0.5	0.5	0.5	0.5	0.5
Distilled water qs to	100	100	100	100	100	100	100	100	100	100	100	100	100	100	100

2.2 Standard Solutions

2.2.1 Preparation of internal standard solution

A stock solution of internal standard was prepared by accurately weighed 5 mg of triamcinolone acetonide into a 10 ml volumetric flask, diluted and adjusted to volume with methanol. The final concentration of triamcinolone acetonide stock solution was 500 µg/ml.

2.2.2 Preparation of standard asiaticoside solutions

The 25 mg part of asiaticoside was accurately weighed and transferred into a 25 ml volumetric flask, diluted and adjusted to volume with methanol. This stock solution had the final concentration of asiaticoside of 1000 µg/ml.

The solutions of 50, 100, 200, 300, 400, 500 µl of asiaticoside standard stock solution, and 100 µl of internal standard stock solution were added into 5 ml volumetric flasks. The dilution to volume with mobile phase gave final concentrations of 10, 20, 40, 60, 80 and 100 µg/ml of asiaticoside, respectively.

The standard solutions were freshly prepared and used for the HPLC run. As a result, the standard curve between concentration and peak area ratio was plotted.

2.3 Validation of the HPLC method

The analysis of parameters in the assay validation for the HPLC method was specificity, linearity, precision and accuracy.

2.3.1 Specificity

The specificity of the method was determined by comparing the test results from analyses of asiaticoside in each film preparation with standard solutions. Under the chromatographic conditions used, the peak of asiaticoside must be completely separated from and not be interfered by the peaks of other components in the preparation.

2.3.2 Linearity

The linearity was determined from the coefficient of determination (R^2). Six concentrations of standard asiaticoside solutions and three replicates of each

concentration were prepared and analyzed. The relation between the peak height ratios and concentrations were plotted and the least square linear regressions were calculated.

2.3.3 Accuracy

a) Accuracy of analysis of solution

The accuracy of an analytical method is the closeness of test results obtained by that method to the true value. The accuracy of the method was determined from the percentage of recovery. Five sets of three concentrations (low, medium, high) of asiaticoside at 30, 50, 90 $\mu\text{g/ml}$ were prepared and analyzed, respectively. The percentage of recovery for each concentration was calculated from the ratio of inversely estimated actual concentration multiplied by 100.

b) Accuracy of analysis of film formulation

The accuracy formulation of an analytical method is the closeness of test results obtained by that method to the true value. The accuracy of the method was determined from the percentage of recovery. Five sets of three concentrations (low, medium, high) of asiaticoside at 30, 50, 90 $\mu\text{g/ml}$ that spiked into selected formulation in topic F1 were prepared and analyzed, respectively. The percentage of recovery for each concentration was calculated from the ratio of inversely estimated actual concentration multiplied by 100.

2.3.4 Precision

a) Within run precision

The within run precision was determined by analyzed five sets of three concentrations of asiaticoside at 30, 50, 90 $\mu\text{g/ml}$ in the same run. Peak height ratios of asiaticoside to triamcinolone acetonide were calculated and the percent of coefficient of variation (%CV) of each concentration was determined.

b) Between run precision

The between run precision was determined by analyzing three concentrations of asiaticoside at 30, 50, 90 $\mu\text{g/ml}$ on five different runs. Peak height ratios of

asiaticoside to triamcinolone acetonide were calculated and the percentage of coefficient of variation for each nominal concentration was determined.

Acceptance criteria:

In order to get high accuracy, the percentage of recovery should be within 98-102% for each nominal concentration, whereas the different coefficient percentage for both within run precision and between run precision should be less than 2%.

3. Evaluation of film prepared from tamarind seed xyloglucan containing *Centella asiatica* extract

3.1 Physical appearances

Physical appearances, thickness, weight, mechanical properties and adhesive force of the film containing *Centella asiatica* extract were investigated as the same procedures mentioned in topic E2.

3.2 Thermal analysis by differential scanning calorimetry

The differential scanning calorimetric (DSC) thermogram was determined by using differential scanning calorimeter (DSC822e, Mettler Toledo, Switzerland). The samples (3-5 mg) were accurately weighed into standard aluminum pans (40 μ l) and then sealed. The DSC runs were conducted over a temperature range 25-360°C at rate of 10°C/min. All tests were performed under a nitrogen atmosphere of 2 ml/min.

3.3 Powder X-ray diffractometry

Powder X-ray diffractograms were carried out by using powder X-ray diffractometer (Bruker AXS model D8 Discover, Germany) with Cu-K radiation as the source of X-rays. The measurement conditions were as follows: voltage of 40 kV, current of 40 mA, scanning speed of 0.2°/min increment the 0.02° angle range of 3-40°.

3.4 In vitro release study of films prepared from tamarind seed xyloglucan containing *Centella asiatica* extract

The *in vitro* release study was performed by using Franz diffusion cell, which consisted of donor and receiver compartments. The dialysis membrane was placed between two compartments of Franz diffusion cell. The membrane was soaked in distilled water for 24 hours, then washed by hot distilled water and soaked in isotonic phosphate buffer saline buffer pH 7.4 for an hour before use. The receiving compartment contained 14 ml of 40% ethanol in isotonic phosphate buffer saline buffer pH 7.4 which was maintained at $37\pm 0.5^{\circ}\text{C}$ by a circulating water jacket (Kabovloi, 2004). The receptor fluid and membranes were equilibrated to the desired temperature for 1 hr before this study. After equilibration, the sample of film (diameter 1.8 cm) was carefully placed into the donor compartment and 200 μl of isotonic phosphate buffer saline buffer pH 7.4 was also dropped into donor compartment then covered with paraffin to prevent evaporation. The receptor fluid was continuously mixed by magnetic stirring bar throughout the time of study. A volume of 1 ml were taken from receiver medium at certain time intervals of 0.25, 0.5, 0.75, 1, 1.5, 2, 4, 6, 8, 10, 12, 15, 18, 21, 24, 28, 32, 36, 40, 44 and 48 hours. The receptor compartment was replaced with receptor solution to keep the constant volume during the experiment. The examination was performed in triplicate. The samples were analyzed for amount of asiaticoside released from the films by HPLC method as mentioned in topic F2.

3.5 Skin permeation of films prepared from tamarind seed xyloglucan containing *Centella Asiatica* extract

Permeation experiments were performed by using Franz diffusion cell, which consisted of donor and receiver compartments. The porcine skin was placed between two compartments of Franz diffusion cell. The porcine skin was soaked in isotonic phosphate buffer saline buffer pH 7.4 for an hour before use. The receiving compartment contained 14 ml of 40% ethanol in isotonic phosphate buffer saline buffer pH 7.4 which was maintained at $37\pm 0.5^{\circ}\text{C}$ by a circulating water jacket. The receptor fluid and porcine skin were equilibrated to the desired temperature for 1 hr before the permeation study. After equilibration, the sample of film (diameter 1.8 cm)

was carefully placed into the donor compartment and 200 µl of isotonic phosphate buffer saline buffer pH 7.4 was also dropped into donor compartment then covered with paraffin to prevent evaporation. The receptor fluid was continuously mixed by magnetic stirring bar throughout the time of study. A volume of 5 ml were taken from receiver medium at certain time intervals of 1, 2, 4, 6, 8, 10, 12, 15, 18, 21 and 24 hours. The receptor compartment was replaced with receptor solution to keep the constant volume during the experiment. The samples were analyzed for amount of asiaticoside permeated from the film into the receptor compartment by HPLC method as mentioned in topic F2. Additionally, at the end of study, the remaining portion of the film in the donor compartment and the porcine skin were removed and analyzed for asiaticoside by the same method. The examination was performed in triplicate.

3.6 Stability of films prepared from tamarind seed xyloglucan containing *Centella asiatica* extract

The films were stored in glass vials, which were tightly sealed with rubber closure and aluminum caps at $40\pm 2^{\circ}\text{C}$ and $75\pm 5\%$ RH for three months (Cartensen, 1990). Samples were withdrawn at 0, 1, 2, and 3 months and were analyzed for the amounts remaining of asiaticoside. The tensiometer study, differential scanning calorimetry study and powder X-ray diffraction study were also performed. The analysis of asiaticoside in film samples followed the previously described HPLC method. The examination was performed in triplicate.

CHAPTER IV

RESULTS AND DISCUSSION

A. Characterization of xyloglucan spray dried powder from Tamarind seeds

1. The percentage yield of xyloglucan spray dried powder

The percentage yield, percentage moisture content and physical appearances of the xyloglucan spray dried powders prepared by four different methods are displayed in Table 5. Figure 15 shows the physical appearances of xyloglucan dried powder from four different methods. From all methods, the physical appearances of xyloglucan spray dried powder were whitish powder, mild aggregation and very bulky. The spray dried powder of method I and II were more bulky than those spray dried powder of method III and IV. The %total yield and %moisture content of xyloglucan spray dried powder (from both collecting chamber and cyclone) from four different methods varied from 18.40-26.21 and 6.26-10.81, respectively. It was notable that the percentages moisture content of the powder in cyclone were slightly higher than in collector. The reason might be due to the higher temperature in the cyclone than in collector.

Table 5 Comparison of the percentage yield, percentage moisture content and physical appearances xyloglucan spray dried powder from four different methods

Method	% Total yield	%moisture content		Appearance
		collecting chamber	cyclone	
I	26.21	9.29	6.63	Whitish powder, bulky
II	23.20	10.81	8.93	Whitish powder, bulky
III	18.40	7.27	6.26	Whitish powder, bulky
IV	19.62	9.36	6.36	Whitish powder, bulky



Figure 15 The xyloglucan spray dried powder from four different methods

2. Determination of xyloglucan in tamarind seed powder

2.1. Validation of HPLC method

The validation of analytical method is the process by which it is established that the performance characteristics of the method meet the requirements for the intended analytical applications. The performance characteristics are expressed in term of analytical parameters. For HPLC assay validation, these include specificity, linearity, accuracy and precision of the method will be determined.

2.1.1 Specificity

The specificity of an analytical method is the ability to measure the analyses accurately and with specificity in the presence of other components in the sample. Figure 16 shows typical chromatograms of standard xyloglucan solution, sample solution and absolute ethanol, respectively. The chromatograms demonstrated that the HPLC condition used in the study had a suitable specificity.

2.1.2 Linearity

The calibration curve data of standard xyloglucan are shown in Table 6. The plot of standard xyloglucan concentrations versus the peak area (Figure 2A) displayed the linear correlation in the concentration range studied of 400-900 µg/ml. The coefficient of determination (R^2) of this line was 0.9997. These results indicated that HPLC method was acceptable for quantitative analysis of xyloglucan in the range studied

2.1.3 Accuracy

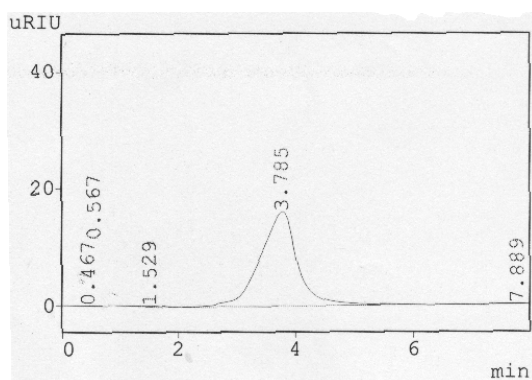
The accuracy of an analytical method is the closeness of test results obtained by the method to the true value. Accuracy is calculated as percent recovery by the assay of known added amount of analyses. The percentages analytical recovery of xyloglucan was in the range of 98.14-100.68% which indicated that this method could be used for analysis in all concentrations studied with a high accuracy (Table 7).

2.1.4 Precision

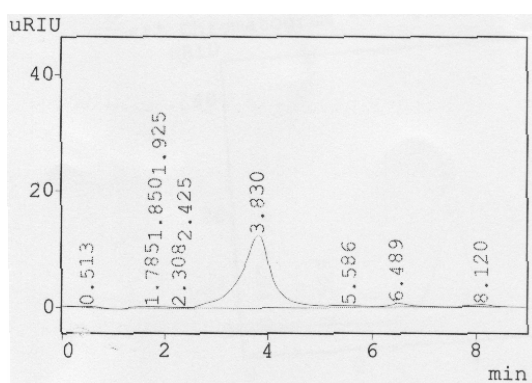
The precision of xyloglucan analyzed by HPLC method were determined both within run precision and between run precision as illustrated in Tables 3A and 4A. All coefficients of variation values were small, as 0.43-1.04% and 1.15-1.78%, respectively. The coefficient of variation of an analytical method should generally be less than 2%. Therefore, the HPLC method was precise for quantitative analysis of xyloglucan in the range studied.

3. The percent xyloglucan, total protein and fat of xyloglucan spray dried powders

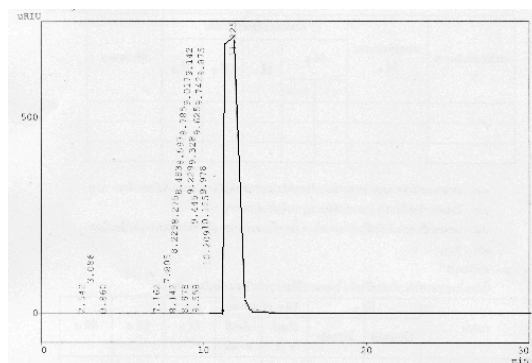
The percentage contents of xyloglucan, total protein and fat of xyloglucan spray dried powder from four different methods and tamarind seed powder are shown in Table 10. The results were obtained by the analysis of variance (ANOVA) at significant level 0.05. According to analytical statistics, all of the methods could significantly reduce the contaminated fat. Moreover, Method I, II and III also reduced significantly the contaminated of protein. However, it revealed that methods resulted to no significant difference of the %xyloglucan content.



(a)



(b)



(c)

Fig 16 HPLC chromatograms of ultrapure water

(a) xyloglucan standard solution

(b) sample solution

(c) absolute ethanol

Table 6 Data of calibration curve of xyloglucan by HPLC method

Concentration ($\mu\text{g/ml}$)	Peak area			Mean	SD	%CV
	Set1	Set2	Set3			
400	3140440	3136673	3127925	3135012.67	6420.58	0.20
500	3946311	3942877	3962926	3950704.67	10722.35	0.27
600	4766031	4718676	4729805	4738170.67	24761.10	0.52
700	5503701	5384933	5497697	5462110.33	66904.91	1.22
800	6309434	6156137	6268376	6244649.00	79355.03	1.27
900	7172318	6924533	7072993	7056614.67	124701.80	1.77
R²	0.9996	0.9994	0.9998	0.9997	-	-

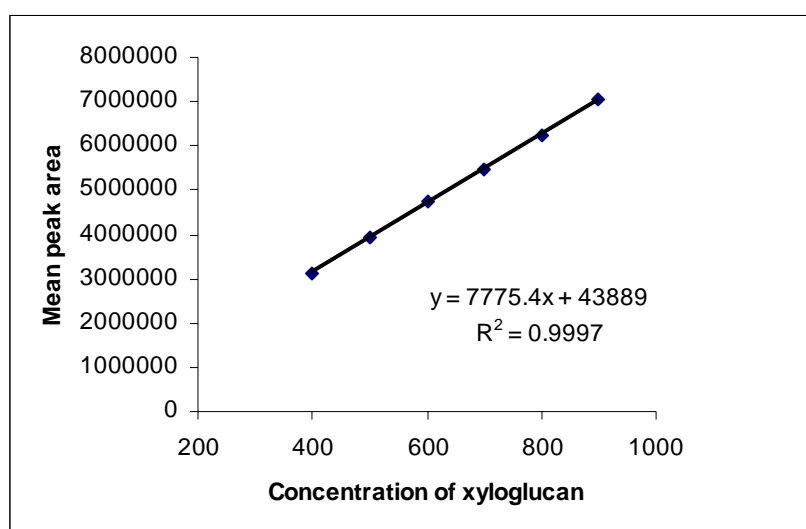


Fig 17 Calibration curve of xyloglucan by HPLC method

Table 7 The percentages of analytical recovery of xyloglucan by HPLC method

Concentration ($\mu\text{g/ml}$)	%Analytical recovery					Mean \pm SD
	1	2	3	4	5	
450	98.35	100.16	99.19	98.12	100.40	99.24 \pm 1.03
650	100.68	100.40	100.31	100.46	98.66	100.10 \pm 0.82
850	98.77	99.14	98.62	98.16	98.14	98.56 \pm 0.43

Table 8 Data of within run precision by HPLC method

Concentration ($\mu\text{g/ml}$)	Concentration ($\mu\text{g/ml}$)					Mean	SD	%CV
	Set1	Set2	Set3	Set4	Set5			
450	442.56	450.71	446.33	441.52	451.78	446.58	4.64	1.04
650	654.42	652.59	652.02	652.97	641.30	650.66	5.31	0.82
850	839.55	842.68	838.23	834.32	834.16	837.79	3.62	0.43

Table 9 Data of between run precision by HPLC method

Concentration ($\mu\text{g/ml}$)	Concentration ($\mu\text{g/ml}$)					Mean	SD	%CV
	Set1	Set2	Set3	Set4	Set5			
450	446.58	465.2	458.43	446.26	452.87	453.87	8.08	1.78
650	650.66	670.94	648.16	644.65	653.07	653.50	10.24	1.57
850	837.79	862.6	842.4	854.29	850.74	849.56	9.79	1.15

Molinarolo (1990) and Sumathi and Ray (2002), a large amount of ethanol was used in extraction of xyloglucan, resulting to high cost of production. In this research, the step of precipitation of xyloglucan with ethanol was removed. Moreover, the defatting with hexane was added in the process of xyloglucan extraction, consequently, xyloglucan powder had low contamination of fat.

Table 10 Comparison of the percentage contents of xyloglucan, total protein and fat of xyloglucan spray dried powder from four different methods and tamarind seed powder (mean \pm SD)

	% xyloglucan	%Protein	%Fat
Tamarind seed powder	-	15.87 \pm 0.35	7.73 \pm 0.27
Method I	42.85 \pm 0.92	14.35 \pm 0.12*	1.09 \pm 0.17*
Method II	43.72 \pm 0.49	14.17 \pm 0.08*	1.15 \pm 0.16*
Method III	42.90 \pm 1.11	14.64 \pm 0.33*	0.89 \pm 0.34*
Method IV	44.62 \pm 0.92	15.19 \pm 0.29	1.19 \pm 0.17*

* Significant at P value = 0.05

4. Morphology of xyloglucan spray dried powder

Figure 18 represented the scanning electron microscopy (SEM) of xyloglucan spray dried powder of four different methods. Particles of all methods were very small and spherical shaped, but some were shrunk and aggregated. The surface particles of xyloglucan spray dried powder from method I and II were rather smooth but method III and IV were rough with shrunk surface.

The results could be explained that method of xyloglucan extraction had effect on the surface topography of particles. In method III and IV, the defatting process by hexane was done with slurry of tamarind seed powder in water.

As the results, all four methods could reduce the %contaminated of total protein and fat. However, defatting process of method III and IV had effect on morphology of xyloglucan spray dried powder. Thus, method III and IV were not suitable for the xyloglucan extraction from tamarind seed. The method II was more time-consuming than method I since it had to leave standing overnight. Consequently, method I was the most appropriate method for xyloglucan extraction

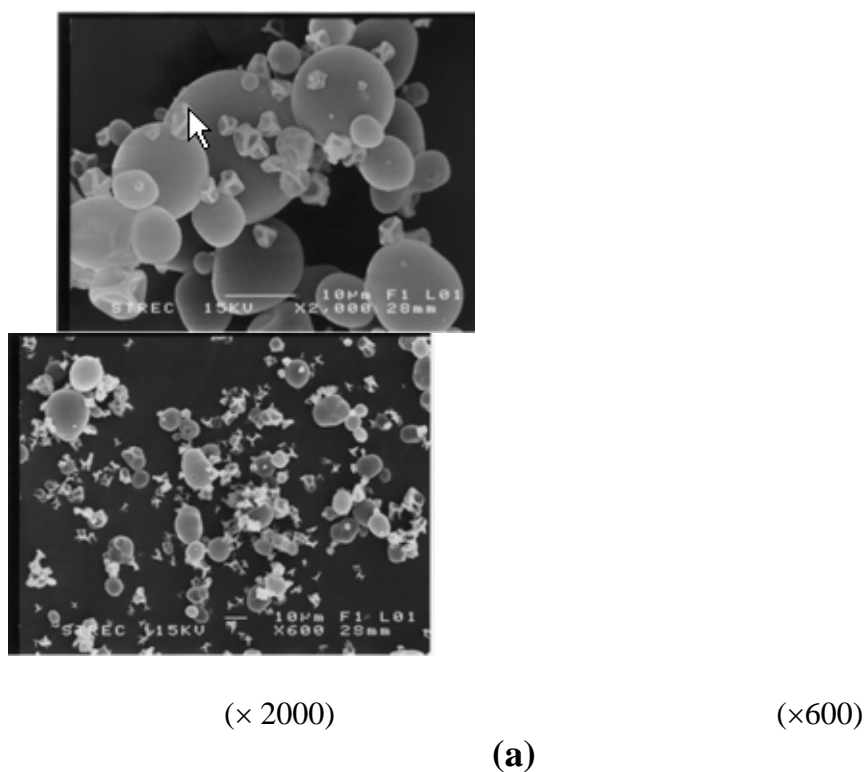
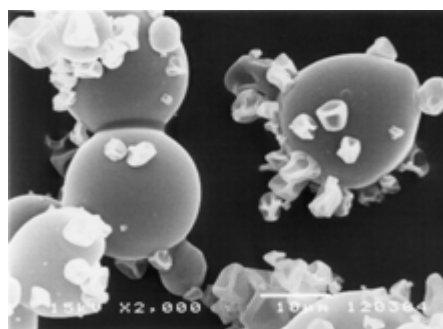
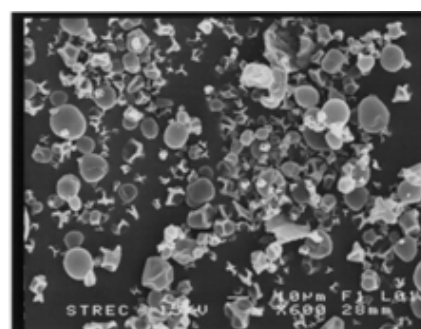


Figure 18 Scanning electron photomicrographs of xyloglucan spray dried powder from four different methods; (a) Method I, (b) Method II, (c) Method III

and (d) Method IV

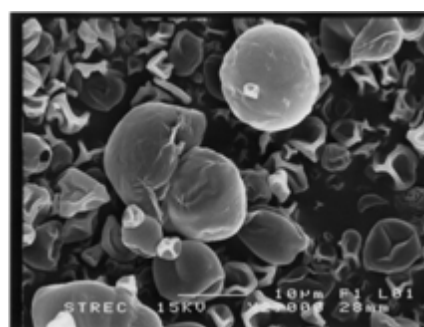


(× 2000)

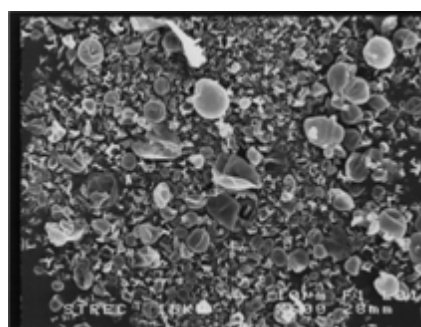


(×600)

(b)

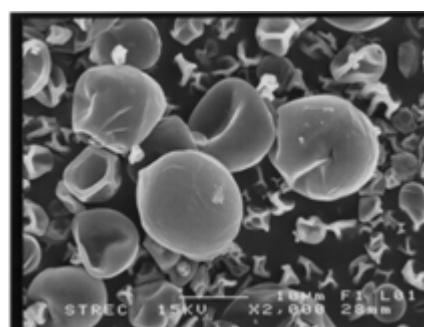


(× 2000)

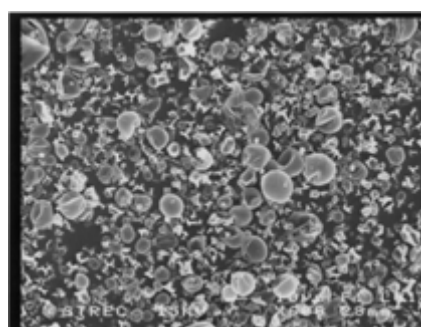


(×600)

(c)



(× 2000)



(×600)

(d)

Figure 18 Scanning electron photomicrographs of xyloglucan spray dried powder from four different methods; (a) Method I, (b) Method II, (c) Method III and (d) Method IV (continued)

B. Optimization of spray drying condition.

1. Optimization of spray drying condition on production yield and moisture

There were many factors effected on yield and powder properties such as concentration of the sample, inlet and outlet air temperature, air flow rate and feed flow rate. In this report, the effect of inlet temperature and air flow rate on the yield and moisture content of spray dried powder were investigated, whereas feed flow rate was fixed at 10%.

To explore the region of the response surface in the neighborhood of the optimum, a second order approximation to the response surface could be developed. A face centered design was used for this purpose. The design matrix with responses is given in Table 11.

The percentage yields and moisture contents varied from 33.64-64.49% and 4.99-7.83%, respectively. The results of the second order, response surface quadratic model fitting in the form of analysis of variance for %yield and the linear model for %moisture content are given in Table 12 and Table 13, respectively.

The analysis of variance of the regression model states that the model of %yield and %moisture content was significant ($P < 0.05$). The response surface quadratic model was an adequate model for %yield and the linear model for %moisture content, as were evident from the F -test ($F_{\%yield} = 10.83$ and $F_{\%moist} = 58.08$) and a very low probability values (%yield: $P_{model} > F = 0.0034$ and %moisture content: $P_{model} > F < 0.0001$) (Table 12 and Table 13). Values of “Prob $> F$ ” were less than 0.05 indicated that model terms were significant ($P < 0.05$) (Myers and Montgomery, 2002). Lack of fit for both models was not significant ($P > 0.05$). Non significant lack of fit was good (Stat-Ease Inc., 2005).

The goodness of fit of the models was checked by the determination coefficient (R^2). The value is always between 0 and 1. The closer the value is to 1, the model is stronger and better predict the response (Myers and Montgomery, 2002). In this study, the values of $R^2 = 0.8856$ and 0.9207 , indicated that 88.56% and 92.07% of variability in the response could be explained by the model for %yield and %moisture content, respectively (Table 14).

Table 11 A face centered design matrix of two parameters and the observed responses

Code	Factor		Responses	
	Inlet temperature (°C)	% Aspirator	%yield	%moisture
C1	120 (-)	80 (-)	33.64	7.83 ± 0.10
C2	200 (+)	80 (-)	46.80	6.05 ± 0.12
C3	120 (-)	100 (+)	40.22	7.05 ± 0.13
C4	200 (+)	100 (+)	50.31	4.99 ± 0.19
C5	120 (-)	90 (0)	40.66	7.23 ± 0.11
C6	200 (+)	90 (0)	45.48	5.86 ± 0.11
C7	160 (0)	80 (-)	58.50	7.06 ± 0.10
C8	160 (0)	100 (+)	52.94	6.33 ± 0.11
C9	160 (0)	90 (0)	62.88	7.03 ± 0.11
C10	160 (0)	90 (0)	60.54	6.50 ± 0.10
C11	160 (0)	90 (0)	61.42	6.66 ± 0.12
C12	160 (0)	90 (0)	64.49	6.32 ± 0.11
C13	160 (0)	90 (0)	53.96	6.59 ± 0.17

The application of P -values is to check the significance of each of the coefficients for essentially understanding the pattern of the mutual interactions between the test variables. To imply the result of %yield, both the first order mainly affected to inlet temperature (A) and second order mainly affected to inlet temperature (A^2) result from their P -values = 0.0337 and 0.0006, respectively. Consequently, they were the most significant effects ($P < 0.05$) (Table 12). For moisture content, the first order main effect of inlet temperature and % aspirator were a significant effect by referring from its P -value < 0.0001 and P -value = 0.0008 ($P < 0.05$), respectively (Table 13).

Table 12 ANOVA for response surface quadratic model of % yield

Source of variations	Sum of squares	df	Mean square	F-value	Probability P (> F)
Model	1026.49	5	205.30	10.83	0.0034*
A-Inlet temp	131.40	1	131.40	6.93	0.0337*
B-% Aspirator	3.42	1	3.42	0.18	0.6835
AB	2.36	1	2.36	0.12	0.7347
A ²	652.10	1	652.10	34.42	0.0006*
B ²	20.36	1	20.36	1.07	0.3344
Residual	132.63	7	18.95		
Lack of Fit	67.56	3	22.52	1.38	0.3689**
Pure Error	65.08	4	16.27		
Corrected Total	1159.13	12			

* Significant at P value = 0.05** Not significant at P value = 0.05

*** R-Squared = 0.8125

Table 13 ANOVA for linear model of % moisture content

Source of variations	Sum of squares	df	Mean square	F-value	Probability P (> F)
Model	5.62	2	2.81	58.08	< 0.0001*
A-Inlet temp	4.52	1	4.52	93.42	< 0.0001*
B-% Aspirator	1.10	1	1.10	22.73	0.0008*
Residual	0.48	10	0.048		
Lack of Fit	0.21	6	0.035	0.51	0.7819**
Pure Error	0.28	4	0.069		
Corrected Total	6.11	12			

* Significant at P value = 0.05** Not significant at P value = 0.05

*** R-Squared = 0.6763

Table 14 Model Summary Statistics of %yield and % moisture content

Responses	Std. Dev.	R-Squared	Adjusted R-Squared	Predicted R-Squared	PRESS
%Yield					
Quadratic	4.35	0.8856	0.8038	0.3672	733.46
%Moisture content					
Linear	0.22	0.9207	0.9049	0.8707	0.79

To apply multiple regression analysis on the experiment data, the experiment results of the face centered design were fitted with a second-order polynomial equation of %yield and linear equation of %moisture content. The coefficients of regression equation associated to the responses to the experimental variables and interactions are represented in Table 15.

Table 15 Coefficients of the regression equation linking the responses to the experimental factors and major interactions (coded units)

Responses	Parameters	Coefficients
%Yield	Intercept	60.02
	A-Inlet temp	4.68
	B-%Aspirator	0.76
	AB	-0.77
	A ²	-15.37
	B ²	-2.72
%Moisture content	Intercept	6.58
	A-Inlet temp	-0.87
	B-%Aspirator	-0.43

Thus the mathematical regression model for % yield and %moisture content fitted in the coded factors were given as following:

$$\begin{aligned} \% \text{Yield} &= 60.02 + (4.68 \times A) + (0.76 \times B) - (0.77 \times AB) - (15.37 \times A^2) \\ &\quad - (2.72 \times B^2) \dots\dots\dots(1) \end{aligned}$$

$$\% \text{Moisture content} = 6.58 - (0.87 \times A) - (0.43 \times B) \dots\dots\dots(2)$$

A and B were the coded values of the test variables;

A: inlet temperature

B: %aspirator

According to the final equation in terms of coded parameters, it may be shown in the equation (1) that increasing of inlet temperature (A) enhanced the %yield while the %aspirator (B) has not significantly affected on %yield (Table15). The results revealed that increasing inlet temperature upto 180°C increased %yield. From higher than 180 °C the opposite results obtained. The reason might be attributed to the compositions of spray drying solution such as carbohydrates that might be stricky as exposed to high temperature. The % yield of different value of the variables could be predicted from the response surface plot (quadratic model).

For %moisture content, the first order main effect of inlet temperature (A) and %aspirator (B) was a significant effect. It was suggested that an increase in inlet temperature and %aspirator were a direct decrease in residual moisture in the products. This finding was consistent with previous research in that the moisture content was decreased with an increased inlet temperature and aspirator capacity (Stahl et al., 2002). The moisture content was possibly forecasted from linear regression plot (linear model). Figure 19 shows the response surface plot for %yield and linear regression plot for %moisture content, respectively.

The normal probability plot of the residuals is an vital diagnostic tool for the detection and explanation of the systematic departures from the assumptions to support errors normally distributed and no affected to each other whose variances are homogeneous (Myers and Montgomery, 2002). Figure 20 are the plots of normal probability of experiment results. The normal probability plot of the “Studentised” residuals indicates almost no violation of the assumptions outlying the analyses.

Based on the two models obtained, a graphical optimization was also conducted the hardness of the Design-Expert version 7.1 statistical software. Recall, the main objective was the maximization of %yield and the minimization of %moisture content. The selection of conditions to overlay plot ranged from 120-200 °C and 80-100% for inlet temperature and %aspirator, respectively. The method basically consisted of overlaying the curves of the models according to the criteria imposed that was to higher %yield as possible and lower %moisture content as possible .

By considering the inverse relationship between %yield and %moisture content, the attained overlaying plot displayed a non-shaded area (white area) where both criterias imposed were satisfied (Figure 21). Hence, a point was selected on the graph (marked by the square). This point was assigned as optimal point and corresponded to 178°C of inlet temperature and 100% of aspirator. Under such conditions, the model predicted 56.90 %yield (a variation of = 49.97 – 63.83% being possible) and 5.77 %moisture content (a variation of = 5.52 – 6.33% being possible) in the confidence range of 95%.

The statistical interpretation of the results concerning both yield and moisture content using the response surface methodology led us to the choice of optimal operating condition. These parameters had to maximize yields while reducing moisture contents.

To confirm the result, three batches were produced using the optimal conditions to validate the fabrication process (Table 16).

According to Table 17, the observed means and standard deviations of the responded obtained for yield and moisture content were found to be $50.40 \pm 4.13\%$ and $6.07 \pm 0.37\%$, respectively. They were in range of the prediction intervals at 95% confidence level. These results can be concluded that the model fitted the experimental data well and described the region studied well

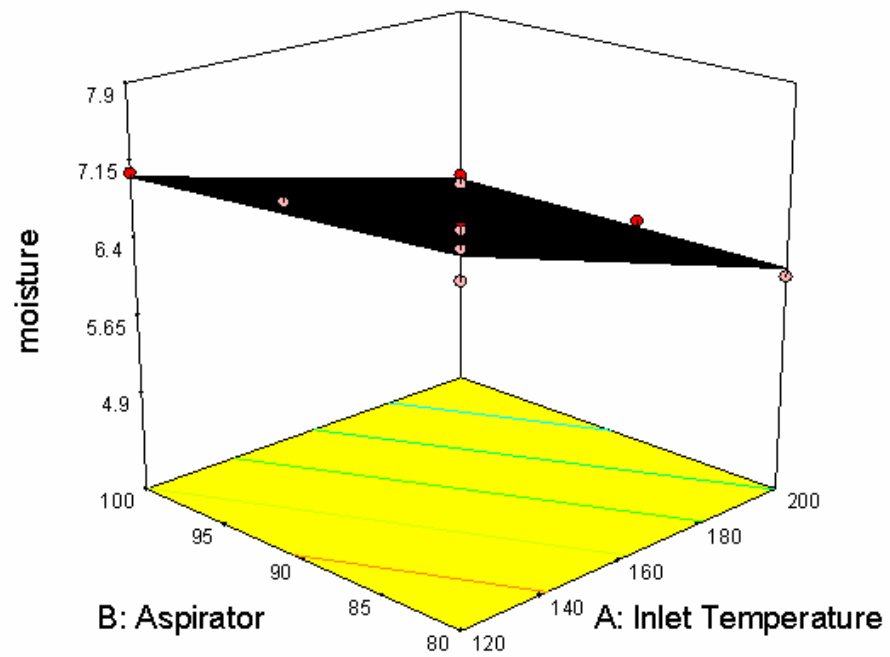
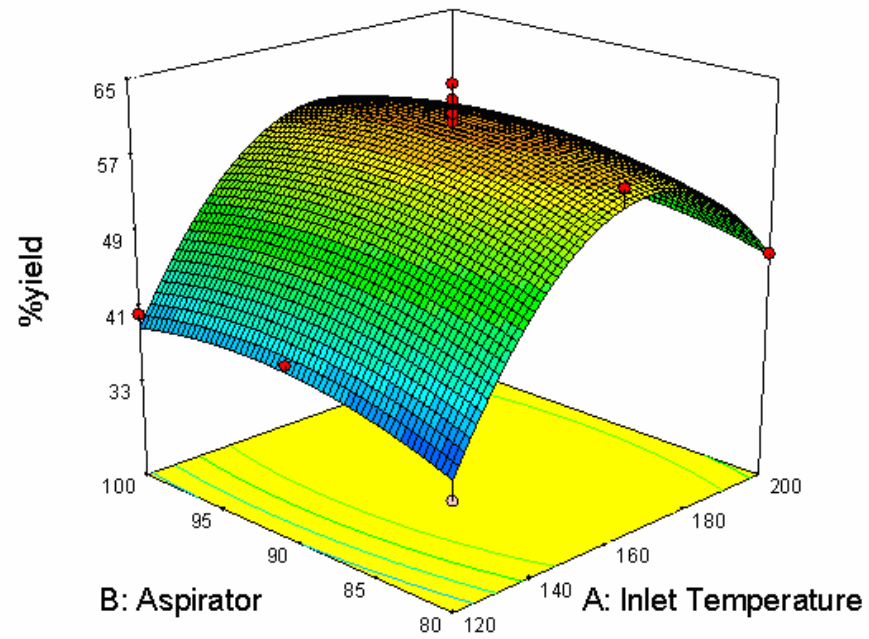
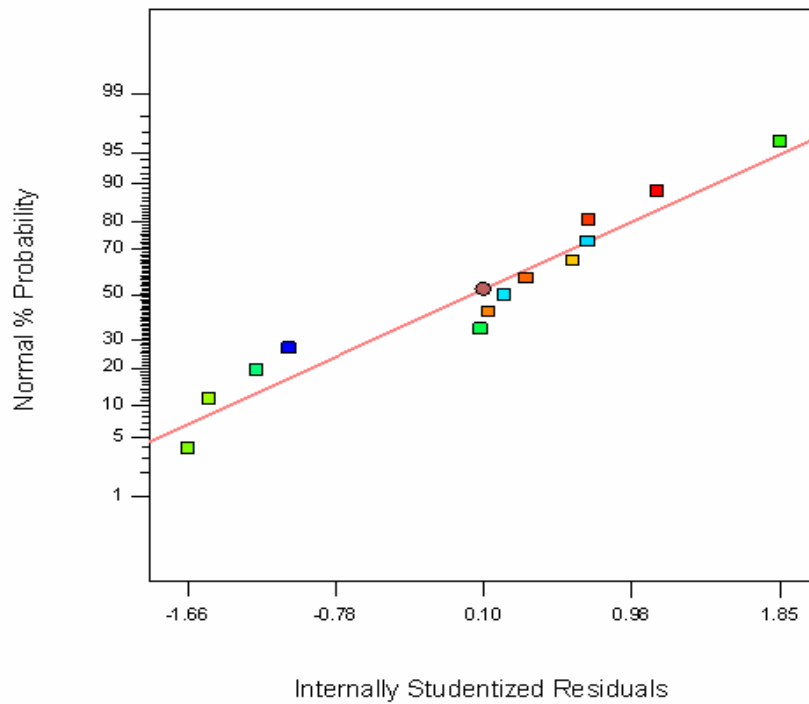


Figure 19 Response surface plot of % yield and linear regression plot of %moisture content; (a) response surface plot of % yield, (b) linear regression plot of %moisture content

Normal plot residuals of %yield results



Normal plot residuals of %moisture content results

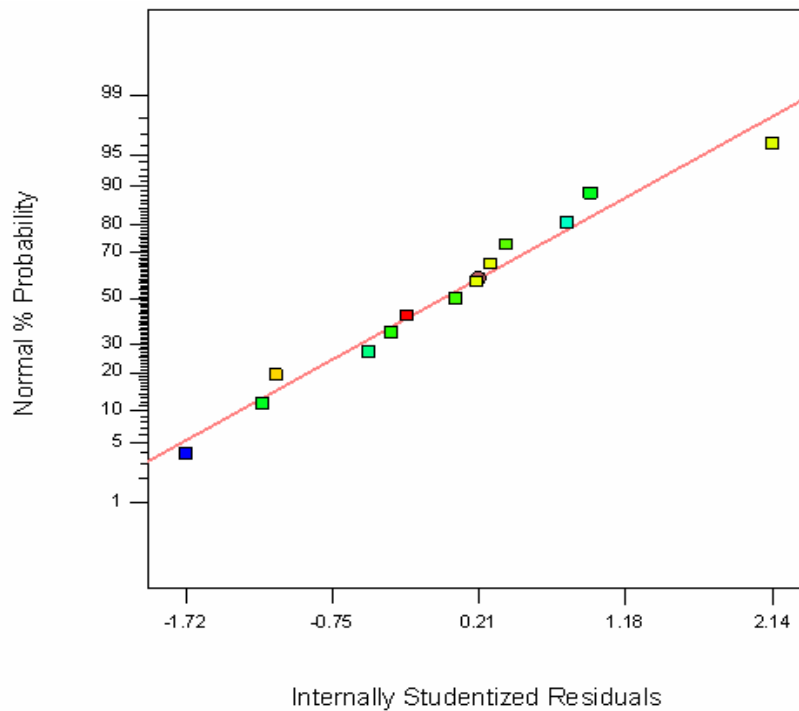


Figure 20 The normal probability plots of the %yield and %moisture content;
 (a) The normal probability plot of the %yield results
 (b) The normal probability plot of the %moisture content results

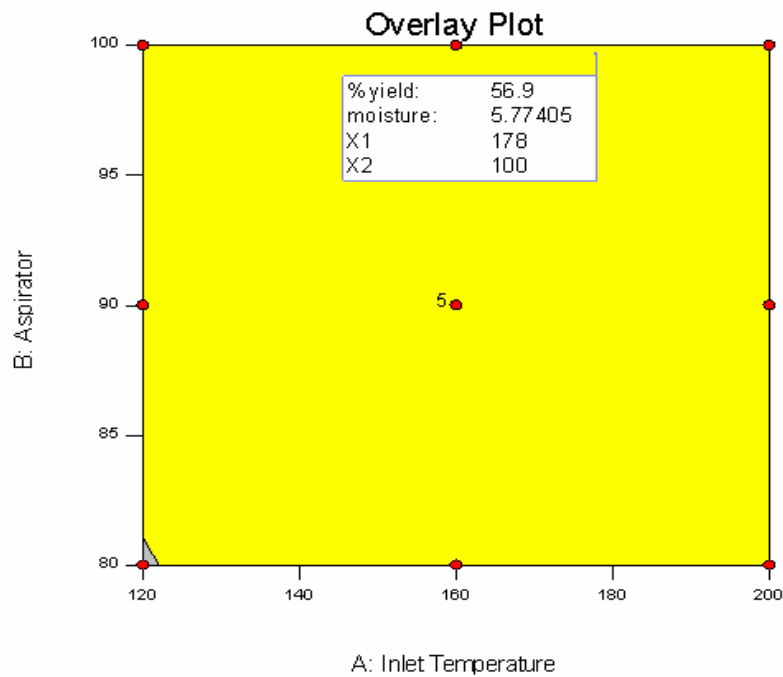


Figure 21 The optimum region by overlay plot of two responses (%yield and %moisture content) evaluated as a function of inlet temperature and %aspirator

Table 16 The optimum region by overlay plot of two parameters and the observed responses

Code	Factor		Responses	
	Inlet temperature (°C)	% Aspirator	%yield	%moisture
O1	178	100	52.49	6.25
O2	178	100	53.06	6.32
O3	178	100	45.84	5.65

Table 17 Observed responses and 95% CI (confidence interval) of optimization spray dried condition

Responses	Values		
	%Observed	%Predicted	95% confidence intervals
Total yield (%)	50.40 ± 4.13	56.90	49.97 – 63.83
Moisture content (%)	6.07 ± 0.37	5.77	5.52 – 6.33

Figure 22 was displayed the optimal xyloglucan spray dried powder obtained as fine particles with whitish color and powder bulkiness.



Figure 22 Xyloglucan spray dried powder of optimal spray dried condition

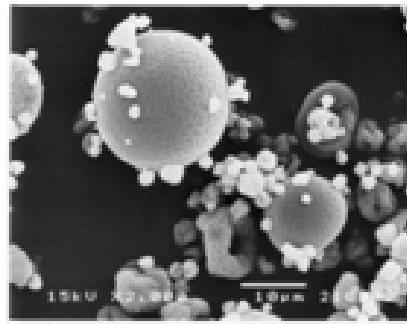
2. Morphology of xyloglucan spray dried powders

The shape and surface topography of the xyloglucan spray dried particles were found to be affected by the spray drying condition. The observation of size, shape and surface topography were done by scanning electron microscopy (SEM). Figure 23 showed the scanning electron photomicrographs of spray dried particles obtained from varied conditions. The particle topography of all conditions were all very small spheres. Some condition such as C8 and C9 gave shrunk particles. At the higher magnification ($\times 10,000$), the particles spray dried from the optimal condition (Figure 23i) showed rough surfaces. The rough surface of particles probably was result from propylene glycol, one of the components in preservative (Sepicide[®] HB) added in spray drying solution. To confirm the postulation, the spray drying solution without preservative (0.5% Sepicide[®] HB) was spray dried by the same optimal condition. Consequently, it was found that the surface topography of the spray dried particle was

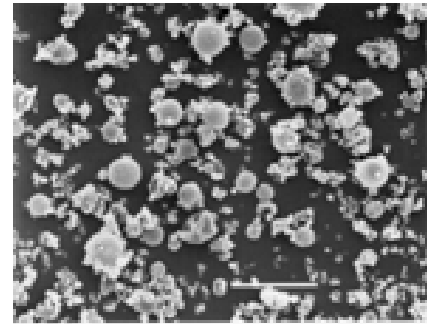
smooth (Figure 23j). From the results, it might be postulated that the shrinkage of particle surfaces was related to the presence of Sepicide[®] HB. Sepicide[®] HB consisted of phenoxyethanol, methylparaben, ethylparaben, propylparaben and butylparaben in propylene glycol. The solvent effect of propylene glycol might affect the evaporation of water from the spraying droplets. This finding also agreement with the previous research that solvent had influenced on particle size and morphology of ZnO preparation (Kanade et al., 2006).

3. Particle size and size distribution

In this study, the average particle size ($D [4, 3]$) and particle size distribution (Span value) were determined and compared between different inlet temperature and %aspirator values of xyloglucan spray dried particles. The particle sizes ranged from 8.26 ± 0.02 to $10.87 \pm 0.06 \mu\text{m}$ and the span values ranged from 2.33 ± 0.01 to $2.64 \pm 0.02 \mu\text{m}$ (Table 18). It was noticed that the particle size obtained from SEM, this method provided the same range of that obtained from light scattering method. As has been shown, an increase in inlet temperature could trended to increase the particle size whereas increasing %aspirator decreased the particle size. The correlation between the particle size and the inlet temperature was in agreement with the previous study that spray-dried insulin intended for inhalation (Stahl et al., 2002).

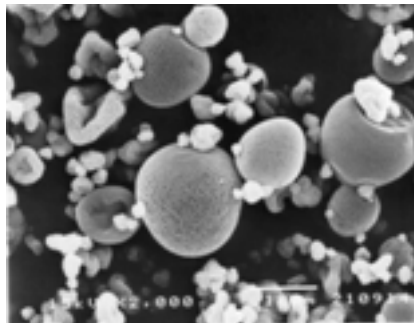


(× 2000)

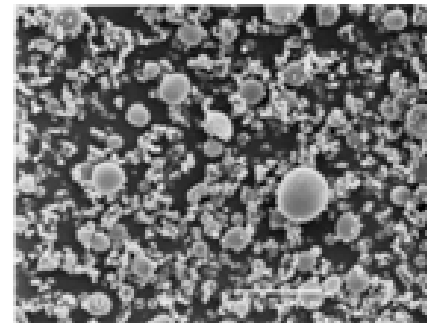


(×500)

(a) C1

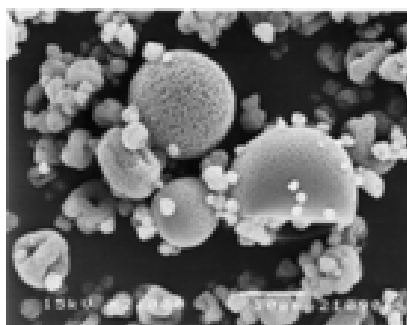


(× 2000)

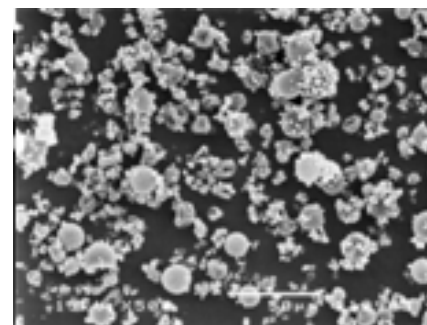


(×500)

(b) C2



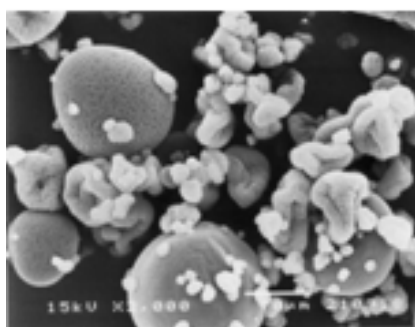
(× 2000)



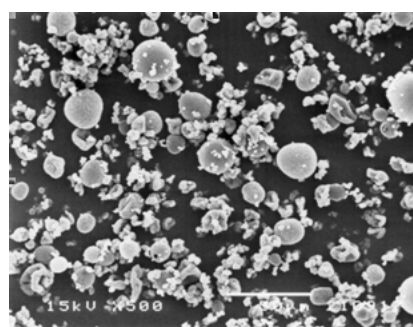
(×500)

(c) C3

Figure 23 Scanning electron photomicrographs of xyloglucan spray dried powder from experimental design

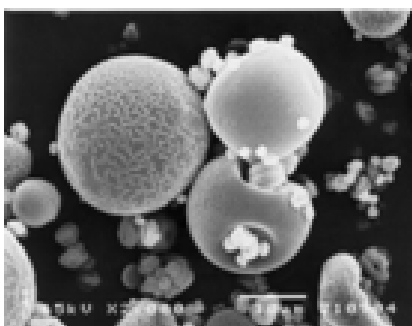


(× 2000)

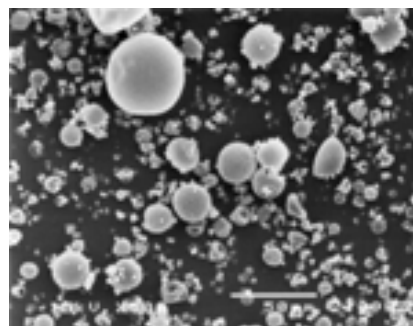


(×500)

(d) C4

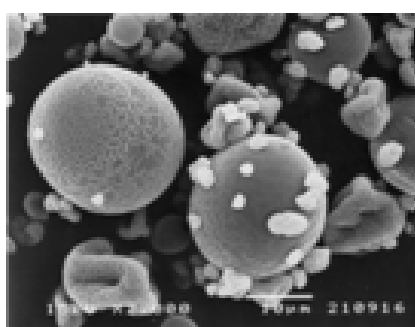


(× 2000)

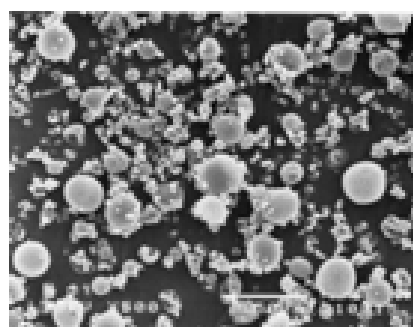


(×500)

(e) C5



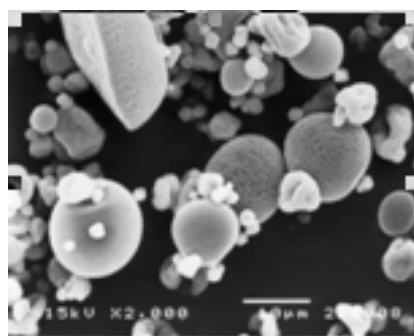
(× 2000)



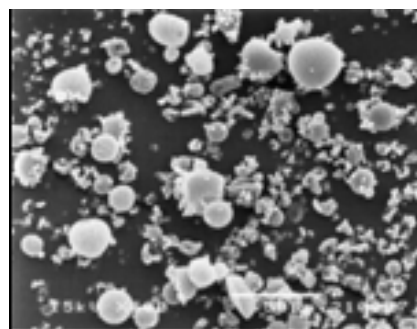
(×500)

(f) C6

Figure 23 Scanning electron photomicrographs of xyloglucan spray dried powder from experimental design (continued)

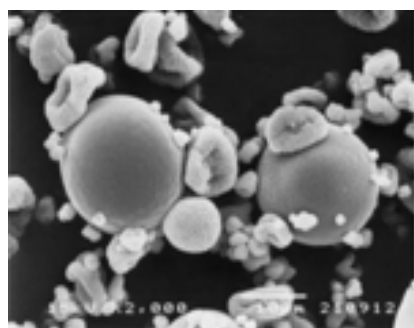


(× 2000)

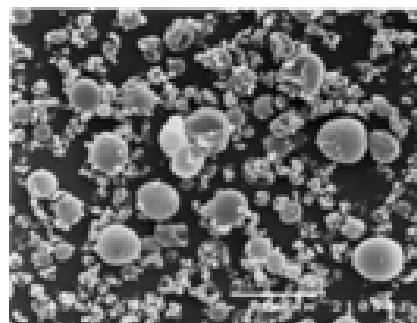


(×500)

(g) C7

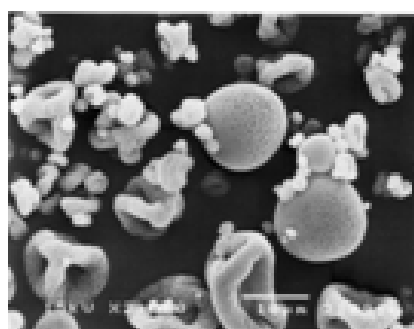


(× 2000)

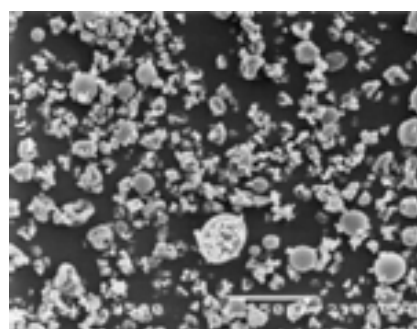


(×500)

(h) C8



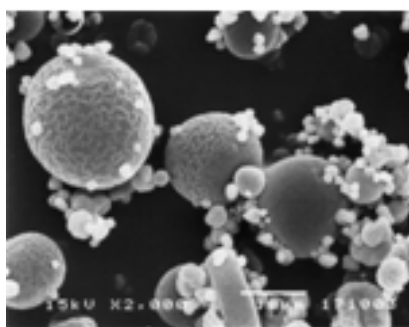
(× 2000)



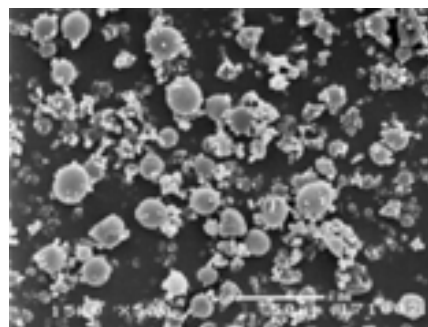
(×500)

(i) C9

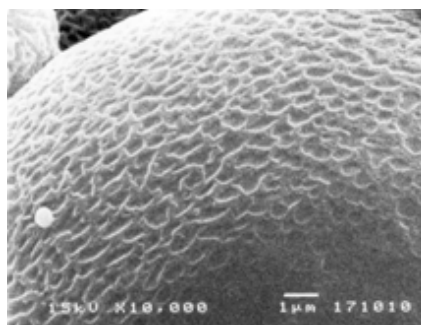
Figure 23 Scanning electron photomicrographs of xyloglucan spray dried powder from experimental design (continued)



(× 2000)

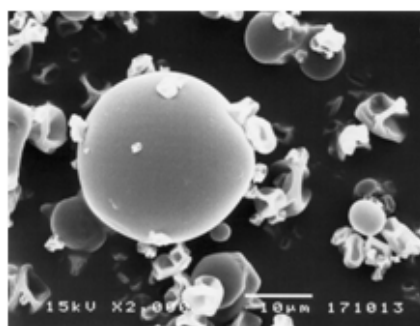


(×500)

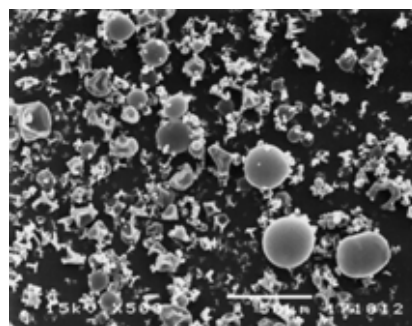


(×10,000)

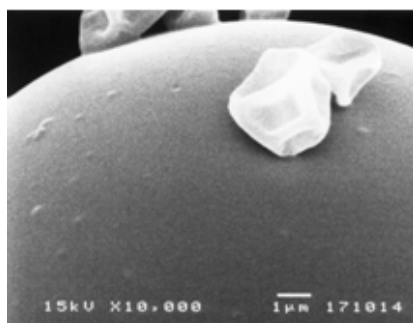
(i) Optimum sample



(× 2000)



(×500)



(× 10,000)

(j) Optimum sample without preservative

Figure 23 Scanning electron photomicrographs of xyloglucan spray dried powder from experimental design (continued)

Table 18 The particle size distributions of the xyloglucan spray dried particles
(mean \pm SD; n=3)

Factor		Average particle size	
Inlet temperature (°C)	% Aspirator	D [4, 3] \pm SD (μm)	Span \pm SD
120	80	11.15 \pm 0.04	2.43 \pm 0.02
200	80	10.86 \pm 0.05	2.63 \pm 0.01
120	100	8.26 \pm 0.02	2.60 \pm 0.02
200	100	9.66 \pm 0.02	2.33 \pm 0.01
120	90	9.16 \pm 0.06	2.37 \pm 0.03
200	90	10.40 \pm 0.03	2.47 \pm 0.01
160	80	9.94 \pm 0.06	2.64 \pm 0.02
160	100	9.66 \pm 0.11	2.45 \pm 0.01
160	90	9.45 \pm 0.14	2.59 \pm 0.01
178	100	10.87 \pm 0.06	2.47 \pm 0.01

C. Evaluation of physicochemical properties of xyloglucan powder from tamarind seeds

Xyloglucan powder was analyzed for the xyloglucan content by HPLC method (Appendix D) was exhibited that the content was 42.30 \pm 0.50%. There are 8 examined physicochemical properties of xyloglucan powder from tamarind seed in this study.

1. pH

The pH value of xyloglucan powder from tamarind seed was 7.83 \pm 0.19. This was in agreement with the report by Megazyme International Ireland Ltd in that the pH of xyloglucan standard ranged neutral.

2. Solubility in water

The solubility value in water of xyloglucan powder from tamarind seed was 6.28 \pm 0.08 mg/ml. This finding was lower than the data reported by Megazyme International Ireland Ltd in that the solubility value in hot water of standard was 10 mg/ml. This might be due to the differences of temperature of water in the studies and in purity of the spray dried powder obtained in this study from the commercial

standard. In this study, the xyloglucan content was approximately 42% and also composed of proteins, fats and other carbohydrates.

3. Viscosity and rheology property

Table 19 displays the viscosity values and rheology properties of 1%, 1.5% and 2% w/w of xyloglucan powder from tamarind seed in purified water. The viscosity of 1%, 1.5% and 2% w/w of xyloglucan powder from tamarind seed ranged from 39.46 ± 0.85 to 168.06 ± 1.83 . Xyloglucan solution of all concentrations exhibited typical Pseudoplastic flow (Figure 24). However, the result conformed with the report by Sims et al (1998) that xyloglucan solution was viscous and displayed non-Newtonian behavior. This was conflicting with the previous report that xyloglucan solution exhibited typical Newtonian flow (13th European Carbohydrate Symposium, 2005). The explanation might be possibly resulted the difference of purity of xyloglucan sample.

Table 19 The viscosity values and rheology properties of 1, 1.5 and 2% w/v of xyloglucan powder from tamarind seed (mean \pm SD)

%w/w of Xyloglucan extract	Viscosity (mPa)	Rheology
1%	39.46 ± 0.85	Pseudoplastic flow
1.5%	93.68 ± 0.91	Pseudoplastic flow
2%	168.06 ± 1.83	Pseudoplastic flow

4. Incompatibility of xyloglucan and ethanol

The study of the incompatibility of xyloglucan and ethanol was operated since ethanol was used in the solubilizing system of *Centella* extract in film formulation in the next study. Whereas, Suttananta (1986) and Tine et al. (2006) reported that xyloglucan could be precipitated by ethanol. In this study, incompatibility of xyloglucan and ethanol of 1% w/v of xyloglucan powder from tamarind seed was determined. Table 20 displays the percentages of remained and reduced xyloglucan after added with ethanol. The percentages of remained and reduced xyloglucan after added with 1-5% ethanol ranged from 82.53 ± 1.60 to 98.51 ± 1.53 and 1.49-17.47,

respectively. As the results, it was shown that the solution of xyloglucan powder from tamarind seed was incompatibility with ethanol in the range 1-5%.

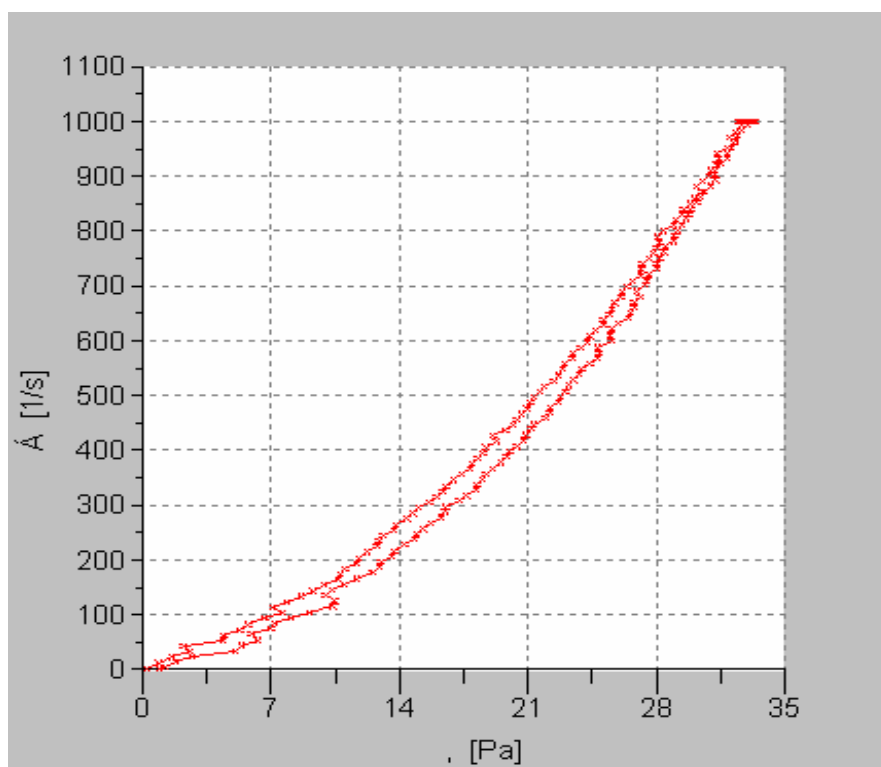


Figure 24 Rheogram of 1% w/v xyloglucan spray dried powder

Table 20 The percentage of remained and reduced xyloglucan after added with ethanol (Mean \pm SD)

%Ethanol	%Remained xyloglucan	% Xyloglucan loss
0	100	-
1	98.51 \pm 1.53	1.49
2	95.14 \pm 0.68	4.86
3	92.38 \pm 1.46	7.62
4	86.16 \pm 1.86	13.14
5	82.53 \pm 1.60	17.47

5. Differential scanning calorimetric thermograms

The DSC thermograms of standard xyloglucan and xyloglucan powder from tamarind seed are shown in Figures 25. It was found that there were broad endotherms in both standard xyloglucan and xyloglucan powder (40-120°C). This might be caused by the loss of moisture absorbed in the standard xyloglucan and xyloglucan powder. From the diffractogram, it was clear that both standard xyloglucan and xyloglucan spray dried powders showed no melting endotherm. However, at high temperatures than 290°C, it was noticed that standard xyloglucan and xyloglucan spray dried powders showed degradation. It might conclude that xyloglucan spray dried powder existed in an amorphous state.

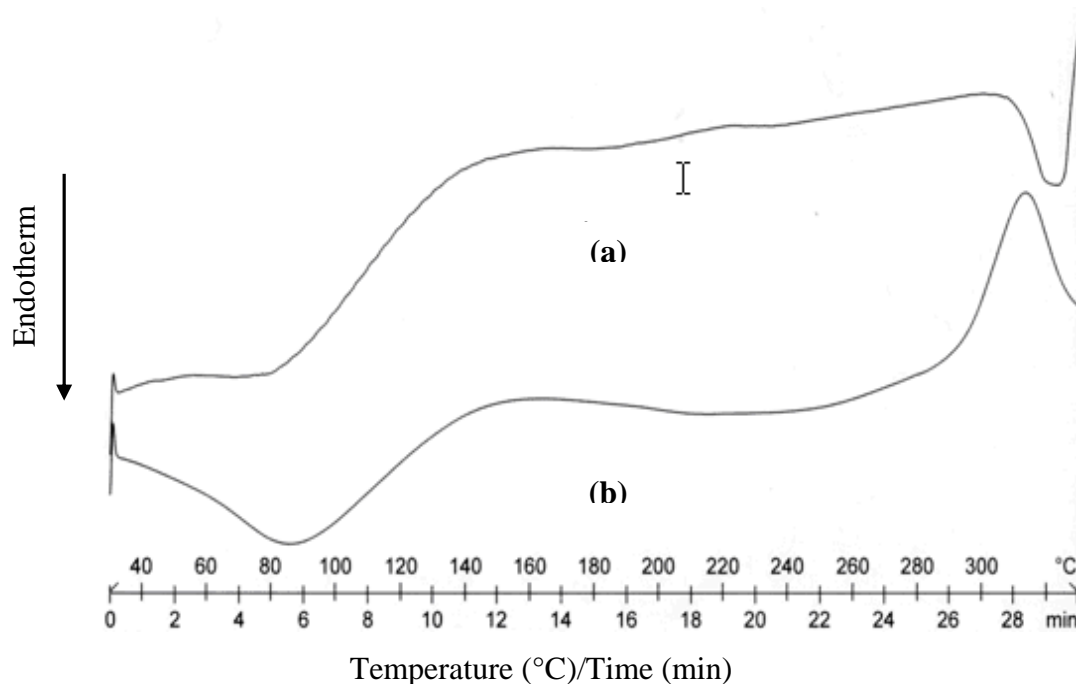


Figure 25 The DSC thermograms of standard xyloglucan and xyloglucan powder from tamarind seed

(a) Standard xyloglucan

(b) Xyloglucan powder from tamarind seed

6. Powder X-ray Diffractometry

Powder X-ray diffractometry may be used to detect crystallinity in the solid state. Figure 26 shows the X-ray diffractograms of standard xyloglucan and xyloglucan powder from tamarind seed. The diffractograms of standard xyloglucan and xyloglucan powder did not present intense diffraction peaks so, the standard xyloglucan and tamarind seed xyloglucan existed in an amorphous state. The result confirmed the observation that obtained from the DSC thermograms.

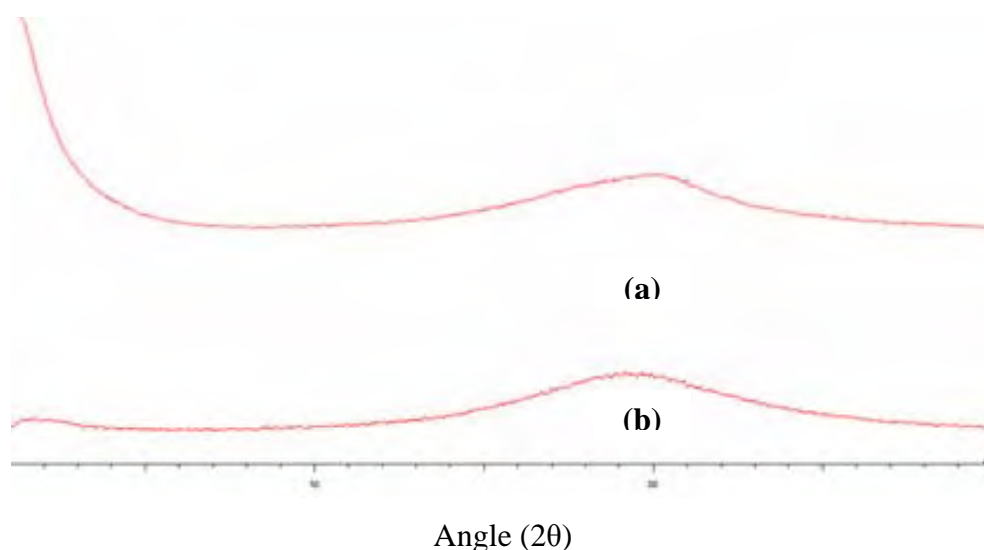


Figure 26 X-ray diffractograms of standard xyloglucan and xyloglucan powder from tamarind seed

(a) Standard xyloglucan

(b) Xyloglucan powder from tamarind seed

7. Particle size and size distribution

Figure 27 displayed scanning electron microscopy (SEM) of xyloglucan powder from tamarind seed. Topography of xyloglucan powder were very small spheres some with smooth surfaced but some were shrunk. The average particle size ($D [4, 3]$) and particle size distribution (Span value) of xyloglucan powder were 11.49 ± 0.11 and 2.47 ± 0.02 , respectively.

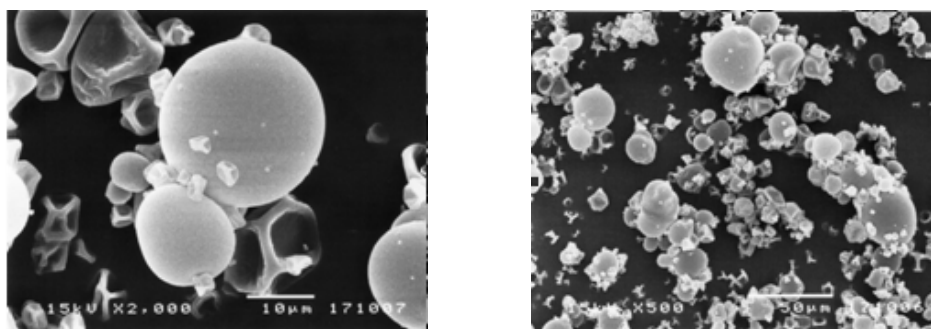


Figure 27 Scanning electron photomicrographs of xyloglucan powder

D. Evaluation of film formulations prepared from xyloglucan spray dried powders containing *Centella asiatica* extract

1. Physical Appearances

All films prepared from xyloglucan spray dried powder were pale brown in color, transparent, smooth and flexible film (Figure 28). The thickness and weight of the films of $1 \times 1 \text{ cm}^2$ were in the range of 0.03-0.07 mm. and 6.90 ± 0.23 - 13.07 ± 0.20 mg, respectively (Table 21). Films formulation prepared from tamarind seed containing *Centella asiatica* extract, the thickness and film weight were 0.047 ± 0.006 mm and 12.71 ± 0.22 mg, respectively. This showed that the addition of *Centella* extract did not affect the physical appearance of the film.

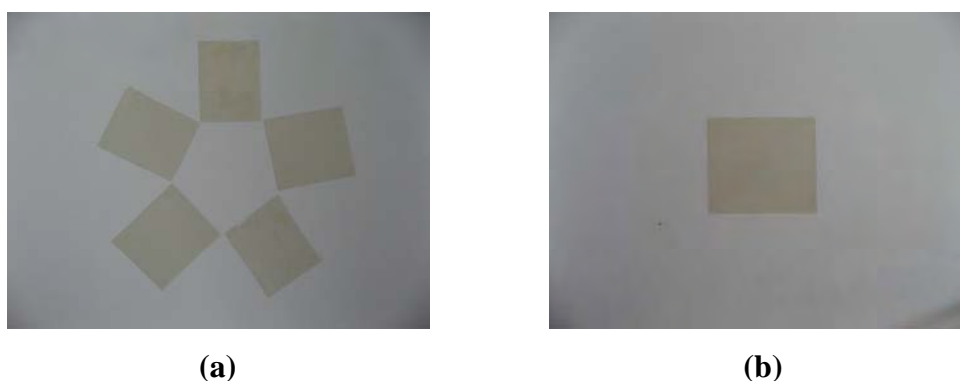


Figure 28 The appearance of films

(a) films prepared from xyloglucan powder

(b) films prepared from xyloglucan powder containing *Centella asiatica* extract

Table 21 The thickness and film weight data of films (mean \pm SD)

Formulation	Thick (mm)	Film weight (mg)
F1	0.05 \pm 0.00	11.54 \pm 0.39
F2	0.06 \pm 0.00	11.23 \pm 0.31
F3	0.03 \pm 0.00	14.99 \pm 0.33
F4	0.03 \pm 0.00	4.81 \pm 0.24
F5	0.03 \pm 0.00	9.72 \pm 0.32
F6	0.06 \pm 0.00	8.73 \pm 0.15
F7	0.06 \pm 0.00	7.72 \pm 0.25
F8	0.07 \pm 0.00	13.07 \pm 0.20
F9	0.07 \pm 0.00	6.90 \pm 0.23
F10	0.06 \pm 0.00	10.44 \pm 0.35
F11	0.05 \pm 0.00	9.58 \pm 0.38
F12	0.04 \pm 0.00	9.07 \pm 0.55
F13	0.04 \pm 0.00	9.36 \pm 0.36
F14	0.05 \pm 0.00	7.87 \pm 0.20
F15	0.04 \pm 0.00	8.21 \pm 0.34
Film with extract	0.05 \pm 0.006	12.71 \pm 0.22

2. Determination of adhesive force of film formulations

The adhesive force evaluated at a predetermined contact time was investigated using porcine skin as a model membrane. The force of maximum detachment force (force of adhesive) and work of adhesive as two parameters were used to evaluate the adhesive properties of films. The results in Table 22 show the adhesive force data of films.

The adhesive forces of films were in range 1.566 \pm 0.74-21.160 \pm 15.49 N/cm². As the results, it showed that the adhesive force of F6 was the highest value in all film formulation. In this study, F6 was selected to prepare the film formulation containing *Centella asiatica* extract. The adhesive force of film containing *Centella asiatica* extract was 3.703 \pm 1.11 N/cm². It was surprising that the incorporation of *Centella*

asiatica extract, the adhesive force of film much decreased. This effect might be resulted from the dispersing of *Centella* extract in film formulation that interfered the adhesive force between the xyloglucan film and porcine skin. It was found from the experimental data, that the standard deviation was high. The high standard derivation was possibly occurred from biological variation of porcine skin using in the test and xyloglucan powder from tamarind seed, which was the natural product resulting high variation, used in film formation.

3. Determination of mechanical properties of films and films formulation

A tensile testing gave an indication of the strength and elasticity of the film reflected by the following parameters: tensile strength, elongation and Young's modulus. Tensile strength or more accurately the ultimate tensile strength is the maximum tensile strength that a film can sustain. Elongation demonstrates the performance of a film to stretch before breaking. Young's modulus or the modulus of elasticity is the ratio of stress to strain over the linear part of stress–strain curve, and it is a measure of film stiffness (Ozdemir and Floros, 2008). It was found that a hard and tough film is greatly appropriate for the intended application as drug delivery systems for the skin. Their flexibility was sufficient for the movements of the skin without breaking, however, at the same time an increased strength for a prevention abrasion of the film caused for example by contact with clothing was apparent (Schroeder et al., 2007). The classification of films according to the value of tensile strength and %elongation is shown in Table 23.

The data of tensile strength, elongation, work of failure and Young's modulus of the films are displayed in Table 24. The tensile strength, elongation, work of failure and Young's modulus of the films were in range 2.77 ± 0.23 to 15.45 ± 3.38 MPa, 87.92 ± 13.38 to $568.60\pm 50.62\%$, 5.16 ± 0.77 to 28.72 ± 8.66 mJ and 2.48 ± 0.22 to 22.33 ± 7.03 MPa, respectively. It was found from the experimental data, that the standard deviations were high. The high standard deviations might possibly occur from xyloglucan powder from tamarind seed, which was the natural product resulting high variation.

Table 22 The force of adhesive data of films. (mean \pm SD)

Formulation	Force of adhesion (N/cm²)
F1	3.366 \pm 0.02
F2	2.616 \pm 0.71
F3	19.560 \pm 7.77
F4	6.029 \pm 2.58
F5	7.156 \pm 4.81
F6	21.160 \pm 15.49
F7	3.704 \pm 0.83
F8	2.312 \pm 2.42
F9	1.566 \pm 0.74
F10	13.480 \pm 10.66
F11	2.212 \pm 0.72
F12	3.659 \pm 0.97
F13	3.029 \pm 1.24
F14	1.733 \pm 0.18
F15	3.393 \pm 1.54
Film with extract	3.703 \pm 1.11

Table 23 The values of tensile strength and %elongation of classification of film (Schroeder et al., 2007).

Typical film	Value	
	Tensile Strength (MPa)	%Elongation
Soft and weak	low	low
Hard and brittle	high	low
Soft and tough	low	high
Hard and tough	high	high

F5 and F6 were composed of 4% w/w of sorbitol solution and 2% w/w glycerin but the percentage amounts of xyloglucan powder were different by 1 and 2% w/w, respectively. By comparison, an increase in % xyloglucan powder resulted in an increase in tensile strength of film but a decrease in Young's modulus and no difference of %elongation. Consequently, increasing %xyloglucan powder enabled film to be harder and tougher.

To compare F9 and F10 which contained different %glycerin, 0 and 4%, respectively but had similar compositions of xyloglucan powder and sorbitol solution, it was found that an increase in % glycerin resulted in lower tensile strength, lower Young's modulus and higher %elongation. As a result, film is softer and tougher when increasing %glycerin.

To compare F7 and F8 which had different percentage amounts sorbitol solution by 2 and 6%, respectively but had similar composition of xyloglucan powder and glycerin, it was found that an increase in sorbitol solution resulted in higher tensile strength, lower %elongation and no difference of Young's modulus. As a result, film is hard and brittle when increasing sorbitol solution.

The tensile strength, elongation, work of failure and Young's modulus of the films containing *Centella asiatica* extract were 15.11 ± 2.32 , 232.73 ± 17.50 , 12.24 ± 2.19 and 5.81 ± 1.18 , respectively. By comparison between F6 and the film containing *Centella asiatica* extract, it was found that adding *Centella asiatica* extract resulted in higher tensile strength, lower %elongation and no difference of Young's modulus. As a result, the film is harder. The previous research reported that a hard and tough film is greatly appropriate for the intended application as drug delivery systems for the skin (Schroeder et al., 2007). So, F6 might be appropriate film formulation.

Table 24 Mechanical property data of film formulations and film containing *Centella asiatica* extract (mean \pm SD)

Formulation	Tensile Strength (MPa)	%Elongation	Work of failure (mJ)	E-Mod (MPa)
F1	15.45 \pm 3.38	176.84 \pm 13.98	10.56 \pm 2.78	8.09 \pm 1.67
F2	4.74 \pm 0.81	375.20 \pm 42.75	13.88 \pm 3.32	2.96 \pm 0.39
F3	4.02 \pm 1.32	491.30 \pm 49.31	9.61 \pm 2.78	4.90 \pm 2.04
F4	14.50 \pm 0.56	128.10 \pm 14.78	5.16 \pm 0.77	17.92 \pm 4.09
F5	4.73 \pm 0.49	360.80 \pm 14.04	7.25 \pm 0.82	5.88 \pm 1.13
F6	12.03 \pm 0.91	357.60 \pm 73.39	23.67 \pm 6.76	4.46 \pm 0.31
F7	3.84 \pm 0.57	547.10 \pm 56.45	20.35 \pm 4.87	3.44 \pm 0.34
F8	6.90 \pm 1.95	164.83 \pm 19.544	5.94 \pm 1.65	3.83 \pm 0.48
F9	10.70 \pm 1.76	87.92 \pm 13.38	5.93 \pm 1.50	22.33 \pm 7.03
F10	2.77 \pm 0.23	494.10 \pm 64.49	11.95 \pm 2.88	2.48 \pm 0.22
F11	7.39 \pm 2.52	561.30 \pm 62.10	28.72 \pm 8.66	5.16 \pm 1.65
F12	3.61 \pm 0.80	525.00 \pm 27.82	15.08 \pm 1.11	3.80 \pm 0.73
F13	6.85 \pm 2.20	568.60 \pm 50.62	25.18 \pm 4.630	5.42 \pm 0.78
F14	5.79 \pm 0.62	513.50 \pm 6.47	20.66 \pm 3.32	3.99 \pm 0.42
F15	7.04 \pm 2.56	503.30 \pm 117.85	23.52 \pm 10.77	6.84 \pm 3.43
Film containing <i>Centella asiatica</i>	15.11 \pm 2.32	232.73 \pm 17.50	12.24 \pm 2.19	5.81 \pm 1.18

4. Differential scanning calorimetric thermograms

The DSC thermograms of *Centella asiatica* extract, film prepared from xyloglucan powder and film prepared from xyloglucan powder containing *Centella asiatica* extract were depicted in Figure 29. The DSC thermogram of the *Centella asiatica* extract showed the endothermic melting peaks at 238°C. The result showed that there was at least one component in *Centella asiatica* extract was in crystalline form. Film prepared from xyloglucan powder exhibited no melting peak. In addition, it was found that the endothermic peak corresponding to *Centella* extract melting was not observed in the thermograms of film formulation containing *Centella asiatica* extract. The

results might be explained that the *Centella* extract in film formulation was uniformly dispersed in an amorphous state.

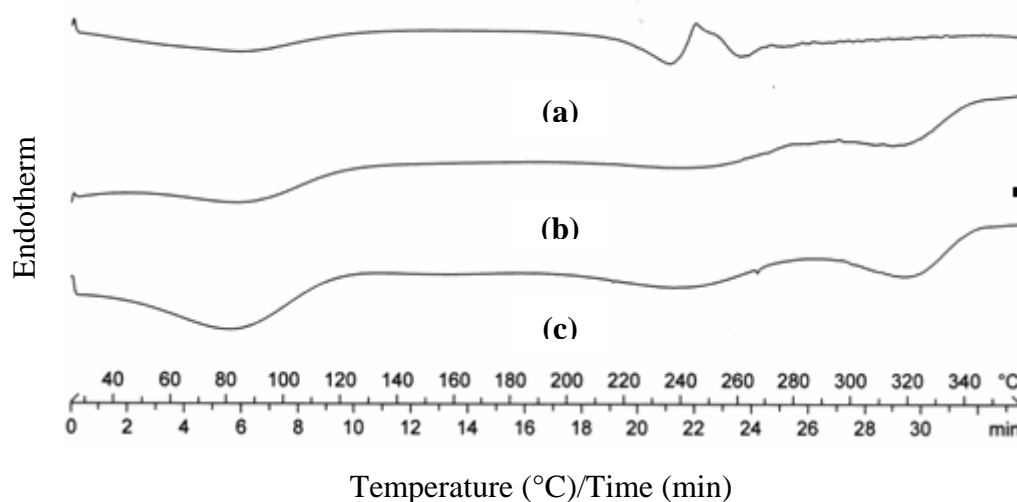


Figure 29 The DSC thermograms of *Centella asiatica* extract, film prepared from xyloglucan powder and film prepared from xyloglucan powder containing *Centella asiatica* extract;

- (a) *Centella asiatica* extract
- (b) Film prepared from xyloglucan powder
- (c) Film prepared from xyloglucan powder containing *Centella asiatica* extract

5. Powder X-ray Diffractometry

The x-ray diffractograms of *Centella asiatica* extract, film prepared from xyloglucan powder and film prepared from xyloglucan powder containing *Centella asiatica* extract are shown in Figure 30.

The diffractograms of *Centella asiatica* extract exhibited a series of intense diffraction peaks, which indicative of their crystalline characteristic. The prominent peaks of x-ray diffractogram of *Centella asiatica* extract were particularly observed at 5.11° , 13.88° , 14.24° and 15.29° , respectively. Whereas the diffractograms of film prepared from xyloglucan powder and film prepared from xyloglucan powder containing *Centella asiatica* extract did not present intense diffraction peak. This result conformed to the DSC thermograms (Figure 28). It might be concluded that the

Centella extract was molecularly dispersed with film prepared from xyloglucan powder or existed in an amorphous state.

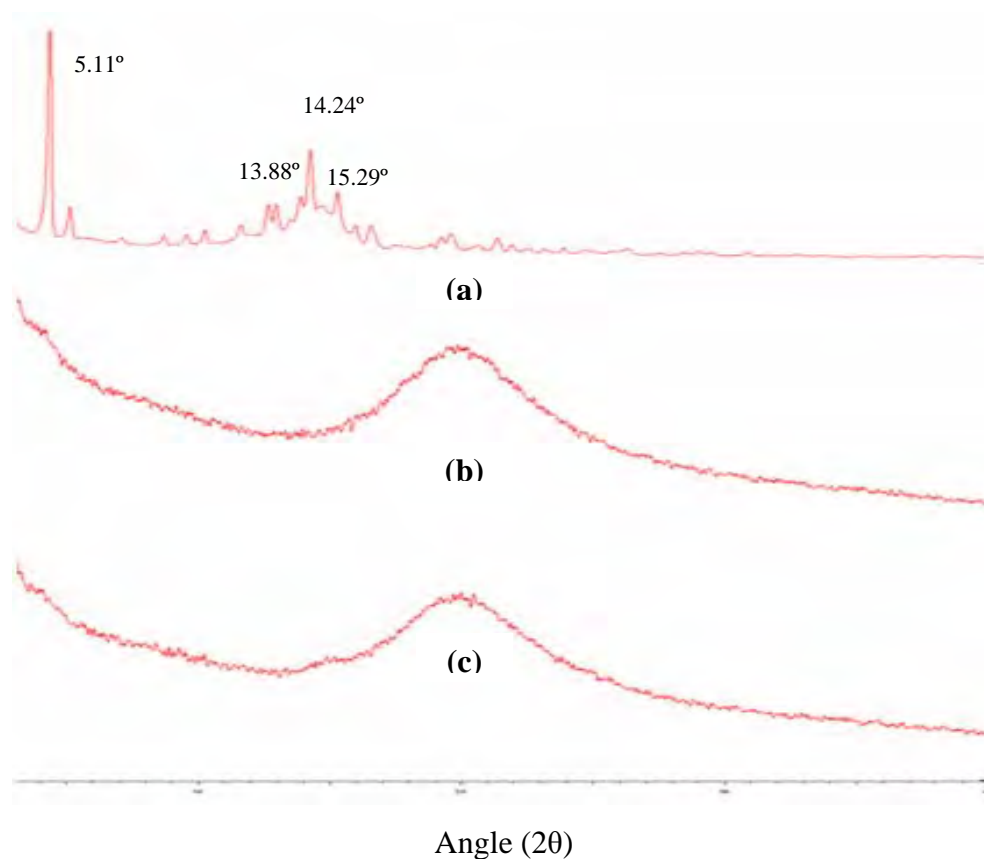


Figure 30 X-ray diffractograms of *Centella asiatica* extract, film prepared from xyloglucan powder and film prepared from xyloglucan powder containing *Centella asiatica* extract;

(a) *Centella asiatica* extract

(b) Film prepared from xyloglucan powder

(c) Film prepared from xyloglucan powder containing *Centella asiatica* extract

6. Release study

Figure 31 and Table 25 presented the release data and release profiles of asiaticoside from film formulation containing *Centella asiatica* extract, respectively. The amount released of asiaticoside was exhibited to be more than 50% within 8 hours from film formulation. The release data over the whole time period were

explained according to the treatment proposed by Higuchi for asiaticoside release from film formulation.

$$Q_t = k_H t^{1/2}$$

where:

Q_t is the amount of drug release at time t

k_H is the release rate constants of Higuchi

t is the release time

Plots of the cumulative amount Q_t of drug released versus the square root of time were a short lag period (initial 50–60% release) (Figure 32). The coefficient of determination of the relationship between cumulative amount releases versus square root of time (R^2) of asiaticoside was $0.9861\%h^{-1/2}$. This finding was in agreement with Takahachi et al. (2002) in percutaneous absorption of non-steroidal anti-inflammatory drugs from in situ gelling xyloglucan formulations. Amount of drugs from formulations were released according to Higuchi model.

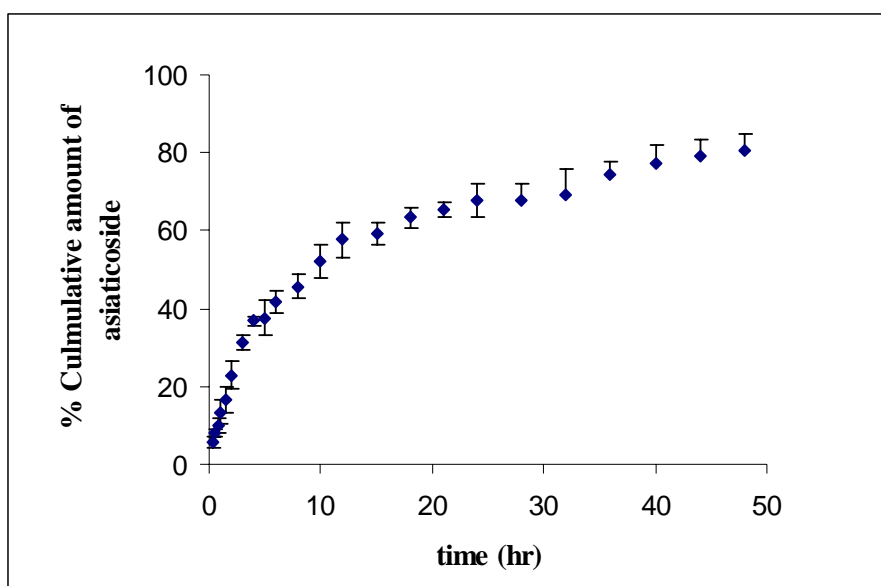


Figure 31 The release profiles of asiaticoside from film formulation

Table 25 The release data of asiaticoside from film formulation (mean \pm SD)

Time (hrs)	% Cumulative release of asiaticoside Mean \pm SD
0	0
0.25	5.69 \pm 1.24
0.5	8.13 \pm 1.07
0.75	9.95 \pm 2.13
1	13.30 \pm 3.08
1.5	16.47 \pm 3.28
2	22.91 \pm 3.43
3	31.28 \pm 2.07
4	36.82 \pm 1.27
5	37.63 \pm 4.57
6	41.64 \pm 2.72
8	45.68 \pm 3.22
10	51.95 \pm 4.23
12	57.60 \pm 4.51
15	59.32 \pm 2.90
18	63.34 \pm 2.63
21	65.37 \pm 2.10
24	67.56 \pm 4.28
28	67.54 \pm 4.45
32	74.61 \pm 2.89
36	77.37 \pm 4.54
40	79.01 \pm 4.24
48	80.75 \pm 3.99

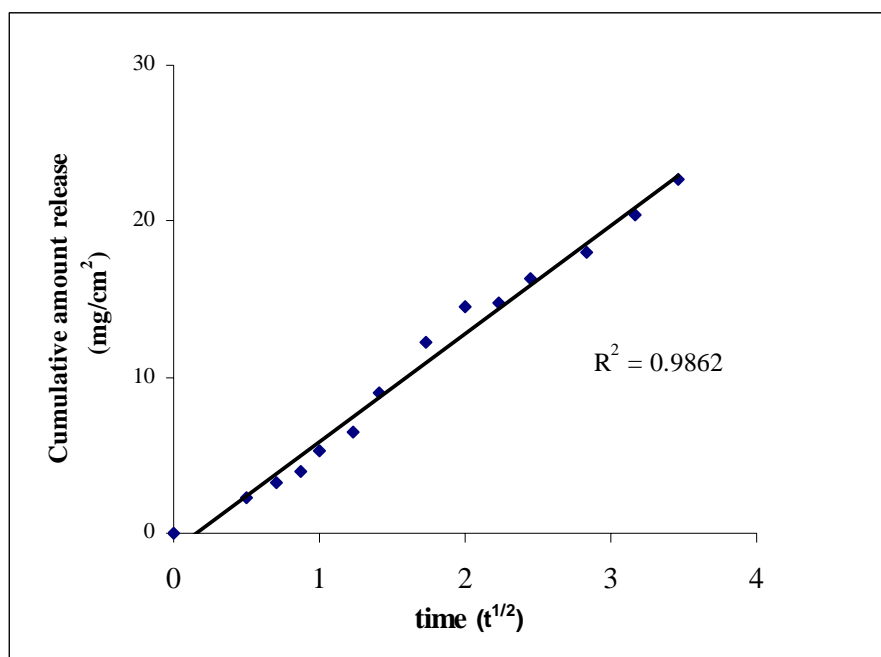


Figure 32 Cumulative releases per unit area, Q , for asiaticoside as a function of square root time from film formulation

7. Permeation study

The permeation study of asiaticoside from film prepared from xyloglucan powder for 24 hours was investigated. The porcine skin was used to be as a model membrane. It found that the asiaticoside which was one of the active components of *Centella asiatica* extract in film formulation could not be detected by HPLC method in the sample taken from the receptor along the study period. The amount asiaticoside inside the porcine skin which, used in the study and film formulation in donor of Franz diffusion cell were determined after the experiment had finished. It found that the percentage of asiaticoside in some porcine skin was so low that it could not be analyzed. The percentage of asiaticoside remaining from film formulation in donor of Franz diffusion cell and porcine skin were $91.14 \pm 1.84\%$ and $1.30 \pm 1.28\%$, respectively (Table 26). Although asiaticoside could not permeate through the porcine skin, it could release from film formulation. This result could confirmed that asiaticoside in film formulation could be used for wound healing due to most wounds lost stratum corneum that was barrier.

From the results, there were some possible explanations as follows. This might be occurred because asiaticoside could not permeate through porcine skin. Since there

was about 7.56% of asiaticoside that could not be detected and explained, this might be the limitation of the analysis of asiaticoside in porcine skin. Moreover, it was possible that asiaticoside might decompose and change to asiatic acid which was the other one active component of *Centella* extract. The HPLC system in the study did not detect and analyse asiatic acid. If this explanation was valid, it was believable that asiaticoside could permeate into the porcine skin and remained present in the form of asiatic acid (Appendix G)

Table 26 The percentage of asiaticoside from film formulations in donor of Franz diffusion cell and porcine skin

Site	% Asiaticoside			Mean	SD
	set 1	set 2	set 3		
Donor's Franz cell	92.51	91.86	89.05	91.14	1.84
Porcine skin	1.33	-	2.56	1.30	1.28

8. Stability study

8.1 Chemical stability study

The stability testing was determined on the film formulation containing *Centella asiatica* extract that had been stored in stressed conditions at the temperature at 40 ± 2 °C and the humidity at $75\pm 5\%$ RH. The amounts of asiaticoside in film prepared from xyloglucan powder was analyzed by HPLC method at the initial time, first, second and third month. The % labeled amount of test preparations which determined at initial time was found to be 93.85%.

From the result, the percentage loss of asiaticoside during 3 months periods was 16.41% (Table 27). The film formulation containing *Centella asiatica* extract were not stable during 3 months periods because the percentage loss of asiaticoside was more than 10% of the initial value (Cartensen, 1990).

It was reported by Hengsawas (2004) that asiaticoside probably be degraded by peroxide, acid and alkaline agents. A degradation of Asiaticoside caused by oxidation mechanism to obtain other compounds while was hydrolyzed by hydronium/hydroxide ion to obtain asiatic acid and sugar moiety, glucose and rhamnose

There were some factors that enhance the degradation of asiaticoside in film formulation containing *Centella asiatica* extract. The first factor, xyloglucan powder

from tamarind seed had hygroscopic property. After the stress condition for 3 periods, asiaticoside was increasingly degraded by hydrolysis due to water content increased in film formulation. The second, the package which used in the study for the film formulation containing *Centella asiatica* extract could not protect the film formulation moisture resulted to hydrolysis.

Table 27 The percentages labeled amount of asiaticoside in film formulation containing *Centella asiatica* extract in stability test (mean \pm SD)

Periods	%Loss of asiaticoside
Initial	0
1 st month	7.37
2 nd month	13.6
3 rd month	16.41

$$\% \text{ loss} = \frac{\text{initial} - \text{final}}{\text{initial}} \times 100$$

% labeled amount

8.2 Adhesive property study

Table 28 displayed adhesive properties of film formulation containing *Centella asiatica* extract at 0, 1, 2 and 3 months period. The results were tested by the analysis of variance (ANOVA) at significant level 0.05. According to analytical statistics, adhesive force reduced significantly after the stress condition for 3 months. This might be resulted to the inappropriate packaging of the moisture sensitive product.

Table 28 Adhesive properties data of asiaticoside in film formulation in stability test (mean \pm SD)

Periods	Force of adhesion (N/cm ²)
Initial	3.703 \pm 1.11
1 st month	2.927 \pm 0.64*
2 nd month	2.825 \pm 0.11*
3 rd month	2.523 \pm 0.29*

* Significant at P value = 0.05

8.3 Mechanical properties study

Table 29 showed mechanical properties of film formulation containing *Centella asiatica* extract at 0, 1, 2 and 3 months period. The results were tested by the analysis of variance (ANOVA) at significant level 0.05. According to analytical statistics, it was found that tensile strength reduced significantly, %elongation increased significantly and work of failure and Young's modulus differ no significant. As a result, film was soft and tough after the stress condition for 3 months due to water content in film formulation increased that would be supported by the endothermic energy increased in DSC thermogram (Figure 33). The similar reason explains the result as in the adhesive property study. In the case of moisture sensitive product such as adhesive film, the appropriate packaging was most important to physical and chemical properties of the film.

Table 29 Mechanical properties data of asiaticoside in film formulation in stability test (mean \pm SD)

Periods	Tensile Strength (MPa)	%Elongation	Work of Failure (mJ)	E-Mod (MPa)
Initial	15.11 \pm 2.32	232.73 \pm 17.50	12.24 \pm 2.19	5.81 \pm 1.18
1 st month	6.71 \pm 0.72*	364.27 \pm 26.85*	12.49 \pm 1.63	3.54 \pm 0.45
2 nd month	5.87 \pm 2.61*	507.47 \pm 29.50*	20.27 \pm 8.31	3.76 \pm 1.33
3 rd month	3.69 \pm 0.13*	472.63 \pm 19.90*	12.03 \pm 0.52	3.46 \pm 0.01

* Significant at *P value* = 0.05

8.4 Differential scanning calorimetric thermograms

The application of DSC thermogram change effectively investigates the physicochemical stability of the film formulation containing *Centella asiatica* extract. As the results of the DSC thermograms of the film formulation, no change in DSC thermograms between three months of stability study as compared to that at the initial was observed. Consequently, the film formulation led to no change in physicochemical properties after the stress condition for 3 months (Figure 33). The *Centella* extract showed the stable existence in film as an amorphous state. Additionally, The very broad endothermic peaks of films formulation containing *Centella* extract after the stress condition at 0, 1, 2 and 3 months were found to be in

range 40-120°C. Moreover, the endothermic energy of peaks after the stress condition at 0, 1, 2 and 3 month were found to be 486.19 mJ, 389.49 mJ, 1120.18 mJ and 719.42 mJ, respectively. These peaks were caused by the loss of moisture absorbed or dehydration in the films (Wang et al., 2002). The endothermic energy after storage were observed clearly higher than that of initial time. These results were conformed that the film prepared tamarind seed xyloglucan had hygroscopic properties. The finding might be explainable to the decomposition by hydrolysis of asiaticoside to asiatic acid in the film, the decrease of adhesive force and the change of mechanical properties of the film.

8.5 Powder X-ray Diffractometry

The powder x-ray diffraction study was carried out to elevating film formulation containing *Centella asiatica* extract. No change in diffractograms between three months of stability study was found when compared with that at the initial time. These results were conformed the DSC study that the film formulation did not change in physicochemical properties after the stress condition for 3 months (Figure 34). The diffraction peak correspond to crystallinity of *Centella asiatica* extract in all diffractograms was not observed.

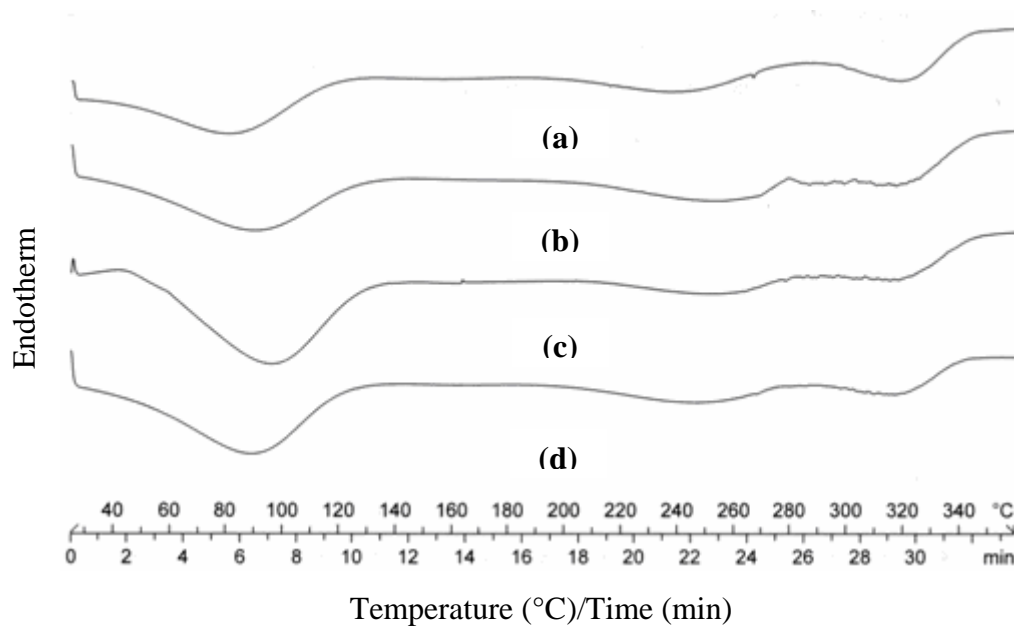


Figure 33 DSC thermograms of film formulation after stress condition (40° C, 75%

RH);

(a) at initial time

(b) at first month

(c) at second month

(d) at third month

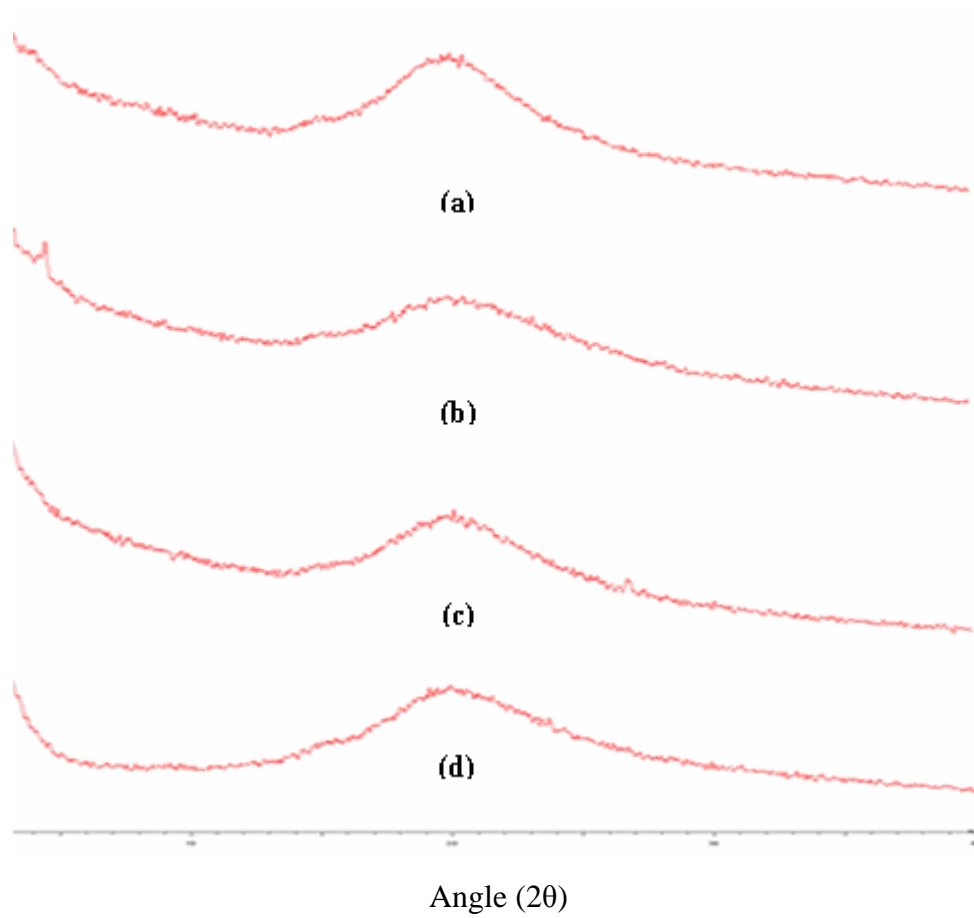


Figure 34 X-ray diffractograms of film formulation after stress condition (40° C, 75% RH);

- (a) at initial time
- (b) at first month
- (c) at second month
- (d) at third month

CHAPTER V

CONCLUSIONS

The present study was aimed to develop the extraction method of xyloglucan from tamarind seed. The appropriate extraction method was evaluated by the defatting and sedimentation technique, and investigation of xyloglucan, total protein and fat contents. The spray drying technique was optimized to obtain the optimal condition for preparing xyloglucan powder. After that, film formulation were prepared from xyloglucan and loaded with *Centella asiatica* extract. The result of the investigation can be concluded as follows:

1. Among the four methods of xyloglucan extraction, method I with direct by soaked tamarind seed powder with hexane and sediment the slurry of tamarind seed powder in water immediately by centrifugation was selected.

2. Xyloglucan contents, which were analyzed by the HPLC method, were not significantly different among four methods. The xyloglucan content obtained ranged from 42.85-44.62%. The extraction method could reduced contaminated total protein and fat content.

3. The optimization techniques were operated for spray drying condition of xyloglucan solution, estimated by response surface methodology. The optimum region of the spray-drying technique by overlay plot was carried out. The optimal condition was inlet temperature 178°C and aspirator 100%. The observed means of the responses obtained, %yield and %moisture content, were in range of the prediction intervals at 95% confidence level. The results clearly showed that the model fitted the experimental data well and described the region studied well.

4. The xyloglucan tamarind seed powder which was obtained from the optimal spray drying condition had small shape average particle size $10.87 \pm 0.06\mu\text{m}$ with spherical shape, and finely rough surface.

5. The physicochemical properties of xyloglucan tamarind seed powder were as follows:

5.1 The pH value of 1% xyloglucan solution was 7.83 ± 0.19 .

5.2 The solubility in water was 6.28 ± 0.08 mg/ml.

5.3 The viscosity of 1%, 1.5% and 2% w/w of xyloglucan tamarind seed powder were ranged from 39.46 ± 0.85 to 168.06 ± 1.83 mPas. At all concentrations of xyloglucan powder from tamarind seed exhibited a typical pseudoplastic flow.

5.4 The 1%w/v solution of xyloglucan tamarind seed powder was not compatible to ethanol added 1-5%.

6. The appropriate film formulations prepared from xyloglucan powder was obtained. The formulation contained 2%w/w xyloglucan powder, 2%w/w glycerin and 4%w/w sorbitol containing *Centella asiatica* extract. The selected formulation exhibited the highest adhesive force at 21.16 ± 15.49 N/cm².

7. The film formulation containing *Centella asiatica* extract was pale brown color, transparent, smooth and flexible. It was hard and tough. The adhesive force of film formulation was reduced to 3.703 ± 1.11 N/cm². The tensile strength, elongation, work of failure and Young's modulus of the films formulation were 15.11 ± 2.32 MPa, $332.73 \pm 17.50\%$, 12.24 ± 2.19 mJ and 5.81 ± 1.18 MPa, respectively.

8. The film formulation containing *Centella asiatica* extract exhibited, from the DSC thermograms and powder X-ray diffactograms, that the *Centella* extract was uniformly dispersed in an amorphous state.

9. The release profile of asiaticoside from film formulation containing *Centella asiatica* extract were fitted with Higuchi model ($R^2 = 0.9862$). The release rate constant was demonstrated to be $6.9233 \%h^{-1/2}$.

10. The permeation study using porcine skin as a model membrane showed the absence of asiaticoside detected in the receptor fluid. The asiaticoside remained in the porcine skin could be detected at $1.30 \pm 1.28\%$.

11. From stability study, the film formulation containing *Centella asiatica* extract during 3 month periods showed the percentage loss of asiaticoside was 16.41% of the initial value. The loss might be due to the degradation by hydrolysis of asiaticoside to asiatic acid in the presence of moisture adsorbed in the film.

REFERENCES

- Belcaro, G.V., Grimaldi, R., and Guidi, G. 1990. Improvement of capillary permeability in patients with venous hypertension after treatment with TTFCa. Angiology 41: 533-540.
- Billona, A., Bataillea, B., Cassanasb, G., and Jacoba, M. 2000. Development of spray-dried acetaminophen microparticles using experimental designs. International Journal of Pharmaceutics 203: 159-168.
- Brinkhaus, B., Lindner, M., Schuppan, D., and Hahn, E.G. 2000. Chemical, pharmacological and clinical profile of the East Asian medical plant *Centella asiatica* Phytomedicine 7: 427-448.
- Broadhead, J., Rouan, S.K.E., Hua, I., and Rhodes, C.T. 1994. The effect of process a formulation variables on the properties of spray-dried β -galactosidase. Journal of Pharmaceutics and Pharmacology 46: 458–467.
- BÜCHI Labortechnik AG. 1997. Training Papers Spray Drying [Online]. Available from: http://www.buchi.com/uploads/media/Distillation_and_Environment.pdf [2007, October 20]
- Burgalassi, S., Panichi, L., Saettone, M.F., Jacobsen, J., and Rassing, M.R. 1996. Development and in vitro/in vivo testing of mucoadhesive buccal patches releasing benzydamine and lidocaine. International Journal of Pharmaceutics 133: 1-7.
- Cartensen, J.T. 1990. Drug stability. New York: Marcel Dekker.
- Chawla, A., Taylor, K.M.G., Newton, J.M., and Johnson, M.C.R. 1994. Production of spray dried salbutamol sulphate for use in dry powder aerosol formulation. International Journal of Pharmaceutics 108: 233-240.
- Cheng, C., and Koo, M. 2000. Effects of *Centella asiatica* on ethanol induced gastric mucosal lesions in rats. Life Sciences 67: 2647–2653.
- Douglas MacKay, D., and Miller, A.L. 2003. Nutritional Support for Wound Healing. Alternative Medicine Review. 8: 359-377.
- Freitasa, R.A., Martinb, S., Santosc, G.L., Valengac, F., Buckeridged, M.S., Reicherb, F., and Sierakowskic, M.R. 2005. Physico-chemical properties of seed xyloglucans from different sources. Carbohydrate polymers 60: 507-514.

- Hadgraft, J., and Guy, R.H. 2002. Transdermal drug delivery: Developmental Issues and Research Initiatives. 2nd ed. New York: Marcel Dekker, Inc.
- Hengsawas, Sorya. 2004. Formulation, evaluation and scale-up production of *Centella asiatica* extract film coated tablets. Master's Thesis, Faculty of Pharmaceutical Sciences, Chulalongkorn University.
- Hiroshi, U., Mitsuru, M., and Kanji, K. 2002. Diversity and Versatility of Plant Seed Xyloglucan. Trends in Glycoscience and Glycotechnology 14: 355–376.
- Hoffman, M., Jia, Z., J. Pena, M., Cash, M., Harper, A., Blackburn II, A.R., Darvill, A., and York, W.S. 2005. Structural analysis of xyloglucans in the primary cell walls of plants in the subclass Asteridae. Carbohydrate Research 340: 1826–1840.
- Ikeda, S., Nitta, Y., Kim, B.S., Temsiripong, T., Pongsawatamanit, R., and Nishinari, K. 2004. Single-phase mixed gels of xyloglucan and gellan. Food Hydrocolloids 18: 669-675.
- Kabovloi, W. 2004. Effect of oils, surfactants and cosurfactants on physicochemical properties and permeation of *Centella Asiatica* extract in microemulsions. Master's Thesis, Faculty of Pharmaceutical Sciences, Chulalongkorn University.
- Kanade, K.G., Kale, B.B., Aiyer, R.C., and Das, B.K. 2006. Effect of solvents on the synthesis of nano-size zinc oxide and its properties. Materials Research Bulletin 41: 590-600.
- Kawasaki, N., Ohkura, R., Miyazaki, S., Uno, Y., Sgimoto, S., and Attwood, D. 1999. Thermally reversible xyloglucan gels as vehicles for oral drug delivery. International Journal of Pharmaceutics 181: 227-234.
- Kongthong, B. 2004. Development of the quantitative determination of asiaticoside, madecassoside, Asiatic acid and madecassia acid in *Centella asiatica* (Linn.) urban by high-performance liquid chromatography. Master's Thesis, Faculty of Pharmaceutical Sciences, Chulalongkorn University.
- Kulkarni, D., Dwivedi, A.K., Sarin, J.P.S., and Singh, S. 1997. Tamarind seed polyose: A potential polysaccharide for sustained release of verapamil hydrochloride as a model drug. Indian Journal of Pharmaceutical Sciences 59: 1-7.

- Lawrence, J.C. 1967. The morphological and pharmacological effects of asiaticoside upon skin in vitro and in vivo. European Journal of Pharmacology 1: 414-424.
- Lewis, Y.S., and Neelakantan, S. 1964. The chemistry, biochemistry and technology of tamarind. Journal Sciences Industry Research 23: 204-206.
- Lu, L., Ying, K., Wei, S., Fang, Y., Liu, Y., Lin, H., Ma, L., and Mao, Y. 2004. Asiaticoside induction for cell-cycle progression, proliferation and collagen synthesis in human dermal fibroblasts. International Journal of Dermatology 43: 801-807.
- MacKay, D., and Miller, A.L. 2003. Nutritional Support for Wound Healing. Alternative Medicine Review 8: 359-377.
- Megazyme International Ireland Ltd. 2002. Xyloglucan oligosaccharides[Online]. (n.d.). Available from: <http://www.megazyme.com/downloads/en/data/O-IPRM.pdf>[2005, Nov 1]
- Master, K. 1979. Spray drying handbook. 3rd ed. New York: John Willey & Sons.
- Mathiowitz, E., Chickering, D.E., and Lehr, C.M. 1999. Bioadhesive Drug Delivery Systems: Fundamentals, Novel Approaches, and Development. 1st ed. New York: CRC Publish.
- Miyazaki, S., Kawasaki, N., Kubo, W., Endo, K., and Attwood, D. 2001. Comparison of in situ gelling formulations for the oral delivery of cimetidine. International Journal of Pharmaceutics 220: 161–168.
- Miyazaki, S., Suisha, F., Kawasaki, N., Shirakawa, M., Yamatoya, K., and Attwood, D. 1998. Thermally reversible xyloglucan gels as vehicles for rectal drug delivery. Journal of Controlled Release 56: 75-83.
- Miyazaki, S., Suzuki, S., Kawasaki, N., Endo, K., Takahashi, A., and Attwood, D. 2001. In situ gelling xyloglucan formulations for sustained release ocular delivery of pilocarpine hydrochloride. International Journal of Pharmaceutics 229: 29–36.
- Molinariolo, S.E., Thompson, N.S., and Stratton, R.A. 1990. Xyloglucan sorption onto cellulose. Atlanta, Georgia: the Institute, Georgia Institute of Technology 363: 1-5.

- Myers, R.H. and Montgomery, D.C. 2002. Building Empirical Models. In A. Wayne (ed.), Response Surface Methodology: Process and Product Optimization Using Designed Experiments. 2nd ed. John Wiley & Sons (Asia) Pte Ltd.
- Ozdemir, M., and Floros, J.D. 2008. Optimization of edible whey protein films containing preservatives for mechanical and optical properties. Journal of Food Engineering 84: 116-123.
- Picout, D.R., Ross-Murphy, S.B., Errington, N., and Harding, S.E. 2003. Pressure cell assisted solubilization of xyloglucan: Tamarind seed polysaccharide and Detarium gum. Biomacromolecules 4: 799-807.
- Pongsawatmanit, R., Temsiripong, T., Ikeda, S., and Nishinari, K. 2006. Influence of tamarind seed xyloglucan on rheological properties and thermal stability of tapioca starch. Journal of Food Engineering 17: 41-50.
- Pongsawatmanit, R., Temsiripong, T., and Suwonsichon, T. 2007. Thermal and rheological properties of tapioca starch and xyloglucan mixtures in the presence of sucrose. Food Research International 40: 239-148.
- Sano, M., Miyata, E., Tamano, S., Hagiwara, A., Ito, N., and Shirai, T. 1996. Lack of carcinogenicity of tamarind seed polysaccharide in B6C3F₁ mice. Food and Chemical Toxicology 34: 463-467.
- Schroeder, I.Z., Franke, P., Schaefer, U.F., and Lehr, C.M. 2007. Development and characterization of film forming polymeric solutions for skin drug delivery. European Journal of Pharmaceutics and Biopharmaceutics 65: 111-121.
- Shabde, V.S. and Hoo, K.A. 2008. Optimum controller design for a spray drying process. Control Engineering Practice 16: 541-552
- Shetty, B.S., Udupa, S.L., Udupa, A.L. and Somayaji, S.N. 2006. Effect of *Centella asiatica* L (Umbelliferae) on normal and dexamethasone-suppressed wound healing in Wistar Albino rats. Lower Extremity Wounds 5: 137-143.
- Shim, P.J., Park, J.H., Chang, M.S., Lim, M.J., Kim, D.H., Jung, Y.H., Jew, S.S., Park, E.H., and Kim, H.D. 1996. Asiaticoside mimetics as wound healing agent. Bioorganic and Medicinal Chemistry Letters 6: 2937-2940.
- Shirakawa, M., Yamatoya, K., and Nishinari, K. 1998. Tailoring of xyloglucan properties using an enzyme. Food Hydrocolloids 12: 25-28.

- Shirakawa, M., and Yamatoya, K. 2003. Xyloglucan: Its Structure and Function. Foods, Food Ingredients Journal Japan 208: 11.
- Shukla, A., Rasik, A. M., Jain, G. K., Shankar, R., Kulshrestha, D. K., and Dhawan, B.N. 1999. In vitro and in vivo wound healing activity of asiaticoside isolater from *Centella asiatica*. Journal of Ethnopharmacology 65: 1-11.
- Sims, I.M., Gane, A.M., Dunstan, D., Allan, G.C., Boger D.V., Melton, L.D., and Bacic, A. 1998. Rheological properties of xyloglucans from different plant species. Carbohydrate Polymers 37: 61-69.
- Somsiri, A. 1997. Pilot scale production of tamarind seed polysaccharide. Master's Thesis, Faculty of Pharmaceutical Sciences, Mahidol University.
- .Stahl, K., Claesson, M., Lilliehorn, P., Linden, H., and Backstrom, K. 2002. The effect of process variables on the degradation and physical properties of spray dried insulin intended for inhalation. International Journal of Pharmaceutics 233: 227-237.
- Stat-Ease, Inc. 2005. Design-Expert statguide [Computer software]. U.S.A.: Stat-Ease, Inc. Design-Expert statistical software [2008, March 15]
- Suisha, F., Kawasaki, N., Miyazaki,S., Shirakawa,M., Yamatoya, K., Sasaki, M., and Attwood, D. (1998) Xyloglucan gels as sustained release vehicles for the intra peritoneal administration of mitomycin C. International Journal of Pharmaceutics 172: 27–32.
- Sumathi, S., and Ray, A.R. 2002. Role of modulating factors on release of caffeine from tamarind seed polysaccharide tablets. Trends in Biomaterial and Artificial Organs 17: 41-46.
- Sumathi, S., and Ray, A.R. 2003. Release behaviour of drugs from tamarind seed polysaccharide tablets. Journal of Pharmacy and Pharmaceutic Sciences 5: 12-18.
- Suttananta, W. 1986. Rheological studies on tamarind seed polysaccharide dispersion. Master's Thesis, Faculty of Pharmaceutical Sciences, Mahidol University.

- Takahashi, A., Suzuki, S., Kawasaki, N., Kubo, W., Miyazaki, S., Loebenberg, R., Bachynsky, J., and Attwood, D. 2002. Percutaneous absorption of non-steroidal anti-inflammatory drugs from in situ gelling xyloglucan formulations in rats. International Journal of Pharmaceutics 246: 179-186.
- Temsiripong, T., Pongsawatmanit, R., Ikeda, S., and Nishinari, K. 2005. Influence of xyloglucan on gelling and retrogradation of tapioca starch. Food Hydrocolloids 19:1054-1063.
- The Guideline of the American Society for Testing and Material ASTM. 1995. Annual Book of ASTM standards; D-882; Standard Test Method for Tensile Properties of Thin Plastic Sheeting; New York.
- The European Agency for the Evaluation of Medicinal Products Veterinary Medicines Evaluation Unit. Committee for veterinary medicinal products *Centellae asiaticae* extractum. 1998.
- The 13th European Carbohydrate Symposium. The biological function and the enzymatic modification of xyloglucan. 2005.
- Tine, M.A.S., Silva, C.O., Lima, D.U., Carpita, N.C., and Buckeridge, M.S. 2006. Fine structure of a mixed-oligomer storage xyloglucan from seeds of *Hymenaea courbaril*. Carbohydrate Polymers 66: 444-454.
- Tinmanee, R. 2004. Development of buccal mucoadhesive films containing triamcinolone acetate from durian-fruit hull gel. Master's Thesis, Faculty of Pharmaceutical Sciences, Chulalongkorn University.
- Tyle, P. 1988. Drug Delivery Devices: Fundamentals and applications. 1st ed. New York: Marcel Dekker, Inc.
- Wang, F.J., Yang, Y.Y., Zhang, X.Z., Zhu, X., Chung, T.S., and Mochhala, S. 2002. Cellulose acetate membranes for transdermal delivery of scopolamine base. Materials Science and Engineering C 20: 93-100.
- Williams, A.C. 2003. Structure and function of human skin. Transdermal and Topical Drug Delivery. USA: Pharmaceutical Press.
- Wille, J.J. 2006. Skin Delivery System: Transdermals Dermatologicals and Cosmetic Actives. 1st ed. USA: Blackwell Publishing.

- Yamanaka, S., Yuguchia, Y., Urakawaa, H., Kajiwara, K., Shirakawa, M., and Yamatoya, K. 2000. Gelation of tamarind seed polysaccharide xyloglucan in the presence of ethanol. Food Hydrocolloids 14: 125–128.
- Yoshimura, M., Takaya, T., and Nishinari, K. 1999. Effects of xyloglucan on the gelatinization and retrogradation of corn starch as studied by rheology and differential scanning calorimetry. Food Hydrocolloids 13: 101-111.

APPENDIX

APPENDIX A: Validation of Analytical Method

APPENDIX B: Experimental data of xyloglucan tamarind seed extract and optimal spray dried condition

APPENDIX C: Experimental data of size and size distribution of spray drying condition

APPENDIX D: Experimental data of physicochemical properties of xyloglucan powder from tamarind seeds

APPENDIX E: Experimental data of mechanical properties of film formulations and film containing *Centella Asiatica* extract

APPENDIX F: Experimental data of adhesive properties of film formulations and film containing *Centella Asiatica* extract

APPENDIX H: Experimental data of stability study

APPENDIX G: Experimental data of release and permeation study

APPENDIX A

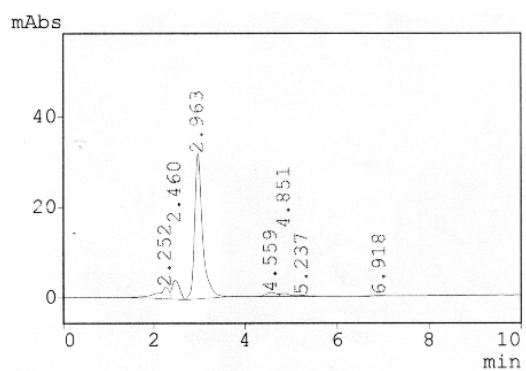
Validation of Analytical Method

1. Analysis of xyloglucan by high performance liquid chromatographic (HPLC) method

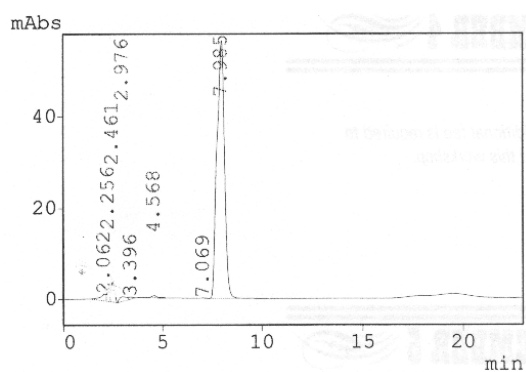
The validation of analytical method is the process by which it is established that the performance characteristics of the method meet the requirements for the intended analytical applications. The performance characteristics are expressed in term of analytical parameters. For HPLC assay validation, these include specificity, linearity, accuracy and precision.

1.1.1 Specificity

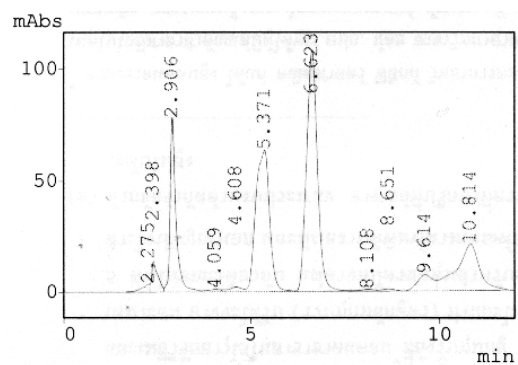
The specificity of an analytical method is the ability to measure the analyte accurately and with specificity in the presence of other components in the sample. Figures 1A were shown typical chromatogram of asiaticoside standard solution, internal standard solution, titrated extract of *Centella asiatica* (TECA) solution, blank sample solution (blank film formulation), respectively. The chromatograms demonstrated that the HPLC condition used in the study had a suitable specificity.



(a)



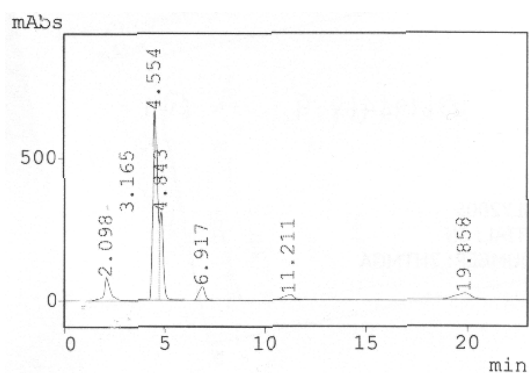
(b)



(c)

Fig 16 HPLC chromatograms of mobile phase

- (a) asiaticoside standard solution
- (b) triamcinolone acetonide solution
- (c) *Centella* extract solution
- (d) Blank film formulation



(d)

Fig 16 HPLC chromatograms of mobile phase (continued)

- (a) asiaticoside standard solution
- (b) triamcinolone acetonide solution
- (c) TECA solution
- (d) Blank film formulation

Table 1A Data for calibration curve of asiaticoside by HPLC method

Concentration ($\mu\text{g/ml}$)	Peak height ratio			Mean	SD	%CV
	Set1	Set2	Set3			
10	0.4903	0.4985	0.4997	0.4962	0.0051	1.03
20	1.0119	1.0361	1.0279	1.0253	0.0123	1.20
40	2.0353	2.0470	2.0313	2.0378	0.0081	0.40
60	3.0187	3.0398	3.0425	3.0336	0.0130	0.43
80	4.0820	4.0793	4.0709	4.0774	0.0058	0.14
100	5.2119	5.1913	5.2225	5.2085	0.0158	0.30
R²	0.9994	0.9997	0.9995	0.9996	-	-

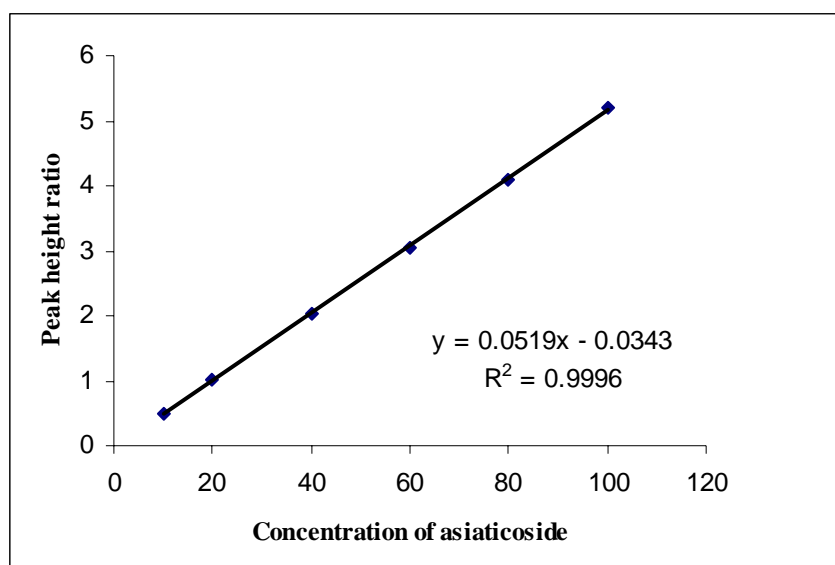


Fig 2A Calibration curve of a by HPLC method

1.1.3 Accuracy

The accuracy of an analytical method is the closeness of test results obtained by the method to the true value. Accuracy is calculated as percent recovery by the assay of known added amount of analyses. The percentages of analytical recovery of asiaticoside solution and film formulation were shown in Table 7 and 8. The percentages analytical recovery of asiaticoside was in the range of 98.13-101.96% and 98.20-101.18%, respectively which indicated that this method could be used for analysis in all concentrations studied with a high accuracy.

Table 2A The percentages of analytical recovery of asiaticoside solution by HPLC method

Concentration ($\mu\text{g/ml}$)	%Analytical recovery					Mean \pm SD
	1	2	3	4	5	
30	100.78	101.96	99.65	100.27	101.55	100.84 \pm 0.93
50	100.11	100.38	101.50	101.75	100.50	100.85 \pm 0.73
90	99.48	98.13	100.74	101.66	99.70	99.94 \pm 1.33

Table 3A The percentages of analytical recovery of asiaticoside film formulation by HPLC method

Concentration ($\mu\text{g/ml}$)	%Analytical recovery					Mean \pm SD
	1	2	3	4	5	
30	99.31	99.29	99.48	100.16	99.01	99.45 \pm 0.43
50	99.37	100.57	98.38	99.93	98.20	99.29 \pm 1.01
90	100.17	100.99	100.85	101.18	100.81	100.80 \pm 0.38

1.1.4 Precision

The precision of asiaticoside analyzed by HPLC method were determined both within run precision and between run precision as illustrated in Tables 9 and 10. All coefficients of variation values were small, as 0.38-1.02% and 0.98-1.23%, respectively. The coefficient of variation of an analytical method should generally be less than 2%. Therefore, the HPLC method was precise for quantitative analysis of asiaticoside in the range studied.

Table 4A Data of within run precision by HPLC method

Concentration ($\mu\text{g/ml}$)	Peak height ratio					Mean	SD	%CV
	Set1	Set2	Set3	Set4	Set5			
30	29.79	29.79	29.84	30.05	29.70	29.83	0.13	0.43
50	49.69	50.29	49.19	49.97	49.10	49.65	0.50	1.02
90	90.15	90.89	90.76	91.06	90.73	90.72	0.34	0.38

Table 5A Data of between run precision by HPLC method

Concentration ($\mu\text{g/ml}$)	Peak height ratio					Mean	SD	%CV
	Set1	Set2	Set3	Set4	Set5			
30	29.47	28.92	29.83	29.67	29.22	29.42	0.36	1.23
50	49.45	48.46	49.64	49.05	49.52	49.22	0.48	0.98
90	88.93	89.81	90.71	90.22	91.25	90.18	0.88	0.98

2. Analysis of protein by UV Spectrophotometric Method

2.1. Validation of UV Spectrophotometric Method

The validation of analytical method is the process for evaluation that the method is suitable and reliable for the intended analytical applications. The analytical parameters used for the UV spectrophotometric assay validation were linearity, accuracy and precision.

2.1.1 Linearity

The data for calibration curve of BSA are shown in Table 1B. Linear regression analysis of the absorbance versus the concentration curve was performed and the coefficient of determination (R^2) was calculated. The coefficients of determination were 0.9998 (Figure 1B).

Table 6A Data for calibration curve of BSA

Concentration ($\mu\text{g/ml}$)	Absorbance			Mean	SD	%CV
	Set1	Set2	Set3			
50	0.1705	0.1707	0.1674	0.1695	0.0019	1.09
100	0.3064	0.3062	0.2999	0.3042	0.0037	1.22
150	0.4316	0.4354	0.4368	0.4346	0.0027	0.62
200	0.5571	0.5564	0.5671	0.5602	0.0060	1.07
250	0.6973	0.7112	0.6921	0.7002	0.0099	1.41
300	0.8153	0.8363	0.8127	0.8214	0.0129	1.58
R^2	0.9996	0.9992	0.9995	0.9998	-	-

2.1.2 Accuracy

The accuracy of an analytical method is the closeness of test results obtained by the method to the true value. Accuracy is calculated as percent recovery by the assay of known added amount of analyses. Table 7A displayed the percentage of analytical recovery of BSA. All percentages analytical recovery of BSA was in the range of 91.39-105.17% which indicated the high accuracy of this method. Thus, it could be used for analysis of BSA in all studied concentrations.

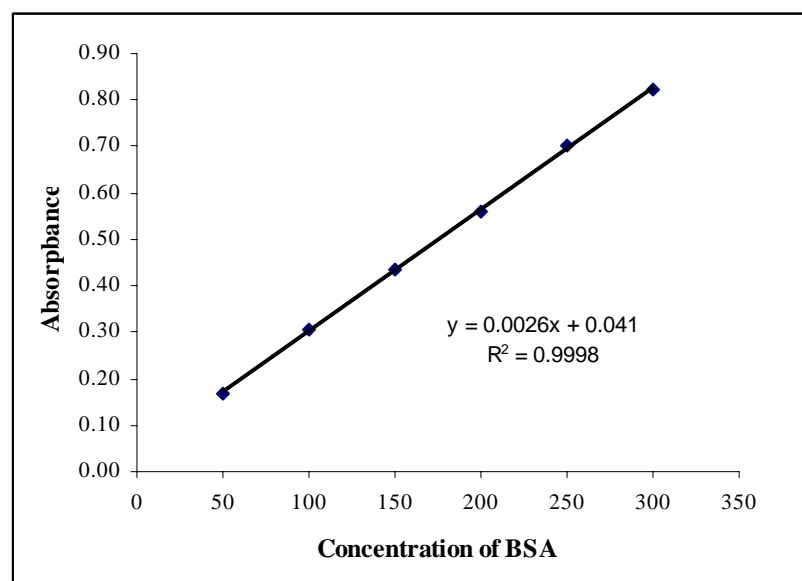


Fig 3A Calibration curve of BSA by UV spectrophotometric method

Table 7A The percentages of analytical recovery of BSA by UV spectrophotometric method

Concentration (µg/ml)	%Analytical recovery					Mean ± SD
	1	2	3	4	5	
80	94.62	94.38	91.39	98.17	98.80	95.47±3.04
160	104.21	105.17	102.52	100.63	104.98	103.50±1.92
240	102.00	99.29	103.09	101.36	101.30	101.41±1.38

2.1.3 Precision

The precision of BSA analyzed by UV spectrophotometric method were determined both within run and between run precisions as depicted in Table 3B and 4B, respectively. The coefficients of variation were in the range of 1.40-1.86% for within run precision and 1.93-3.81% for between run precision. Both within run and between run precisions of BSA provided the coefficient of variation less than 15%. Thus, the UV spectrophotometric method was accurate for the quantitative analysis of BSA in the range of studied.

Table 8A Data of within run precision by UV spectrophotometric method

Concentration ($\mu\text{g/ml}$)	Absorbance					Mean	SD	%CV
	Set1	Set2	Set3	Set4	Set5			
80	79.28	79.12	82.00	81.84	82.00	80.85	1.51	1.86
160	165.76	171.76	169.76	166.88	168.36	168.50	2.36	1.40
240	237.32	236.28	237.76	236.28	244.40	238.40	3.41	1.43

Table 9A Data of between run precision by UV spectrophotometric method

Concentration ($\mu\text{g/ml}$)	Absorbance					Mean	SD	%CV
	Set1	Set2	Set3	Set4	Set5			
80	80.85	88.33	81.84	80.75	82.27	82.81	3.15	3.81
160	168.50	168.23	161.71	170.14	167.43	167.20	3.22	1.93
240	238.41	238.63	247.58	254.22	243.70	244.51	6.64	2.71

APPENDIX B

Experimental data of xyloglucan tamarind seed extract and optimal spray dried condition

Table 1B The percentage yield of xyloglucan spray dried powder from four different methods

	%Xyloglucan			Mean	SD
	set 1	set 2	set 3		
method1	43.56	41.81	43.17	42.85	0.92
method2	44.12	43.87	43.17	43.72	0.49
method3	42.13	44.17	42.41	42.90	1.11
method4	43.57	45.26	45.03	44.62	0.92

Table 2B The percent of total protein of xyloglucan spray dried powder from four different methods and tamarind seed powder

	%Protein			Mean	SD
	set 1	set 2	set 3		
Tamarind seed powder	15.72	15.62	16.27	15.87	0.35
method1	14.21	14.39	14.44	14.35	0.12
method2	14.15	14.10	14.25	14.17	0.08
method3	14.27	14.75	14.89	14.64	0.33
method4	14.92	15.49	15.17	15.19	0.29

Table 3B The percent of fat of xyloglucan spray dried powder from four different methods and tamarind seed powder

	%Fat			Mean	SD
	set 1	set 2	set 3		
Tamarind seed powder	7.99	7.69	7.50	7.73	0.25
method1	0.99	1.29	0.99	1.09	0.17
method2	0.98	1.29	1.19	1.15	0.16
method3	0.70	1.29	0.69	0.89	0.34
method4	1.09	1.09	1.38	1.19	0.17

Table 4B ANOVA for the percentage xyloglucan of four different methods

	Sum of Squares	df	Mean Square	F	Sig.
Between Groups	6.253	3	2.084	2.848	0.120
Within Groups	6.297	8	0.787		
Total	12.550	11			

Table 5B ANOVA for the %total protein of four different methods and tamarind seed powder

	Sum of Squares	df	Mean Square	F	Sig.
Between Groups	5.771	4	1.443	21.839	0.000
Within Groups	0.661	10	0.066		
Total	6.432	14			

Table 6B ANOVA for the %fat of four different methods and tamarind seed powder

	Sum of Squares	df	Mean Square	F	Sig.
Between Groups	106.156	4	26.539	506.212	0.000
Within Groups	0.524	10	0.052		
Total	106.680	14			

Table 7B Tukey HSD test of the percentage xyloglucan of four different methods

Method	Method	Sig.
I	II	0.640
	III	1.000
	IV	0.144
II	I	0.640
	III	0.684
	IV	0.620
III	I	1.000
	I	0.684
	IV	0.166
V	I	0.144
	II	0.620
	III	0.161

* The mean difference is significant at the 0.05 level.

Table 8B Tukey HSD test of the %total protein of four different methods and tamarind seed powder

Method	Method	Sig.
I	II	0.906
	III	0.651
	IV	0.016*
	Tamarind seed powder	0.000*
II	I	0.906
	III	0.241
	IV	0.004*
	Tamarind seed powder	0.000*
III	I	0.651
	II	0.241
	IV	0.133
	Tamarind seed powder	0.001*
IV	I	0.016*
	II	0.004*
	III	0.133
	V	0.055*
Tamarind seed powder	I	0.000*
	II	0.000*
	III	0.001*
	IV	0.055

* The mean difference is significant at the 0.05 level.

Table 9B Tukey HSD test of the %fat of four different methods and tamarind seed powder

Method	Method	Sig.
I	II	0.997
	III	0.826
	IV	0.984
	Tamarind seed powder	0.000*
II	I	0.997
	III	0.646
	IV	1.000
	Tamarind seed powder	0.000*
III	I	0.826
	II	0.646
	IV	0.546
	Tamarind seed powder	0.000*
IV	I	0.984
	II	1.000
	III	0.546
	V	0.000*
	Tamarind seed powder	0.000*
Tamarind seed powder	I	0.000*
	II	0.000*
	III	0.000*
	IV	0.000*

* The mean difference is significant at the 0.05 level

Table 10B A face centered design matrix of two parameters, the viscosity, outlet temperature, %yield and %moisture content (n=3)

Code	Temperature (°C)	Aspirator	Outlet Temperature (°C)	Viscosity (mPas)	%Moisture content			Mean	SD
					1	2	3		
C1	120 (-)	80 (-)	74±1	329.9	7.77	7.77	7.95	7.83	0.10
C2	200 (+)	80 (-)	117±2	329.3	5.98	5.99	6.19	6.05	0.12
C3	120 (-)	100 (+)	77±2	325.7	6.97	7.20	6.99	7.05	0.13
C4	200 (+)	100 (+)	99±2	323.3	4.80	4.99	5.17	4.99	0.19
C5	120 (-)	90 (0)	73±2	322.1	7.36	7.16	7.17	7.23	0.11
C6	200 (+)	90 (0)	120±2	304.1	5.98	5.79	5.80	5.86	0.11
C7	160 (0)	80 (-)	96±2	335.9	7.17	7.00	7.00	7.06	0.10
C8	160 (0)	100 (+)	82±3	316.7	6.40	6.39	6.20	6.33	0.11
C9	160 (0)	90 (0)	100±3	304.1	7.16	6.97	6.97	7.03	0.11
C10	160 (0)	90 (0)	100±3	323.9	6.56	6.56	6.39	6.50	0.10
C11	160 (0)	90 (0)	101±1	309.5	6.59	6.59	6.79	6.66	0.12
C12	160 (0)	90 (0)	101±1	298.1	6.37	6.19	6.39	6.32	0.11
C13	160 (0)	90 (0)	101±2	296.9	6.60	6.57	6.60	6.59	0.02

Table 11B The optimum region by overlay plot of two parameters, the viscosity, outlet temperature and %moisture content (n=3)

Code	Temperature (°C)	Aspirator	Outlet Temperature (°C)	Viscosity (mPas)	%Moisture content			Mean	SD
					1	2	3		
O1	178	100	114±2	382.1	6.18	6.39	6.19	6.25	0.12
O2	178	100	113±2	411.5	6.37	6.39	6.20	6.32	0.10
O3	178	100	112±2	5.59	5.77	5.59	5.65	0.10	5.59

APPENDIX C

Experimental data of size and size distribution of spray drying condition

Figure 1C Size and size distribution of C1

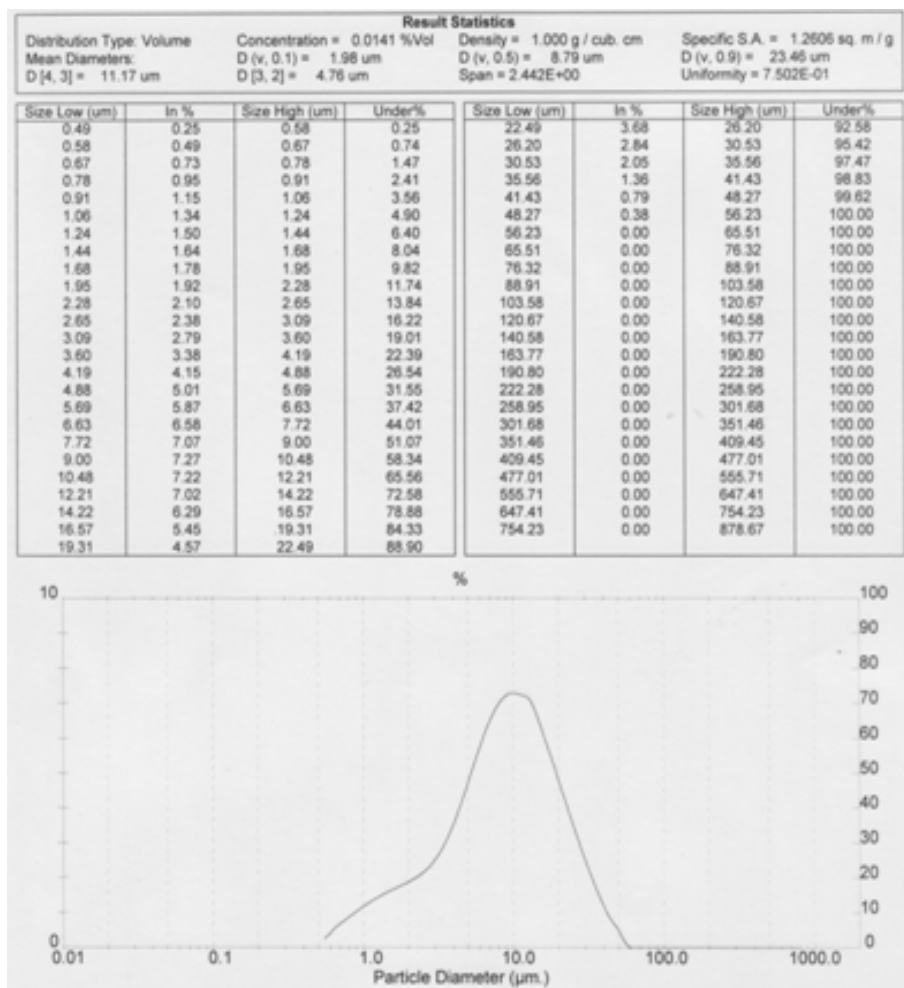


Figure 2C Size and size distribution of C2

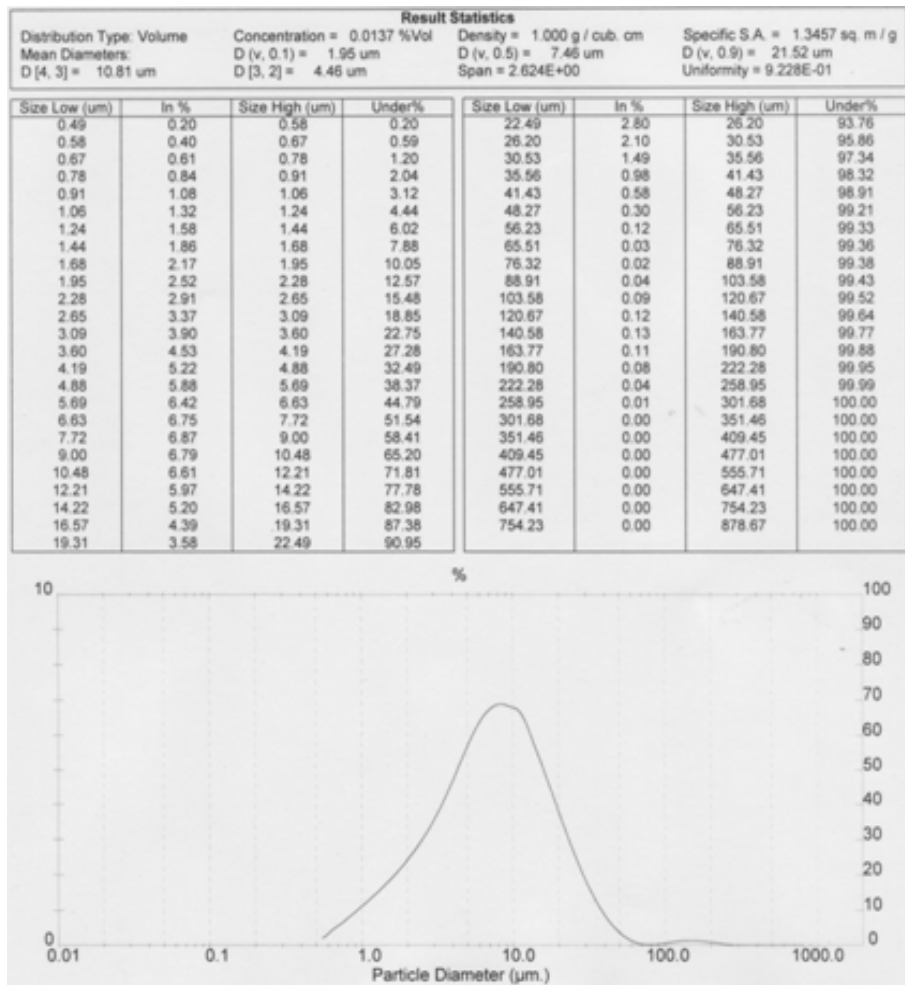


Figure 3C Size and size distribution of C3

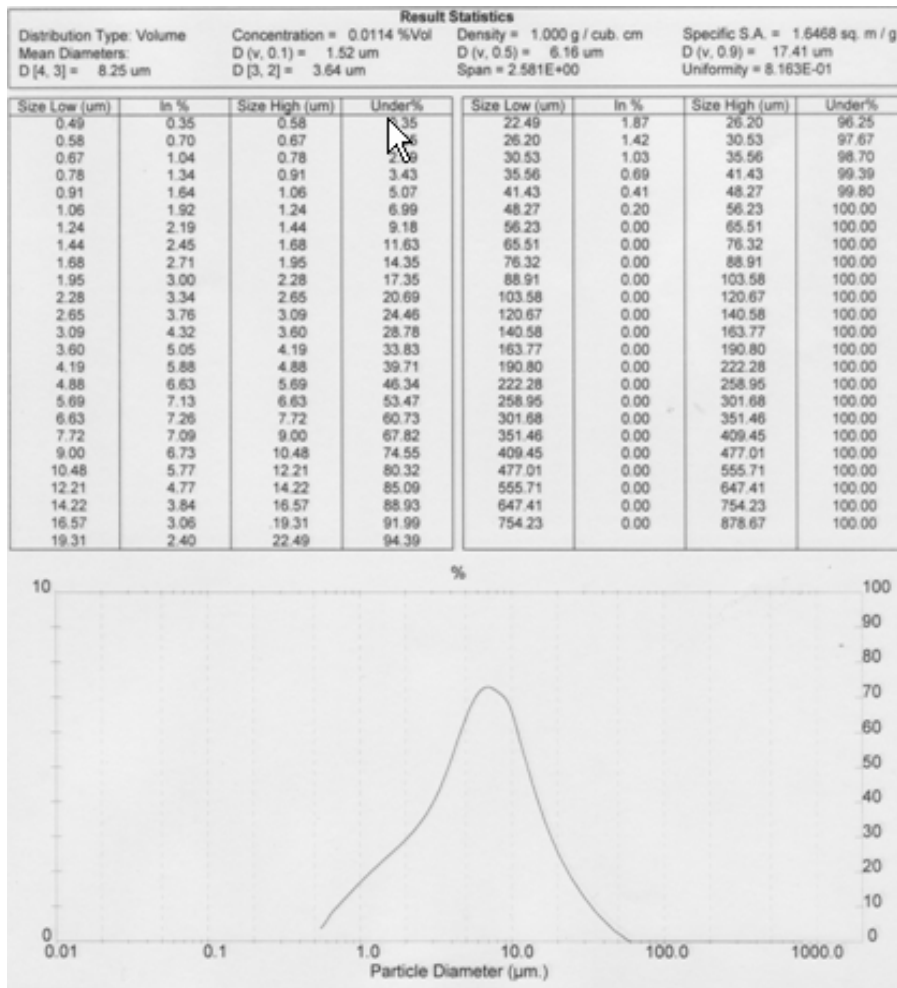


Figure 4C Size and size distribution of C4

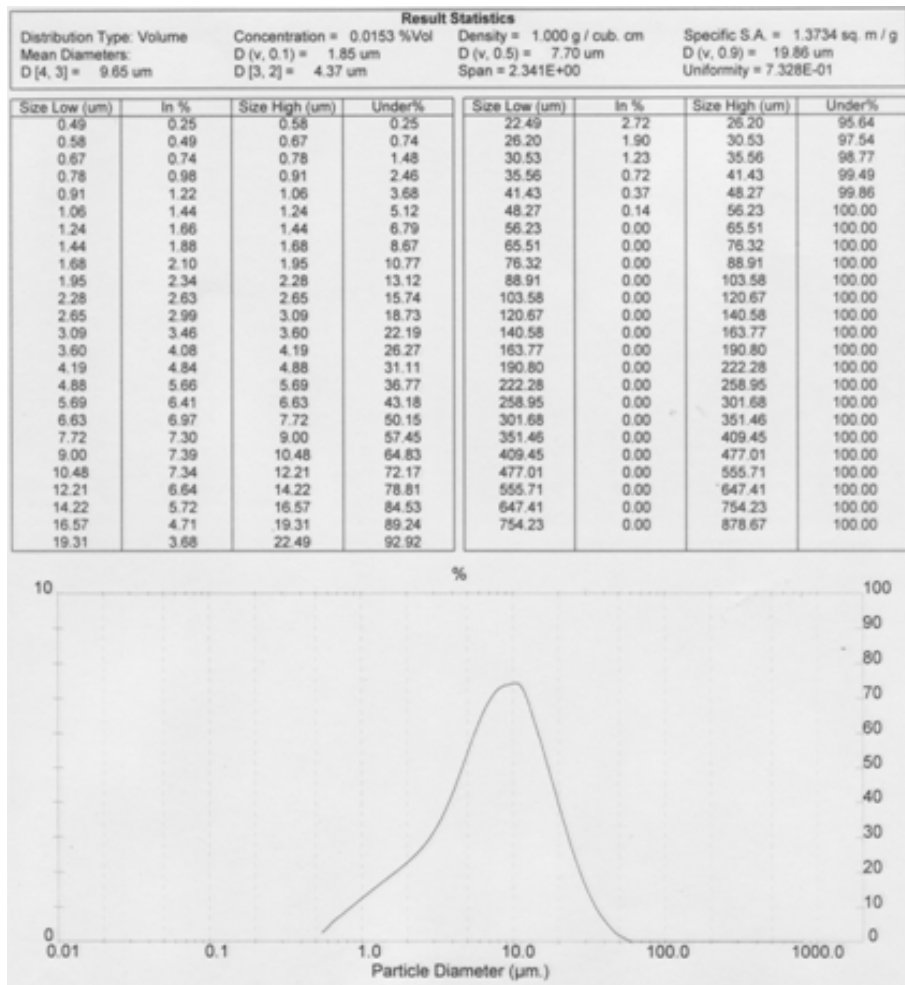


Figure 5C Size and size distribution of C5

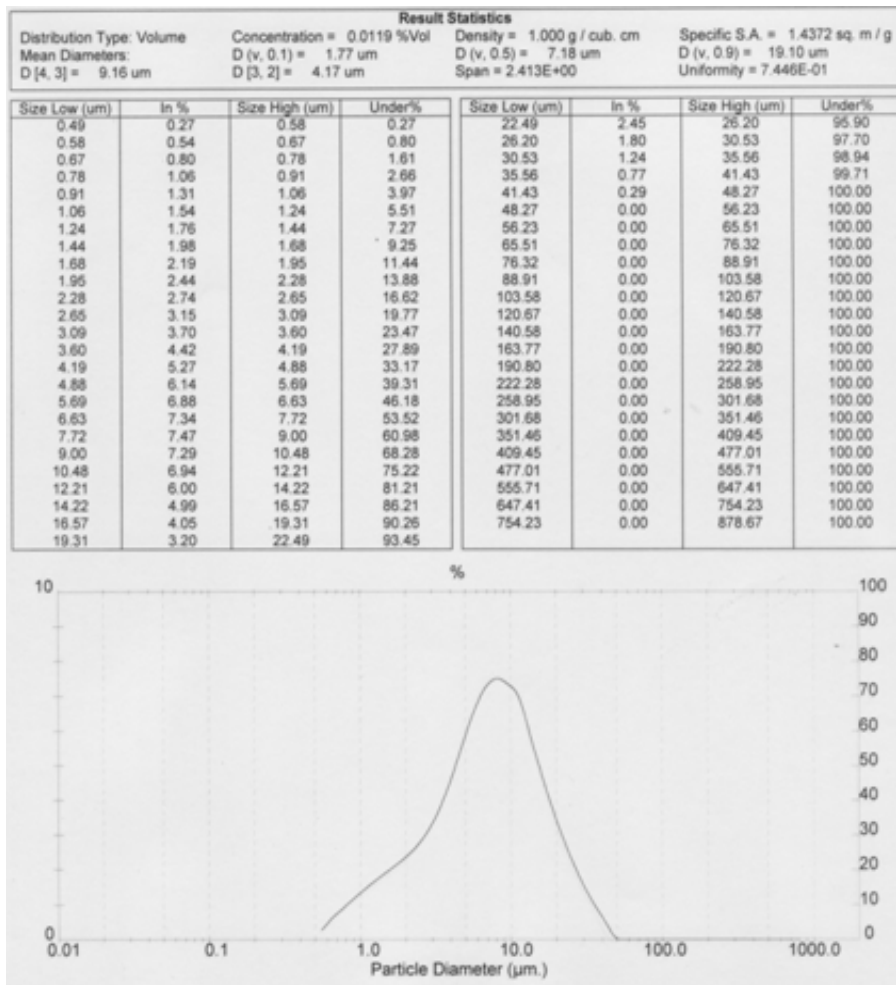


Figure 6C Size and size distribution of C6

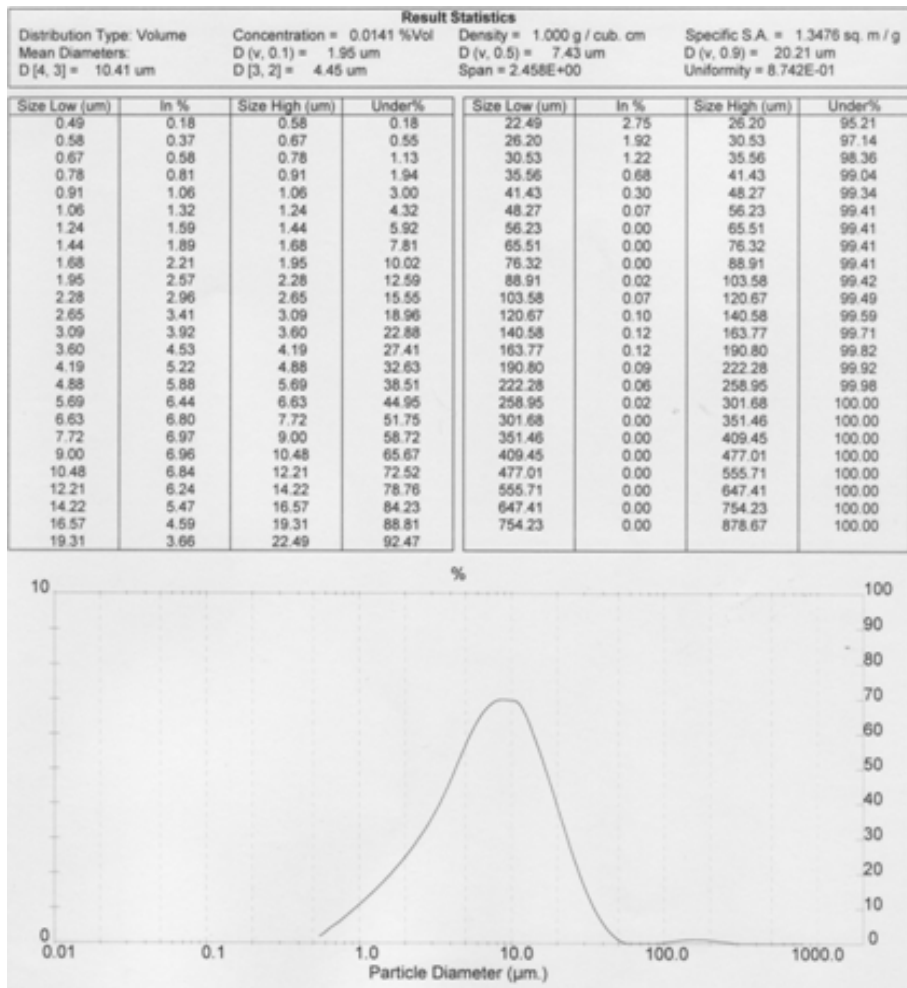


Figure 7C Size and size distribution of C7

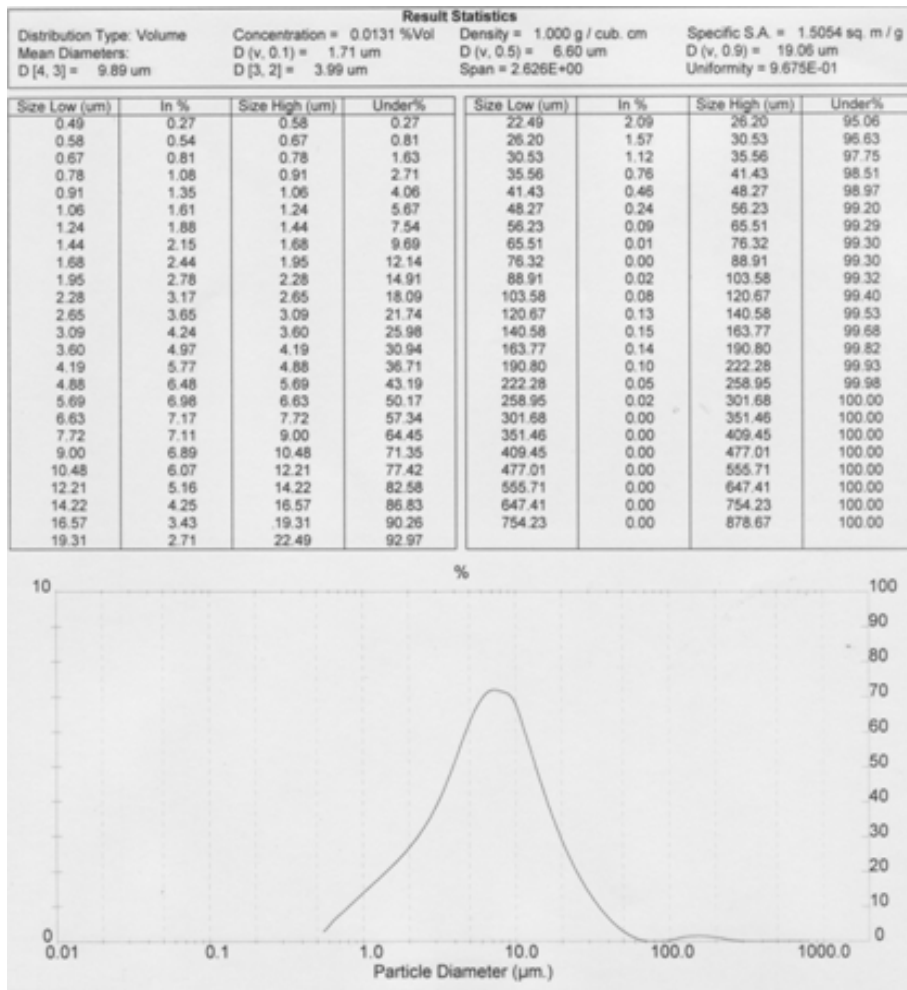


Figure 8C Size and size distribution of C8

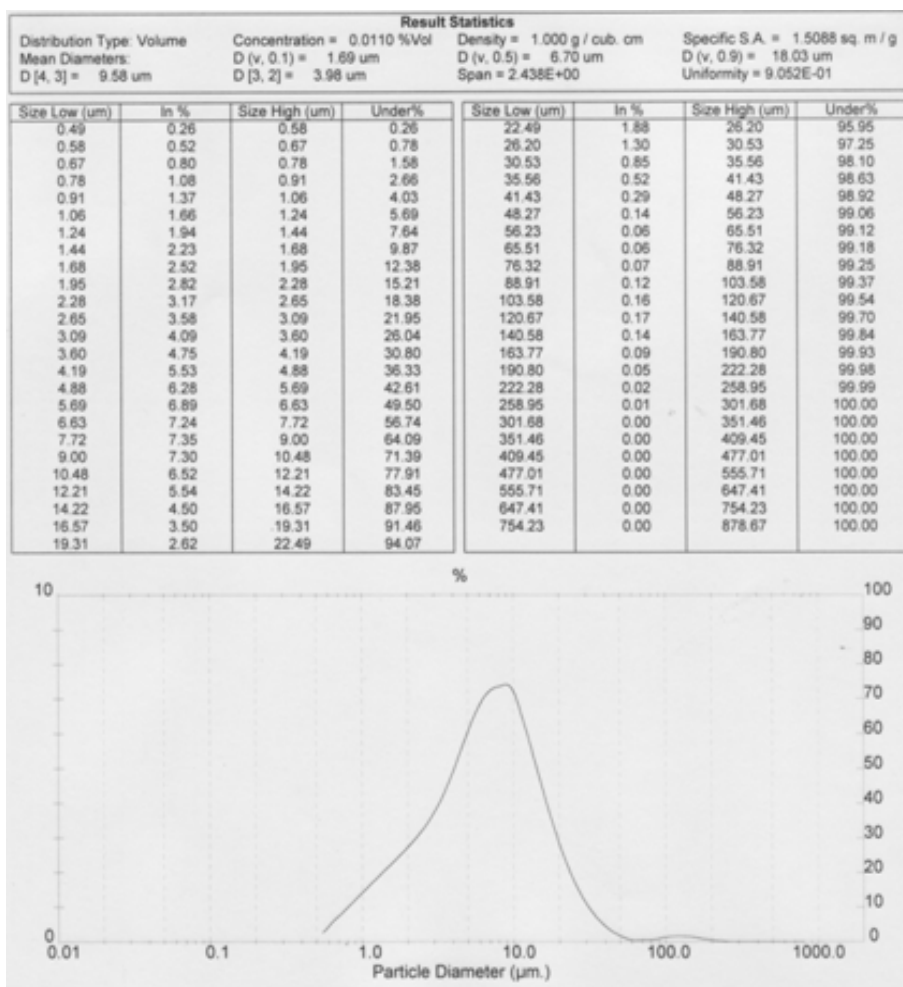


Figure 9C Size and size distribution of C9

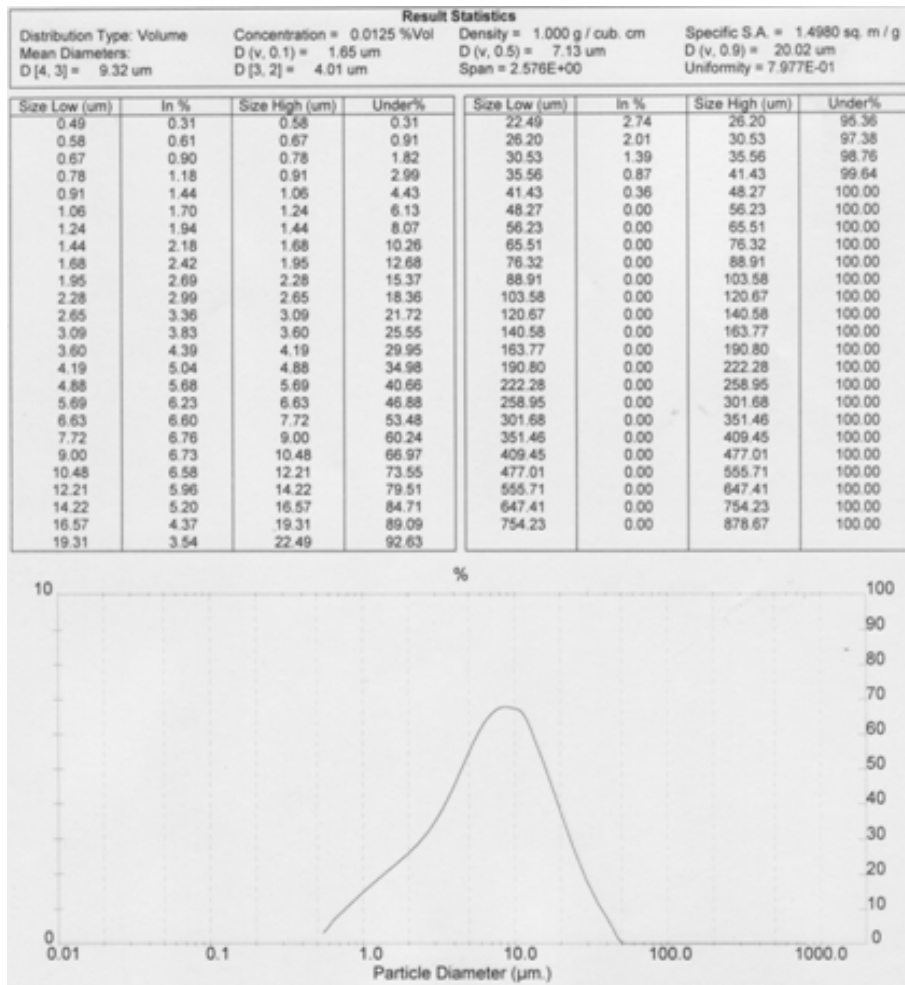


Figure 10C Size and size distribution of optimization spray dried condition

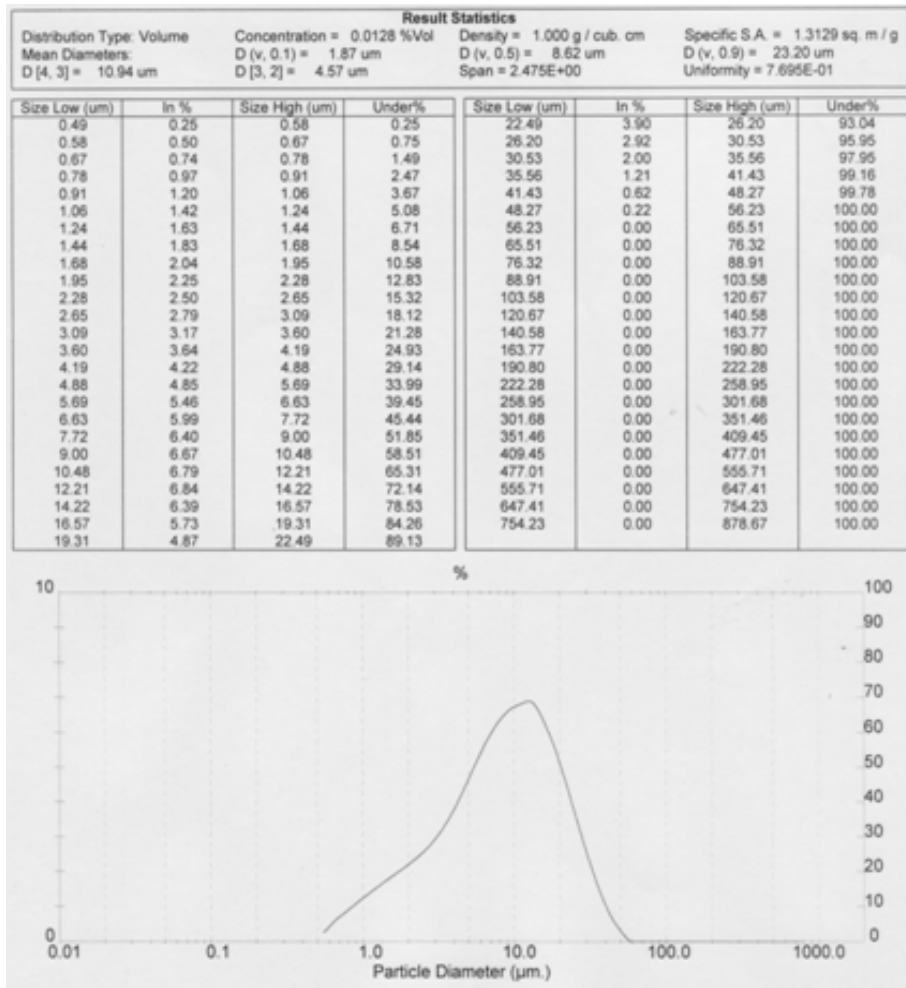
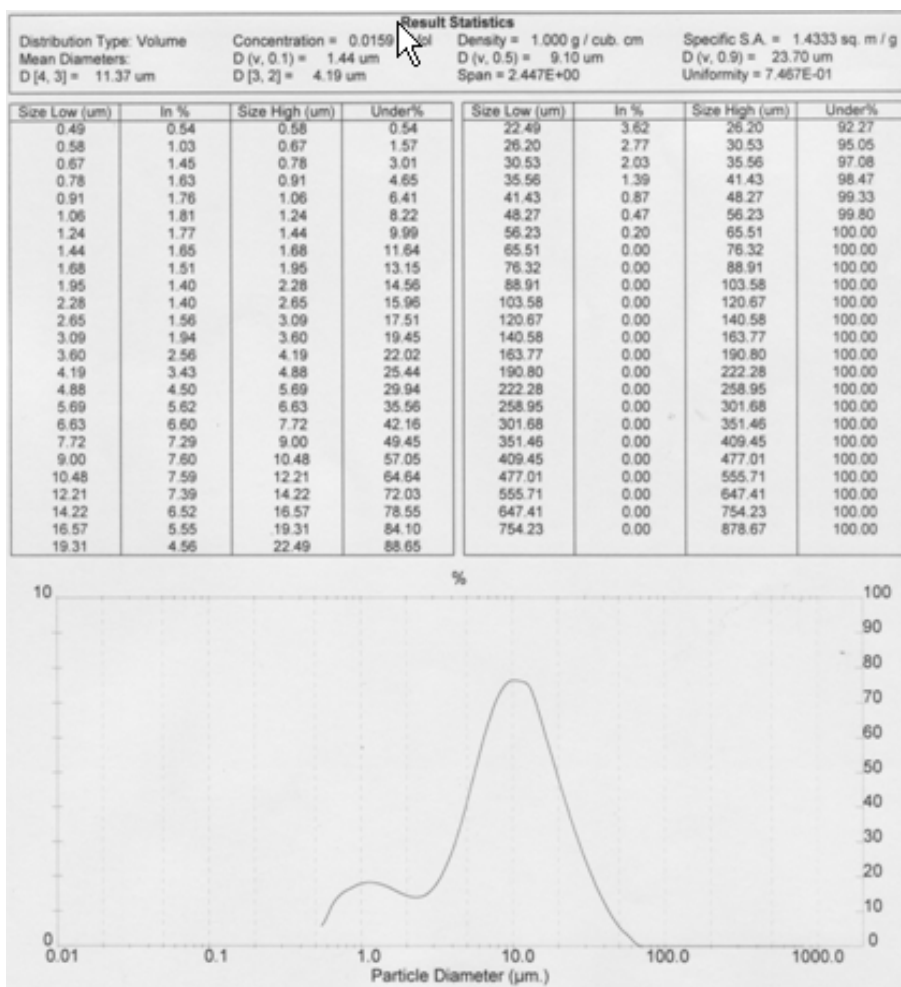


Figure 11C Size and size distribution of xyloglucan spray dried powder



APPENDIX D

Experimental data of physicochemical properties of xyloglucan powder from tamarind seeds

Table 1D The percentage of xyloglucan in xyloglucan spray dried powder

Run	%Xyloglucan			mean	SD
	set1	set2	set3		
1	42.21	42.99	43.35	42.85	0.58
2	41.96	42.00	41.71	41.89	0.16
3	41.98	42.18	42.32	42.16	0.17

Table 2D The pH value of xyloglucan spray dried powder

	set 1	set 2	set 3	AVG	SD
pH	7.61	7.93	7.94	7.83	0.1877

Table 3D The viscosity value of 1%, 1.5% and 2% w/v of xyloglucan spray dried powder

conc.	Viscosity (mPas)			Mean	SD
	set 1	set 2	set 3		
1%	40.135	39.742	38.513	39.463	0.8461
1.5%	94.264	92.630	94.150	93.681	0.9123
2%	166.729	170.146	167.292	168.056	1.8320

Table 4D The percentage of remained xyloglucan after added ethanol

%Ethanol	%Remained xyloglucan			Mean	SD
	set 1	set 2	set 3		
1	97.82	97.45	100.26	98.51	1.53
2	95.85	94.49	95.07	95.14	0.68
3	91.51	91.56	94.06	92.38	1.46
4	85.14	85.04	88.31	86.16	1.86
5	83.14	80.72	83.74	82.53	1.60

Figure 1D Rheogram of 1% w/v xyloglucan spray dried powder

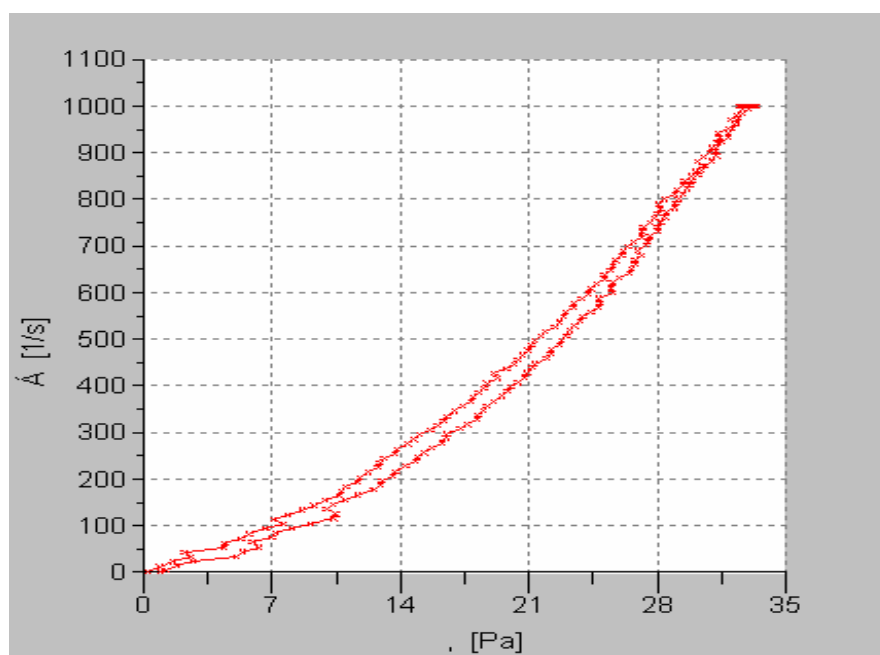


Figure 2D Rheogram of 1.5%w/v xyloglucan spray dried powder

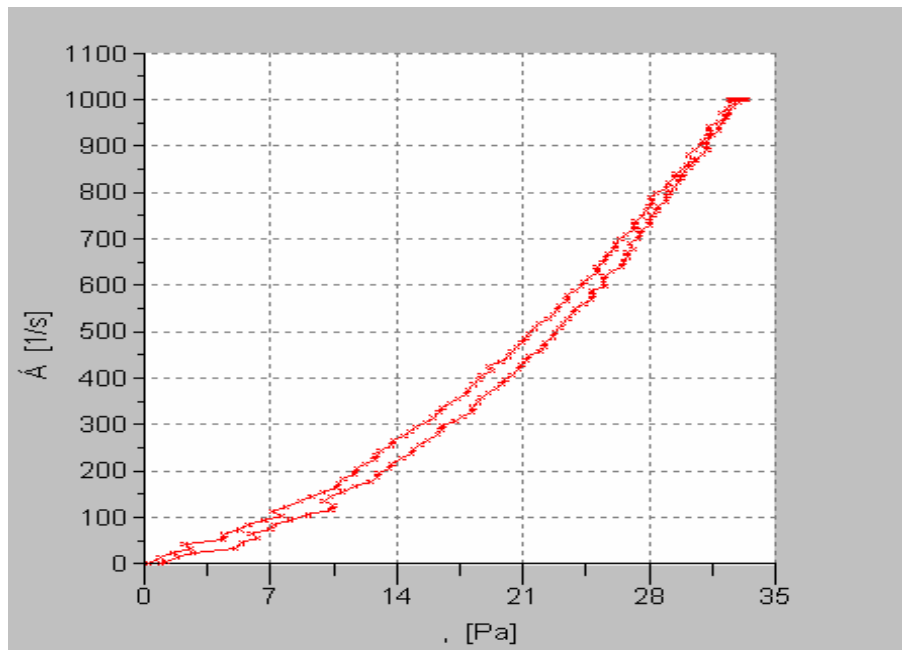
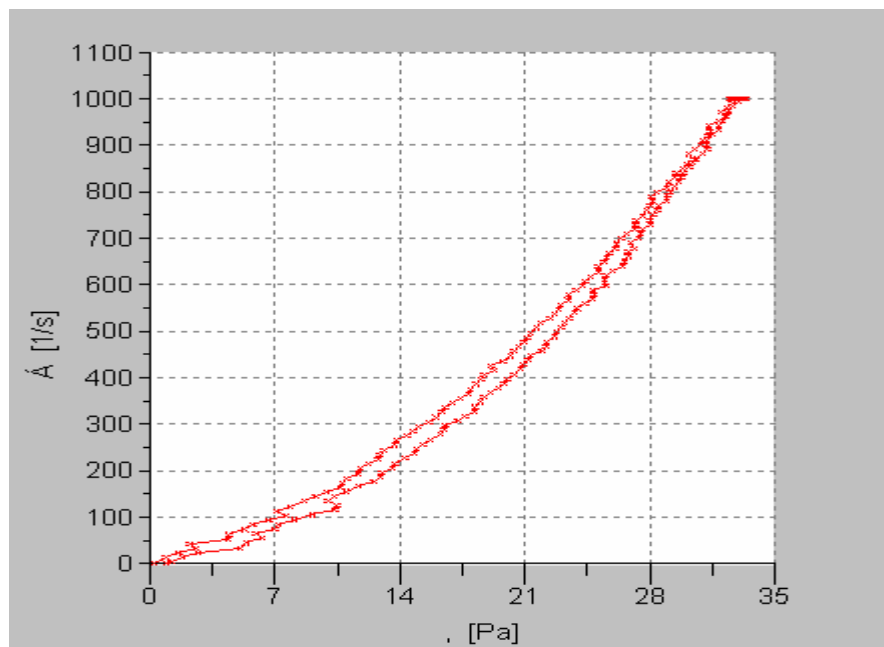


Figure 3D Rheogram of 2%w/v xyloglucan spray dried powder



APPENDIX E

Experimental data of mechanical properties of film formulations and film containing *Centella Asiatica* extract

Table 1E The film weights of film formulations and film containing *Centella Asiatica* extract

Formulation	Film weight (mg)					mean	SD
	1	2	3	4	5		
F1	11.92	11.60	11.88	11.03	11.27	11.54	0.39
F2	10.85	11.28	11.47	11.58	10.97	11.23	0.31
F3	15.50	14.89	15.13	14.76	14.68	14.99	0.33
F4	4.68	5.04	4.97	4.89	4.45	4.81	0.24
F5	9.39	9.55	9.60	9.88	10.20	9.72	0.32
F6	8.79	8.74	8.49	8.91	8.71	8.73	0.15
F7	7.60	8.15	7.60	7.51	7.75	7.72	0.25
F8	13.02	12.94	12.85	13.30	13.26	13.07	0.20
F9	7.14	6.65	7.02	6.65	7.05	6.90	0.23
F10	10.15	10.50	10.18	10.33	11.02	10.44	0.35
F11	9.50	9.76	10.13	9.34	9.16	9.58	0.38
F12	8.41	9.50	9.76	8.88	8.79	9.07	0.55
F13	9.21	9.78	9.67	9.26	8.89	9.36	0.36
F14	8.05	8.13	7.72	7.75	7.70	7.87	0.20
F15	8.35	8.33	7.93	8.64	7.80	8.21	0.34
Film with extract 1	11.63	12.55	13.21	11.83	13.15	12.474	0.73
Film with extract 2	11.67	11.63	12.02	11.98	11.56	11.772	0.21
Film with extract 3	12.72	13.42	12.08	12.12	13.50	12.768	0.68

Table 2E The max force, force of adhesive, work of adhesive and thick value of F1

Run	Max Force (N)	Force of adhesion (N/cm²)	Work of Adhesion (mJ)	Thick (mm)
1	0.0357	2.856	0.0286	0.05
2	0.0230	1.840	0.0136	0.05
3	0.0227	1.816	0.0149	0.05
4	0.0577	4.616	0.0346	0.05
5	0.0713	5.704	0.0319	0.05
Mean	0.0421	3.366	0.0247	0.05
SD	0.02	1.73	0.01	0

Table 3E The max force, force of adhesive, work of adhesive and thick value of F2

Run	Max Force (N)	Force of adhesion (N/cm²)	Work of Adhesion (mJ)	Thick (mm)
1	0.0383	2.553	0.0243	0.06
2	0.0553	3.687	0.0326	0.06
3	0.0370	2.467	0.0156	0.06
4	0.0403	2.687	0.0216	0.06
5	0.0253	1.687	0.0159	0.06
Mean	0.0392	2.616	0.022	0.06
SD	0.01	0.71	0.01	0

Table 4E The max force, force of adhesive, work of adhesive and thick value of F3

Run	Max Force (N)	Force of adhesion (N/cm²)	Work of Adhesion (mJ)	Thick (mm)
1	0.2777	37.02	0.027	0.03
2	0.2543	33.91	0.0502	0.03
3	0.2593	34.58	0.019	0.03
4	0.1534	20.45	0.0767	0.03
5	0.1643	21.91	0.0436	0.03
Mean	0.2218	29.58	0.0433	0.03
SD	0.06	7.77	0.02	0

Table 5E The max force, force of adhesive, work of adhesive and thick value of F4

Run	Max Force (N)	Force of adhesion (N/cm²)	Work of Adhesion (mJ)	Thick (mm)
1	0.0747	9.96	0.0495	0.03
2	0.0470	6.27	0.0220	0.03
3	0.0490	6.53	0.0240	0.03
4	0.0267	3.56	0.0193	0.03
5	0.0287	3.83	0.0158	0.03
Mean	0.0452	6.029	0.0261	0.03
SD	0.02	2.58	0.01	0.00

Table 6E The max force, force of adhesive, work of adhesive and thick value of F5

Run	Max Force (N)	Force of adhesion (N/cm²)	Work of Adhesion (mJ)	Thick (mm)
1	0.0357	4.76	0.0140	0.03
2	0.0563	7.51	0.0208	0.03
3	0.0220	2.93	0.0133	0.03
4	0.0400	5.33	0.0276	0.03
5	0.1143	15.24	0.0300	0.03
Mean	0.0537	7.156	0.0211	0.03
SD	0.04	4.81	0.01	0.00

Table 7E The max force, force of adhesive, work of adhesive and thick value of F6

Run	Max Force (N)	Force of adhesion (N/cm²)	Work of Adhesion (mJ)	Thick (mm)
1	0.5403	36.02	0.0906	0.06
2	0.2083	13.89	0.0598	0.06
3	0.0700	4.67	0.0316	0.06
4	0.1787	11.91	0.0405	0.06
5	0.5893	39.29	0.0746	0.06
Mean	0.3173	21.16	0.0594	0.06
SD	0.23	15.49	0.02	0.00

Table 8E The max force, force of adhesive, work of adhesive and thick value of F7

Run	Max Force (N)	Force of adhesion (N/cm²)	Work of Adhesion (mJ)	Thick (mm)
1	0.0373	4.973	0.0257	0.03
2	0.0233	3.107	0.0145	0.03
3	0.0243	3.240	0.0141	0.03
4	0.0310	4.133	0.0202	0.03
5	0.0230	3.067	0.0150	0.03
Mean	0.0278	3.704	0.0179	0.03
SD	0.01	0.83	0.01	0.00

Table 9E The max force, force of adhesive, work of adhesive and thick value of F8

Run	Max Force (N)	Force of adhesion (N/cm²)	Work of Adhesion (mJ)	Thick (mm)
1	0.0223	1.274	0.0142	0.07
2	0.0137	0.781	0.0078	0.07
3	0.0290	1.657	0.0147	0.07
4	0.0217	1.238	0.0097	0.07
5	0.1157	6.610	0.0480	0.07
Mean	0.0405	2.312	0.0189	0.07
SD	0.04	2.42	0.02	0.00

Table 10E The max force, force of adhesive, work of adhesive and thick value of F9

Run	Max Force (N)	Force of adhesion (N/cm²)	Work of Adhesion (mJ)	Thick (mm)
1	0.1393	0.929	0.0295	0.07
2	0.1833	1.222	0.0431	0.07
3	0.2353	1.569	0.0582	0.07
4	0.4250	2.833	0.0864	0.07
5	0.1917	1.278	0.0387	0.07
Mean	0.2349	1.5662	0.0512	0.07
SD	0.11	0.74	0.02	0

Table 11E The max force, force of adhesive, work of adhesive and thick value of F10

Run	Max Force (N)	Force of adhesion (N/cm²)	Work of Adhesion (mJ)	Thick (mm)
1	0.1223	8.16	0.0214	0.06
2	0.0597	3.98	0.0298	0.06
3	0.2870	19.13	0.0468	0.06
4	0.0993	6.62	0.0270	0.06
5	0.4427	29.51	0.0667	0.06
Mean	0.2022	13.48	0.0383	0.06
SD	0.16	10.66	0.02	0

Table 12E The max force, force of adhesive, work of adhesive and thick value of F11

Run	Max Force (N)	Force of adhesion (N/cm²)	Work of Adhesion (mJ)	Thick (mm)
1	0.0373	2.984	0.0243	0.05
2	0.0343	2.744	0.0179	0.05
3	0.0297	2.376	0.0162	0.05
4	0.0157	1.253	0.0092	0.05
5	0.0213	1.704	0.0143	0.05
Mean	0.0277	2.212	0.0164	0.05
SD	0.01	0.72	0.01	0

Table 13E The max force, force of adhesive, work of adhesive and thick value of F12

Run	Max Force (N)	Force of adhesion (N/cm²)	Work of Adhesion (mJ)	Thick (mm)
1	0.0460	4.600	0.0250	0.04
2	0.0413	4.133	0.0233	0.04
3	0.0410	4.100	0.0181	0.04
4	0.0333	3.333	0.0145	0.04
5	0.0213	2.130	0.0126	0.04
Mean	0.0366	3.659	0.0187	0.04
SD	0.01	0.97	0.01	0

Table 14E The max force, force of adhesive, work of adhesive and thick value of F13

Run	Max Force (N)	Force of adhesion (N/cm²)	Work of Adhesion (mJ)	Thick (mm)
1	0.0210	1.680	0.0133	0.05
2	0.0280	2.240	0.0153	0.05
3	0.0617	4.936	0.0285	0.05
4	0.0413	3.304	0.0219	0.05
5	0.0373	2.984	0.0224	0.05
Mean	0.0379	3.029	0.0203	0.05
SD	0.02	1.24	0.01	0

Table 15E The max force, force of adhesive, work of adhesive and thick value of F14

Run	Max Force (N)	Force of adhesion (N/cm²)	Work of Adhesion (mJ)	Thick (mm)
1	0.0233	1.864	0.0193	0.05
2	0.0220	1.760	0.0195	0.05
3	0.0237	1.896	0.0171	0.05
4	0.0180	1.440	0.0165	0.05
5	0.0213	1.704	0.0172	0.05
Mean	0.0217	1.7328	0.0179	0.05
SD	0.002	0.18	0.001	0

Table 16E The max force, force of adhesive, work of adhesive and thick value of F15

Run	Max Force (N)	Force of adhesion (N/cm²)	Work of Adhesion (mJ)	Thick (mm)
1	0.0317	3.170	0.0159	0.04
2	0.0410	4.100	0.0188	0.04
3	0.0557	5.567	0.0210	0.04
4	0.0263	2.630	0.0142	0.04
5	0.0150	1.500	0.0039	0.04
Mean	0.0339	3.393	0.0147	0.04
SD	0.02	1.54	0.01	0

Table 17E The max force, force of adhesive, work of adhesive and thick value of
Film with extract 1

Run	Max Force (N)	Force of adhesion (N/cm²)	Work of Adhesion (mJ)	Thick (mm)
1	0.04530	4.530	0.0181	0.04
2	0.03900	3.900	0.0219	0.04
3	0.06270	6.270	0.0279	0.04
4	0.05430	5.430	0.0324	0.04
5	0.02270	2.267	0.0109	0.04
Mean	0.0448	4.479	0.0223	0.04
SD	0.02	1.53	0.01	0

Table 17E The max force, force of adhesive, work of adhesive and thick value of
Film with extract 2

Run	Max Force (N)	Force of adhesion (N/cm²)	Work of Adhesion (mJ)	Thick (mm)
1	0.06270	5.0160	0.0320	0.05
2	0.03870	3.0960	0.0223	0.05
3	0.07800	6.2400	0.0387	0.05
4	0.02370	1.8930	0.0129	0.05
5	0.05930	4.7440	0.0240	0.05
Mean	0.0525	4.198	0.026	0.05
SD	0.02	1.71	0.01	0

Table 17E The max force, force of adhesive, work of adhesive and thick value of
Film with extract 3

Run	Max Force (N)	Force of adhesion (N/cm²)	Work of Adhesion (mJ)	Thick (mm)
1	0.03230	2.5840	0.0218	0.05
2	0.01330	1.0640	0.0107	0.05
3	0.03570	2.8560	0.0236	0.05
4	0.03070	2.4530	0.0149	0.05
5	0.04000	3.2000	0.0257	0.05
Mean	0.0304	2.431	0.0193	0.05
SD	0.01	0.82	0.01	0

APPENDIX F

Experimental data of adhesive properties of film formulations and film containing *Centella Asiatica* extract

Table 1F Mechanical properties data of F1

Run	Tensile Strength (MPa)	%Elongation	Work of failure (mJ)	E-Mod (MPa)
1	15.03	178.20	10.31	7.80
2	18.00	198.80	13.65	8.05
3	12.32	161.00	7.48	7.19
4	12.15	176.20	8.24	6.52
5	19.73	170.00	13.12	10.87
Mean	15.447	176.84	10.559	8.086
SD	3.38	13.98	2.78	1.6664

Table 2F Mechanical properties data of F2

Run	Tensile Strength (MPa)	%Elongation	Work of failure (mJ)	E-Mod (MPa)
1	3.378	368	10.54	2.403
2	4.978	356	13.19	3.271
3	5.306	336	13.21	3.315
4	5.382	448	19.45	3.062
5	4.639	368	12.99	2.730
Mean	4.736	375.2	13.876	2.956
SD	0.81	42.75	3.32	0.39

Table 3F Mechanical properties data of F3

Run	Tensile Strength (MPa)	%Elongation	Work of failure (mJ)	E-Mod (MPa)
1	2.167	416.0	5.83	3.267
2	3.683	524.0	8.03	3.097
3	5.400	542.4	10.06	4.208
4	3.633	500.0	11.13	6.011
5	5.211	474.0	13.00	7.911
Mean	4.019	491.3	9.611	4.899
SD	1.32	49.31	2.78	2.04

Table 4F Mechanical properties data of F4

Run	Tensile Strength (MPa)	%Elongation	Work of failure (mJ)	E-Mod (MPa)
1	14.80	138.20	5.68	17.53
2	15.33	149.10	6.20	13.68
3	14.17	120.20	5.04	24.70
4	13.95	116.00	4.43	17.20
5	14.23	117.20	4.47	16.47
Mean	14.497	128.1	5.163	17.917
SD	0.56	14.78	0.77	4.09

Table 5F Mechanical properties data of F5

Run	Tensile Strength (MPa)	%Elongation	Work of failure (mJ)	E-Mod (MPa)
1	5.242	352	7.83	5.32
2	3.928	348	5.93	7.60
3	4.789	382	7.13	4.99
4	4.692	368	7.32	5.04
5	4.983	354	8.01	6.44
Mean	4.727	360.8	7.245	5.88
SD	0.49	14.04	0.82	1.13

Table 6F Mechanical properties data of F6

Run	Tensile Strength (MPa)	%Elongation	Work of failure (mJ)	E-Mod (MPa)
1	13.01	420.0	30.49	4.731
2	12.39	450.0	30.99	4.220
3	12.58	300.0	19.59	4.765
4	10.93	285.9	15.89	4.059
5	11.21	332.0	21.39	4.530
Mean	12.026	357.6	23.67	4.461
SD	0.91	73.39	6.76	0.31

Table 7F Mechanical properties data of F7

Run	Tensile Strength (MPa)	%Elongation	Work of failure (mJ)	E-Mod (MPa)
1	3.483	528	16.75	3.342
2	3.694	548	20.37	3.362
3	3.847	466	17.60	3.334
4	3.372	576	18.29	3.144
5	4.800	618	28.73	4.025
Mean	3.839	547.1	20.35	3.441
SD	0.57	56.45	4.87	0.33

Table 8F Mechanical properties data of F8

Run	Tensile Strength (MPa)	%Elongation	Work of failure (mJ)	E-Mod (MPa)
1	9.56	184.2	8.59	4.421
2	4.66	150.7	5.17	3.952
3	8.16	157.0	5.92	3.883
4	5.98	145.1	4.12	3.791
5	6.11	187.2	5.89	3.097
Mean	6.893	164.83	5.941	3.829
SD	1.95	19.54	1.65	0.48

Table 9F Mechanical properties data of F9

Run	Tensile Strength (MPa)	%Elongation	Work of failure (mJ)	E-Mod (MPa)
1	11.7	96.8	6.62	17.59
2	10.62	95.6	6.46	17.20
3	12.23	82.4	6.33	23.66
4	7.73	66.8	3.27	34.05
5	11.19	98.0	6.96	19.12
Mean	10.695	87.92	5.926	22.33
SD	1.76	13.38	1.50	7.04

Table 10F Mechanical properties data of F10

Run	Tensile Strength (MPa)	%Elongation	Work of failure (mJ)	E-Mod (MPa)
1	2.600	510.4	11.76	2.554
2	3.040	580.0	16.00	2.405
3	2.988	508.0	13.13	2.635
4	2.550	404.0	8.29	2.139
5	2.683	468.0	10.57	2.688
Mean	2.772	494.1	11.951	2.484
SD	0.23	64.49	2.88	0.22

Table 11F Mechanical properties data of F11

Run	Tensile Strength (MPa)	%Elongation	Work of failure (mJ)	E-Mod (MPa)
1	8.57	646.4	35.73	5.860
2	3.48	540.0	13.89	2.516
3	7.13	532.0	30.93	5.931
4	7.43	600.0	33.77	6.790
5	10.32	488.0	29.29	4.725
Mean	7.386	561.3	28.72	5.164
SD	2.52	62.10	8.66	1.65

Table 12F Mechanical properties data of F12

Run	Tensile Strength (MPa)	%Elongation	Work of failure (mJ)	E-Mod (MPa)
1	4.542	488	16.34	4.439
2	3.313	526	15.47	4.183
3	4.342	522	15.72	3.791
4	3.225	522	13.59	2.570
5	2.642	566	14.30	4.007
Mean	3.613	525	15.083	3.798
SD	0.80	27.82	1.12	0.73

Table 13F Mechanical properties data of F13

Run	Tensile Strength (MPa)	%Elongation	Work of failure (mJ)	E-Mod (MPa)
1	4.46	618	22.90	4.99
2	6.99	576	21.57	4.79
3	4.89	594	22.78	4.82
4	8.33	484	25.64	6.44
5	9.60	572	33.02	6.08
Mean	6.853	568.6	25.18	5.424
SD	2.20	50.62	4.63	0.78

Table 14F Mechanical properties data of F14

Run	Tensile Strength (MPa)	%Elongation	Work of failure (mJ)	E-Mod (MPa)
1	5.31	498	17.93	3.393
2	6.32	426	16.43	4.390
3	6.08	568	24.32	4.236
4	4.96	580	22.39	3.701
5	6.28	496	22.21	4.220
Mean	5.789	513.5	20.66	3.988
SD	0.62	62.47	3.32	0.42

Table 15F Mechanical properties data of F15

Run	Tensile Strength (MPa)	%Elongation	Work of failure (mJ)	E-Mod (MPa)
1	6.13	510	22.38	5.21
2	3.52	520	13.14	4.34
3	8.21	512	20.54	5.57
4	10.43	500	41.75	12.84
5	6.94	474	19.79	6.22
Mean	7.044	503.3	23.52	6.835
SD	2.56	17.85	10.77	3.43

Table 16F Mechanical properties data of Film with extract n 1

Run	Tensile Strength (MPa)	%Elongation	Work of failure (mJ)	E-Mod (MPa)
1	11.89	249.9	12.75	5.575
2	13.11	255.9	10.95	4.486
3	10.39	210.0	6.87	4.086
4	10.89	198.0	7.21	4.285
5	15.95	252.0	12.70	4.176
Mean	12.446	233.2	10.095	4.522
SD	2.22	27.04	2.89	0.61

Table 17F Mechanical properties data of Film with extract 2

Run	Tensile Strength (MPa)	%Elongation	Work of failure (mJ)	E-Mod (MPa)
1	17.81	202.0	11.90	7.89
2	16.75	232.0	13.47	6.67
3	14.00	222.0	10.82	5.76
4	16.05	183.2	9.44	6.68
5	18.72	236.0	15.08	7.14
Mean	16.666	215	12.143	6.829
SD	1.80	22.13	2.21	0.78

Table 18F Mechanical properties data of Film with extract 3

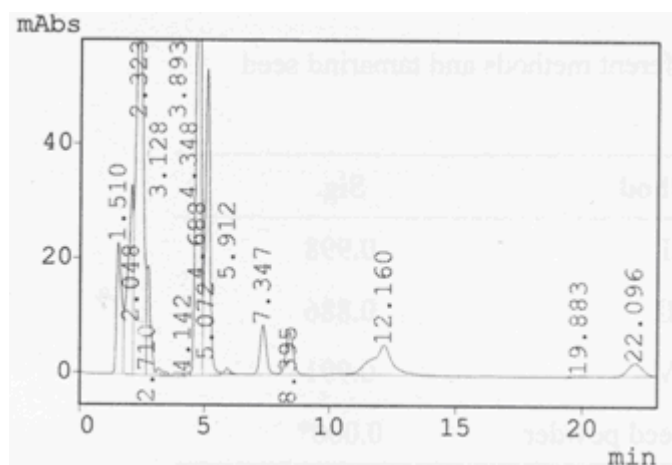
Run	Tensile Strength (MPa)	%Elongation	Work of failure (mJ)	E-Mod (MPa)
1	15.43	252.0	12.97	5.40
2	15.90	240.0	13.03	5.29
3	17.23	254.1	15.14	6.62
4	15.70	261.9	17.70	6.93
5	16.85	242.0	13.55	6.08
Mean	16.223	250	14.475	6.064
SD	0.78	9.03	2.00	0.73

APPENDIX G

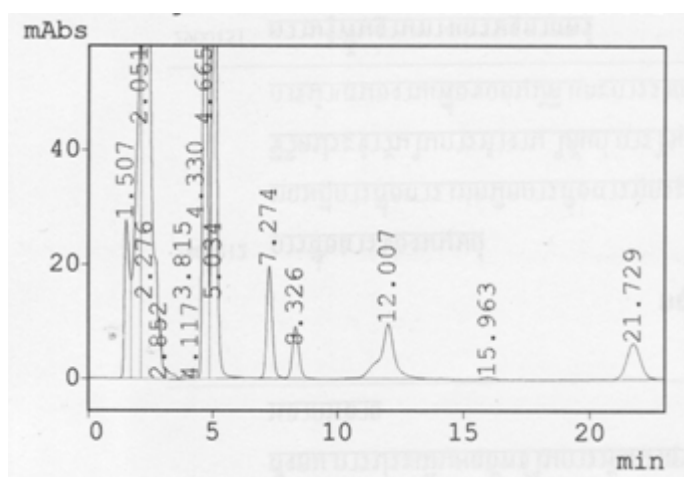
Experimental data of release and permeation study

Table 1G The release data of asiaticoside from film formulations

Time (hr)	%Cumulative release of asiaticoside			Mean	SD
	set 1	set 2	set 3		
0	0	0	0	0	0
0.25	5.97	4.34	6.77	5.69	1.24
0.5	7.10	8.04	9.24	8.13	1.07
0.75	8.80	8.65	12.41	9.95	2.13
1	10.81	12.34	16.74	13.30	3.08
1.5	14.20	14.97	20.23	16.47	3.28
2	19.10	23.89	25.74	22.91	3.43
3	29.14	31.42	33.27	31.28	2.07
4	35.74	36.49	38.22	36.82	1.27
5	34.12	35.96	42.80	37.63	4.57
6	39.96	40.19	44.77	41.64	2.72
8	42.83	45.05	49.17	45.68	3.22
10	48.33	50.91	56.60	51.95	4.23
12	52.53	59.05	61.20	57.60	4.51
15	55.97	61.12	60.87	59.32	2.90
18	60.33	65.18	64.50	63.34	2.63
21	63.13	65.69	67.29	65.37	2.10
24	70.61	62.67	69.40	67.56	4.28
28	70.57	62.42	69.62	67.54	4.45
32	72.61	61.94	73.57	69.37	6.45
36	77.37	71.61	74.86	74.61	2.89
40	79.05	72.23	80.84	77.37	4.54
44	79.72	74.46	82.85	79.01	4.24
48	80.98	76.65	84.62	80.75	3.99



(a)



(b)

Figure 1G HPLC chromatograms of asiatic acid from permeation study at different time.

- (a) Peak of asiatic acid at 2 hours (retention time at 12.160 minutes)
- (b) Peak of asiatic acid at 24 hours (retention time at 12.007 minutes)

APPENDIX H

Experimental data of stability study

Table 1H The percentages labeled amount of asiaticoside in film formulations containing *Centella asiatica* extract in stability test

Periods	% Asiaticoside			Mean	SD
	set 1	set 2	set 3		
Initial	89.4506	99.392	92.7002	93.85	5.07
1 st month	84.0113	92.1003	84.6858	86.93	4.49
2 nd month	80.5896	86.0523	76.629	81.09	4.73
3 rd month	76.2121	83.6113	75.5291	78.45	4.48

Table 2H Adhesive properties data of film formulations in initial period

Run	Max Force (N)	Force of adhesion (N/cm ²)	Work of Adhesion (mJ)	Thick (mm)
1	0.0448	4.479	0.0223	0.04
2	0.0525	4.198	0.0260	0.05
3	0.0304	2.431	0.0193	0.05
Mean	0.0426	3.703	0.0225	0.047
SD	0.01	1.11	0.003	0.01

Table 33H Adhesive properties data of film formulations in 1st month period

Run	Max Force (N)	Force of adhesion (N/cm ²)	Work of Adhesion (mJ)	Thick (mm)
1	0.0274	2.191	0.0208	0.05
2	0.0415	3.322	0.0229	0.05
3	0.0409	3.269	0.0216	0.05
Mean	0.0366	2.927	0.0218	0.05
SD	0.01	0.64	0.001	0

Table 4H Adhesive properties data of film formulations in 2nd month period

Run	Max Force (N)	Force of adhesion (N/cm²)	Work of Adhesion (mJ)	Thick (mm)
1	0.0529	5.287	0.0174	0.04
2	0.0357	2.853	0.0217	0.05
3	0.0365	2.917	0.0212	0.05
Mean	0.0353	2.825	0.0215	0.05
SD	0.001	0.11	0.0003	0

Table 5H Adhesive properties data of film formulation in 3rd month period

Run	Max Force (N)	Force of adhesion (N/cm²)	Work of Adhesion (mJ)	Thick (mm)
1	0.0285	2.854	0.0176	0.04
2	0.0300	2.402	0.0216	0.05
3	0.0289	2.314	0.0211	0.05
Mean	0.0291	2.523	0.0201	0.0467
SD	0.001	0.29	0.002	0.006

Table 6H ANOVA for the adhesive forces data of film formulation

	Sum of Squares	df	Mean Square	F	Sig.
Between Groups	0.000	3	0.000	0.793	0.531
Within Groups	0.000	8	0.000		
Total	0.000	11			

Table 7H Tukey HSD test of the adhesive forces data of film formulation

Periods	Method	Sig.
Initial	1 st month	0.028*
	2 nd month	0.018*
	3 rd month	0.006*
1 st month	Initial	0.028*
	2 nd month	0.989
	3 rd month	0.632
2 nd month	Initial	0.018*
	1 st month	0.989
	3 rd month	0.800
3 rd month	Initial	0.006*
	1 st month	0.632
	2 nd month	0.800

* The mean difference is significant at the 0.05 level

Table 8H Mechanical properties data of film formulation in initial period

Run	Tensile Strength (MPa)	%Elongation	Work of failure (mJ)	E-Mod (MPa)
1	12.446	233.2	10.095	4.522
2	16.666	215	12.143	6.829
3	16.223	250	14.475	6.064
Mean	15.11	232.73	12.24	5.81
SD	2.32	17.50	2.19	1.18

Table 9H Mechanical properties data of film formulation in 1st month period

Run	Tensile Strength (MPa)	%Elongation	Work of failure (mJ)	E-Mod (MPa)
1	7.362	334.4	10.678	4.027
2	5.934	386.4	12.947	3.155
3	6.829	372	13.834	3.426
Mean	6.71	364.27	12.49	3.54
SD	0.72	26.85	1.63	0.45

Table 10H Mechanical properties data of film formulation in 2nd month period

Run	Tensile Strength (MPa)	%Elongation	Work of failure (mJ)	E-Mod (MPa)
1	6.797	539.7	24.97	4.361
2	2.922	500.9	10.676	2.226
3	7.896	481.8	25.16	4.682
Mean	5.87	507.47	20.27	3.76
SD	2.61	29.50	8.31	1.33

Table 11H Mechanical properties data of film formulation in 3rd month period

Run	Tensile Strength (MPa)	%Elongation	Work of failure (mJ)	E-Mod (MPa)
1	3.836	490.7	12.621	4.101
2	3.621	451.3	11.631	3.2
3	3.61	475.9	11.828	3.073
Mean	3.69	472.63	12.03	3.46
SD	0.13	19.90	0.52	0.56

Table 12H ANOVA for the tensile strength of film formulation

	Sum of Squares	df	Mean Square	F	Sig.
Between Groups	225.789	3	75.263	23.625	0.000
Within Groups	25.485	8	3.186		
Total	251.274	11			

Table 13H Tukey HSD test of the tensile strength of film formulation

Periods	Method	Sig.
Initial	1 st month	0.002*
	2 nd month	0.001*
	3 rd month	0.000*
1 st month	Initial	0.002*
	2 nd month	0.937
	3 rd month	0.240
2 nd month	Initial	0.001*
	1 st month	0.937
	3 rd month	0.481
3 rd month	Initial	0.000*
	1 st month	0.240
	2 nd month	0.481

* The mean difference is significant at the 0.05 level

Table 14H ANOVA for the %elongation of film formulation

	Sum of Squares	df	Mean Square	F	Sig.
Between Groups	137845.776	3	45948.592	80.126	0.000
Within Groups	4587.607	8	573.451		
Total	142433.38	11			

Table 15H Tukey HSD test of the %elongation of film formulation

Peroids	Method	Sig.
Initial	1 st month	0.001*
	2 nd month	0.000*
	3 rd month	0.000*
1 st month	Initial	0.001*
	2 nd month	0.000*
	3 rd month	0.002*
2 nd month	Initial	0.000*
	1 st month	0.000*
	3 rd month	0.347
3 rd month	Initial	0.000*
	1 st month	0.002*
	2 nd month	0.347

* The mean difference is significant at the 0.05 level

Table 16H ANOVA for the work of failure of film formulation

	Sum of Squares	df	Mean Square	F	Sig.
Between Groups	144.982	3	48.327	2.519	0.132
Within Groups	153.500	8	19.188		
Total	298.483	11			

Table 17H Tukey HSD test of the work of failure of film formulation

Peroids	Method	Sig.
Initial	1 st month	1.000
	2 nd month	0.191
	3 rd month	1.000
1 st month	Initial	1.000
	2 nd month	0.209
	3 rd month	0.999
2 nd month	Initial	0.191
	1 st month	0.209
	3 rd month	0.176
3 rd month	Initial	1.000
	1 st month	0.999
	2 nd month	0.176

* The mean difference is significant at the 0.05 level

Table 18H ANOVA for the Young's modulus of film formulation

	Sum of Squares	df	Mean Square	F	Sig.
Between Groups	11.248	3	3.749	4.079	0.050
Within Groups	7.353	8	0.919		
Total	18.601	11			

Table 19H Tukey HSD test of the Young's modulus of film formulation

Peroids	Method	Sig.
Initial	1 st month	0.077
	2 nd month	0.114
	3 rd month	0.067
1 st month	Initial	0.077
	2 nd month	0.992
	3 rd month	1.000
2 nd month	Initial	0.114
	1 st month	0.992
	3 rd month	0.980
3 rd month	Initial	0.067
	1 st month	1.000
	2 nd month	0.980

* The mean difference is significant at the 0.05 level

VITA

Miss. Jirunya Assanee was born on December 8, 1981 in Bangkok, Thailand. She received her Bachelor degree of Science in Pharmacy from the Faculty of Pharmaceutical Sciences, Srinakarinwirot University in 2003. She worked for the Rajvitee hospital, Thailand.